TECHNISCHE UNIVERSITÄT MÜNCHEN

FACHGEBIET FÜR ORGANISCHE CHEMIE

Enantio-recognition of Oxoanions by Chiral Bicyclic Guanidinium Hosts

Ashish Tiwari

Vollständiger Abdruck der von der Fakultät für Chemie der Technischen Universität München zur Erlangung des akademischen Grades eines Doktors der Naturwissenschaften genehmigten Dissertation.

Vorsitzender:	Univ.-Prof. Dr. M. Schuster
Prüfer der Dissertation:	1. Univ.-Prof. Dr. F. P. Schmidtchen
	2. Univ.-Prof. Dr. K. Köhler

Die Dissertation wurde am 18.01.2012 bei der Technischen Universität München eingereicht und durch die Fakultät für Chemie am 22.02.2012 angenommen.

To my parents

Acknowledgements

Work presented in this thesis was carried out from January 2009 to December 2011 in the Department of Organic Chemistry and Biochemistry at Technical University of Munich.

I would like to thank Prof. Dr. F. P. Schmidtchen for his continuous encouragement and support. The work would not have been complete without his patience and understanding. His vast experience in the field of organic and supramolecular chemistry helped me to overcome every obstacle during the work.

I would like to thank Mrs. Otte, Mr. Kaviani and Mr. Cordes for providing me mass spectra of the compounds prepared in this work. I would also like to thank Prof. Dr. Herbert Mayr for allowing me to use ITC facilities in his lab.

I would take the opportunity to thank Dr. Wiebke Antonius and Dr. Laxman Malge for their continuous help throughout these years. I wish to thank Andrei Ursu for his help and fruitful discussions during the stay in laboratory.

I thank all my friends for their support and encouragement throughout this period.

I would be grateful to my parents and family members for their love and constant encouragement.

Abbreviations

Ac	Acetyl
Ala	Alanine
AMBER	Assisted Model Building with Energy Refinement
Arg	Arginine
Ar	Aromatic
Bn	Benzyl
t-Boc	tert-Butoxycarbonyl
bp	boiling point
CFF	Consistent Force Field
δ	chemical shift
d	dublet
DABCO	1,4-Diazabicyclo(2.2.2)-octane
DBU	1,8-Diazabicyclo[5.4.0]undec-7-ene
DCM	Dichloromethane
DCE	1,2-Dichloroethane
DMF	N,N-Dimethylformamide
DMSO	Dimethylsulfoxide
DNA	Deoxyribonucleic acid
EDIPA	Ethylenediisopropylamine
ESI	Electron Spray Ionization
FT	Fourier Tansform
GROMOS	GROningen MOlecular Simulation
HPLC	High Performance Liquid Chromatography
IR	Infrared
ITC	Isothermal Titration Calorimetry
K_{ass}	Association Constant
LDA	Lithiumdiisopropylamide
Lys	Lysine
MD	Molecular Dynamics
mp	Melting point

MPLC	Medium pressure liquid chromatography
MS	Mass Spectroscopy
MTBE	Methyl tert butyl ether
NAD^+	Nicotinamide adenine dinucleotide
NMR	Nuclear magnetic resonance
ppm	Parts per million
RCM	Ring closing metathesis
RMSD	Root mean square deviation
RP	Reversed phase
R_t	Retention time
RT	Room temperature
S	singulet
SPE	Solid phase extraction
t	triplet
TBDPS	tert.–butyldiphenylsilyl
t-Bu	tert.-butyl
TEA	Triethylamine
Tf	Trifluoromethanesulfonyl
TFA	Trifluoroacetic acid
THF	Tetrahydrofuran
TLC	Thin Layer Chromatography
Ts	Tosyl
UV	Ultraviolet
Val	Valine
VIS	Visible
ADP	Adenosine 5’-diphosphate
AMP	Adenosine 5’-monophosphate
ATP	Adenosine 5’-triphosphate
GMP	Guanosine monophosphate

Contents

1. Introduction

Whether or not a host-guest complex under study complies with the ultimate model of structural uniqueness, i.e., the lock-and-key picture, is of prime importance for addressing the various goals of molecular recognition[1] The singularity of the binding mode plays a predominant role in all supramolecular applications targeting a peculiar geometrical identity as in assembly processes or in catalyses depending on a specific stereoelectronic disposition of the interaction partners. In contrast, supramolecular interactions aiming at maximum affinity for, e.g., two-phase extraction or rigorous blocking of a receptor site have less demand for structural uniqueness. The discrimination between two structures that exclusively differ in their geometry as it occurs in enantiorecognition clearly belongs to the former domain. Recognition of enantiomers of chiral anions holds an important place among various applications of supramolecular chemistry. Enantioselective anion sensing is included in a number of reviews covering much broader subjects, namely receptors of anions in general [1c, 2] and chromophoric sensors of anions[3]. There are also more specialized reviews dealing with receptors for anions based on amides[4], guanidiniums[5], crown ethers[6], or lanthanoids[7]. The chemical and more importantly biological activity of any chiral substance depends on its stereochemistry, so recognition of these enantiomers depends exclusively on geometrical factors, but not at all on the differences in chemical nature or solvation of the competing partners. This is why design, synthesis and structure-activity relationships of enantioselective receptors are still very vital areas of research.

Chiral separation is an important issue in pharmaceutical research and industries, because most organic compounds and biological molecules, including many drugs and food additives, are chiral compounds. Enantiomerically pure compounds are usually obtained by asymmetric synthesis, crystallisation of diastereomeric salts, kinetic resolution of racemic mixtures or chiral chromatography. An interesting alternative to these methods is the separation of enantiomers based on the complementarity to a receptor. Those processes occurring through translocation of a guest between immiscible phases (chromatography, extraction, membrane transport) are particularly attractive. If the receptor is chiral, one of the enantiomers can be complexed preferentially and a kinetic resolution could be achieved. Moreover, the process needs only a catalytic amount of receptor since it can transfer several substrate molecules, one at a time,

across the phase boundary, without being removed from its own (stationary or liquid) phase. There is a rule of thumb – based on both experience and highly sophisticated calculations valid for the design of new enantioselective receptors: "Chiral recognition requires a minimum of four simultaneous interactions between receptor and at least one of the enantiomers, with at least one of these interactions being stereochemically dependent".[8] It should be stressed that this four-point rule does not require all four interactions to be attractive (i.e., bonding). In many cases, repulsive steric interactions are invoked, usually in combination with one or more bonding interactions to explain chiral recognition. In practice it means that the exchange of one enantiomer for the other is accompanied by the loss or profound change of at least one of these interactions. The study of enantioselective receptors consists in the measurement of the difference in Gibb's free energy caused by these two, attractive and repulsive processes. The magnitude of this difference is directly proportional to the efficiency of chiral recognition. Gibb's free energy is given by following thermodynamic equations:

$$\Delta G = \Delta H - T\Delta S$$

$$\Delta G^{\circ} = -RT \ln K_{ass}$$

It should be noted that the free energy is resultant of addition of enthalpy and entropy (as TΔS). Enthalpy is negative when a bond is formed between two species. And the entropy is positive when the complexation between two binding partners results in higher disorder in the system. As is evident from the above equation, a negative change in enthalpy and a positive change in entropy would be the ideal situation for the strong complexation between two interacting molecules, resulting in negative free energy. It implies that only strong binding (negative enthalpy) is not necessary or sufficient for strong complexation, rather it needs to be accompanied by a positive change in entropy. Normally, supramolecular complexation results in compensation between these two thermodynamic entities.[9] The chiral discrimination of cationic hosts with anionic guests is governed by a critical counterbalance between the electrostatic interaction of the charged groups in the host and guest and the conventional intracavity interactions of the hydrophobic moiety of the guest, such as hydrophobic, van der Waals, solvation/desolvation, and hydrogen bonding interaction.[10]

1.1 Guanidinium based chiral receptors

In the concrete case of enantio-differentiation of oxoanions like carboxylates or phosphates, biology offers some inspiration in the form of the guanidinium receptor functions. Nature frequently uses guanidinium moieties to coordinate different anion groups. Present in the side chain of the amino acid arginine, the guanidinium group forms strong ion-pairs with oxoanions such as carboxylates or phosphates in enzymes and antibodies, and it also contributes to the stabilisation of protein tertiary structures via internal salt bridges, mainly with carboxylates.[11] Guanidinium salt bridges play also important roles in enzyme active sites. Typical examples are carboxypeptidase A,[12] creatine kinase,[13] fumarate reductase,[14] and malate dehydrogenase.[15] The guanidinium moiety has been a popular choice as an anion binding unit due to its distinct oxoanion binding mode featuring two parallel hydrogen bonds in addition to an electrostatic interaction (Fig. 1.1.1). Additionally, both guanidinium remains protonated over a wide pH range because of their strong basicity (pK_a values typically ranging between 11 and 13).[16] The embedding of an anchor group in an open chain or macrocyclic chiral framework opens an access to dedicated enantioselective recognition of chiral carboxylates.

Figure 1.1.1. Mode of interaction between guanidine and carboxylate/phosphate anions

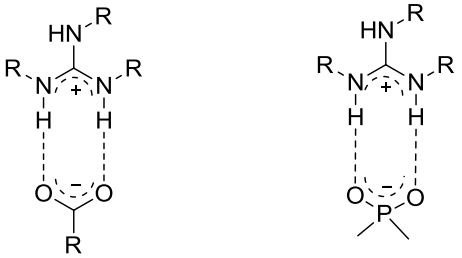

The first example of chiral recognition of a carboxylate by a guanidinium-based receptor was reported by de Mendoza in 1989.[17] Using NMR titration in $CDCl_3$, better chiral recognition was observed upon the complexation of *N*-Ac-tryptophan (K=1,051±20% M^{-1} for the L-enantiomer and K=534±15% M^{-1} for the D-enantiomer) by receptor **1**. The association constants were not as strong as required for complexation studies and with the error in the range of 20%, the difference in the association constants between both enantiomers did not promise much in terms of enantiomeric discrimination, but the host design gave a fundamental idea to improve upon in the future perspective. Another example of enantiomeric recognition by a guanidinium based receptor was reported by Schmidtchen.[18] Here the substituting arms contained the bulkier

diphenyl-*tert*-butylsilyl group and the aza-18-crown-6 unit by a symmetrical triaza analog that is known to recognize the ammonium cation with high selectivity over alkali metal cations. This compound **2** was capable of discrimination between enantiomers of phenylalanine. The L-enantiomer was extracted into chloroform with 40% ee in a wide pH range. This demonstrates that restricting the number of degrees of freedom in the hosts could provide with better alternatives for effective enantiomeric recognition.

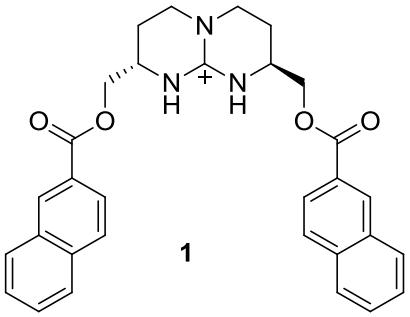

1

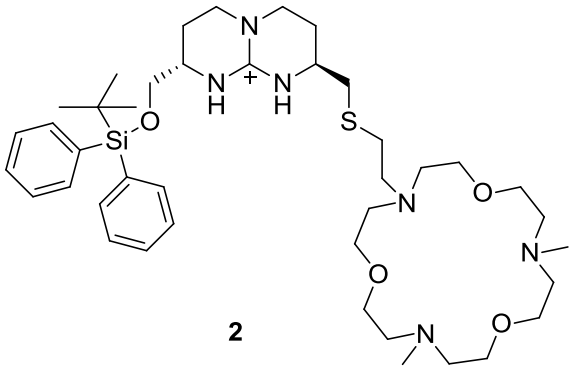

2

Steroid ligands possess an added advantage other than having a rigid structural framework as they have chiral centers which increases the possibility of chiral interaction with the guests. Davis has shown that the steroid skeleton can be used as a very efficient chiral scaffold.[19] A guanidinium group was attached to a lipophilic steroid skeleton, usually in spatial proximity with other anion-binding active groups such as amides, sulfonamide, or urethane. L-Enantiomers of the amino acids *N*-Ac-Ala, *N*-Ac-Phe, *N*-Ac-Val,and *N*-Ac-Trp were extracted with sevenfold preference over the antipodes by ligand **3**. Analogously, ligand **4** was found to be even more efficient, as the L-enantiomeric preference was tenfold.

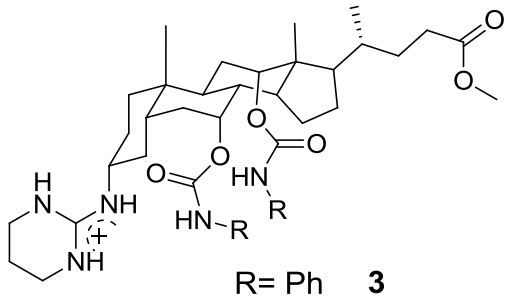

R= Ph **3**

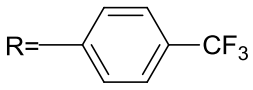

4

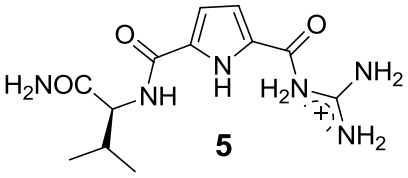

5

A different design was used by Schmuck for guanidinocarbonyl pyrrole ligand **5** to bind carboxylates effectively in aqueous media with binding constants which were much larger than those obtained simply with guanidinium cations.[20] Binding studies with a systematically varied series of ligands showed that the amide NH next to the pyrrole ring was mainly responsible for the stronger binding, whereas the pyrrole NH and the terminal carbamoyl group contributed less to overall binding. Ligand **5** showed preferential binding of the L-enantiomer of *N*-Ac-Ala (K=1,610 M^{-1}) against *N*-Ac-D-Ala (K=930 M^{-1}). Also a barely significant preference for the L-enantiomer of *N*-AcTrp (K=1,145 M^{-1}) over *N*-Ac-D-Trp (K= 1,005 M^{-1}) was observed. On the contrary, the D-enantiomer of *N*-Ac-Phe showed preference over the L-enantiomer, (*N*-Ac-D-Phe: K=680 M^{-1}; *N*-Ac-L-Phe: K=585 M^{-1}). There are two problems connected with this unexpected behavior. First, the ligand is still rather flexible and second, it contains only one chiral centre. Though, the interaction studies give different values for binding constants of enantiomers of amino acids, but the host cannot be qualified at all as a chiral discriminating agent for two reasons. Firstly, the binding constants are too small to bind any anion efficiently and secondly, the difference between the binding constants of enantiomers is within the range of measurement errors normally associated with these experiments. The majority of the artificial guanidinium-based systems are acyclic and analogous to podand hosts for cations. But, as the above examples indicate, making the host structure more rigid by the means of macrocyclization might help in better enantiorecognition of chiral anions. The first examples of macrocyclic guanidinium-based anion receptors **6** and **7** were reported by Lehn et al. in 1978.[21] Both of these systems showed only weak complexation of PO_4^{3-} (log K_s=1.7 and 2.4 in methanol/ water), governed by electrostatic interactions.

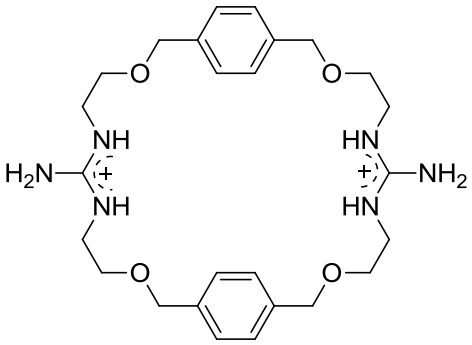

6

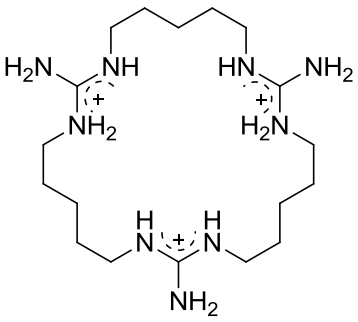

7

A few receptors have also been reported containing a macrocyclic framework as a side chain attached to bicyclic guanidinium unit although guanidine is not the part of the cyclic framework as reported by Schmidtchen (molecule **2)** and de Mendoza[22]. Apart from aza-oxacrown ethers, calixarenes have also been used in combination with guanidinium moieties with the purpose of anion binding. For the binding of a rather complicated zwitterionic substrate, dioctanoyl-1-phosphatidylcholine (DOPC) the receptor **8** was synthesized. Strong binding was observed in chloroform (Ks=7.3 E4) and NMR data as well as molecular modelling supported the anticipated binding mode with the calixarene encapsulating the ammonium group by adopting a cone conformation.[23]

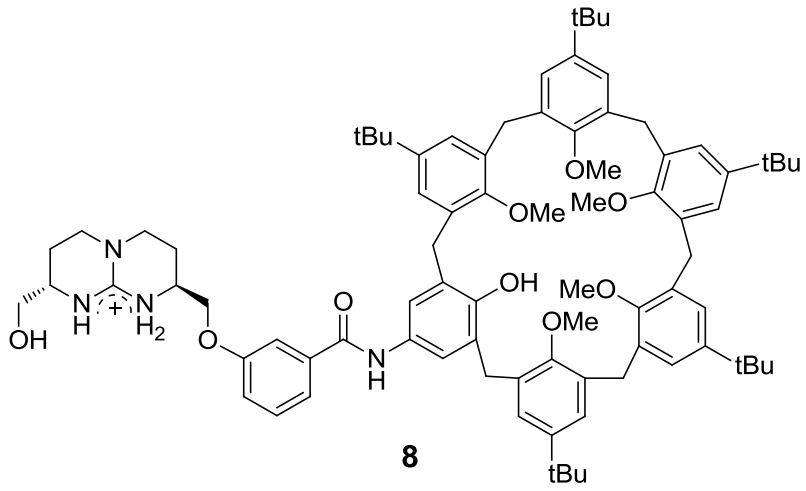

8

An interesting example of a preorganized macrocyclic host based on a bicyclic guanidinium subunit with the purpose of binding tetrahedral oxoanions such as phosphates, is **9**. This receptor was obtained in a one-pot synthesis and contains the chiral bicyclic guanidinium subunit in a macrocyclic framework. Overall, six binding units are arranged in such a way as to wrap around the anion by means of six hydrogen bonds tightly orientated in towards the centre of the cavity.[24] However, NMR evidence showed that despite the fact that phosphates are bound tightly, they do not enter the cavity. In contrast, the chloride complex was found to have a perfect C_2 symmetry at any temperature indicating encapsulation of the anion.

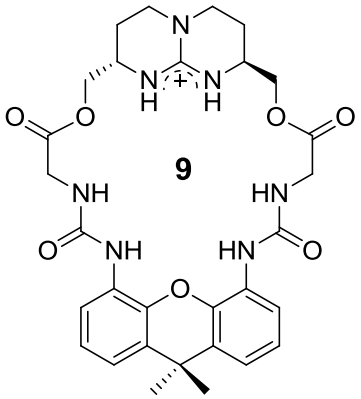

9

Schmidtchen, recently, reported a chirally active macrocyclic host[25] **10** with two guanidinium units attached to each other by two urea functions acting as a supplementary anchor groups for the complexation of anions. Isothermal calorimetric titration studies were done with the optical antipodes of tartrates and aspartates. Traditionally, the diastereomeric host-guest pair is considered to form matched or mismatched configurations merely based on the observed affinity ($\Delta G°$)[26]. ITC titration showed that there was a difference of 7.6 kJ mol^{-1} in the association entropies ($T\Delta S$) of two enantiomers of tartrate, but the ubiquitous enthalpy-entropy compensation[27] almost annihilates this entropic factor leaving behind a factor of 3.5 in terms of the association constant. In other examples also, the matched pair having the more negative entropy of association displayed weaker affinity compared to the mismatched one. So, one is led to conclude that affinity should be disqualified as the only evaluation criterion in enantiodiscrimination and should be replaced by the proper appreciation of the entire energetic signature of the process. For the direct comparison of the chiral discrimination capacity between the macrocyclic host **10** and its open-chain analogue **11**, the enantiomeric tartrates and aspartates were examined under the same conditions. In general, the calorimetric analyses revealed no significant differential effects in enantiomer binding. The affinities ($\Delta G°$) as well as the component entropies ($\Delta S°$) and enthalpies ($\Delta H°$) were identical within experimental error. The lack of enantiodiscrimination ($\Delta\Delta G°$) in these cases did not arise from enthalpy-entropy compensation that is commonly observed in supramolecular interactions but was seen in the energetic components, too.

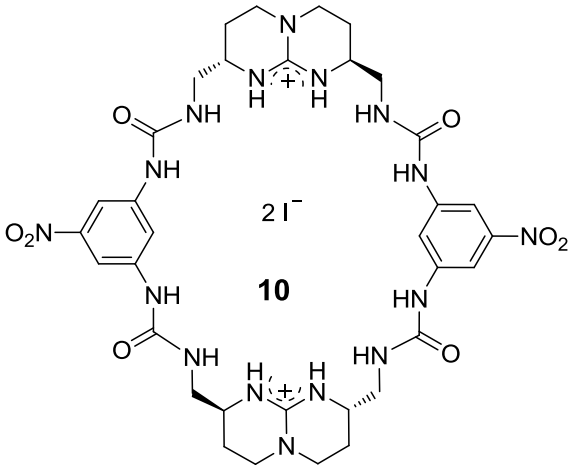

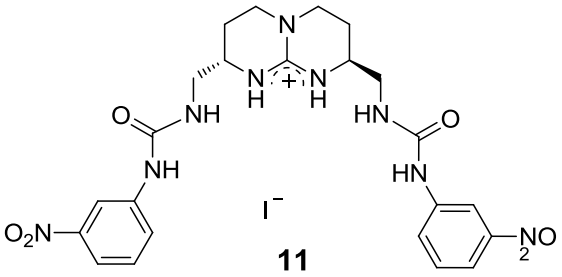

1.2 Enantiorecognition of carboxylates

The selective complexation of carboxylate anions by natural and synthetic hosts is a topic of current interest in bioorganic and supramolecular chemistry[1c, 2d], because these species are involved in several molecular recognition phenomena of biological interest. It is worth noting the special role that carboxylate recognition plays in determining the biological activity of the vancomycin family of antibiotics[28]. The enantioselective recognition of chiral carboxylates is also an important goal, because several pharmaceutical compounds possess this functional group. Efficient synthetic receptors for carboxylate anion recognition have been obtained by incorporating in more complex structures charged guanidinium, amidinium, or ammonium groups[1c] and neutral H-bonding donor groups such as (thio)ureas[29], pyrroles[2c], activated amides[30], and trifluoromethyl alcohols[31].

1.2.1 Binaphthyl based receptors

Over the last two decades, 1,1'-bi-2-naphthol (BINOL) and its derivatives have been extensively used in chiral recognition and asymmetric catalysis.[32] This is because the unique chiral and aromatic structure of the 1,1'-binaphthyl unit could provide both excellent chiral recognition capability and fluorescence signals. Application of 1,1'-binaphthyl-based chiral macrocycles to molecular recognition has been extensively studied as represented by Cram's pioneering work.[33] Separation and NMR methods have revealed that macrocyclic bis-binaphthyl crown ethers are able to carry out highly enantioselective discrimination of amino ester salts. Changes in the UV-VIS absorptions of binaphthyl-containing macrocycles have also been utilized for chiral

recognition. Lin Pu et. al. have exploited the built-in chirality of bisnaphthyl compounds to design a series of chiral hosts for enantiomeric recognition of chiral carboxylates and amino acids. In 2002, they synthesized the bisbinaphthyl-based macrocycle **S-12** which was found to carry out highly enantioselective fluorescent recognition of mandelic acids.[34] It was observed that within a certain concentration range, one enantiomer of the chiral acids could increase the fluorescence intensity of the macrocycles by 2-3-fold, while the other enantiomer scarcely enhanced the fluorescence. Such unusually high enantioselective responses make these macrocycles very attractive as fluorescent sensors in determining the enantiomeric composition of α-hydroxycarboxylic acids.

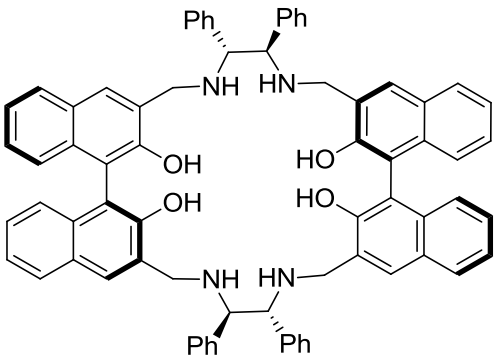

12

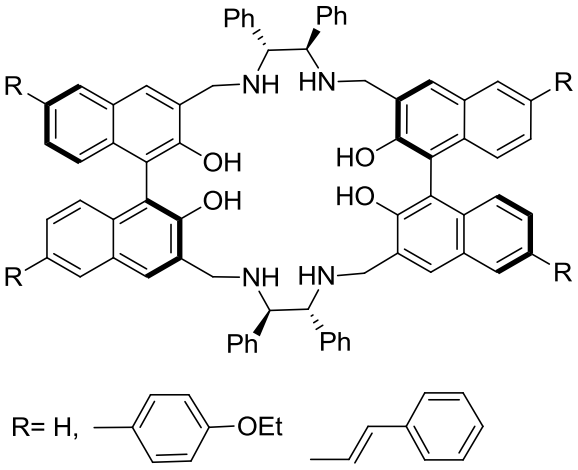

13

They modified the previously reported host by synthesizing the substituted bis-binaphthyl-based macrocyclic compounds **13**.[35] Using the 6, 6'-substituted bis-binaphthyl macrocycles in place of the unsubstituted macrocycles allowed a two orders of magnitude reduction in the sensor concentration for the fluorescence measurements. These macrocycles exhibited highly enantioselective fluorescent enhancements in the presence of chiral *R*-mandelic acid (with average enhancement factor, ef~2) and N-protected *R*-amino acids. They are useful as fluorescent sensors for chiral recognition. In addition, the macrocycles showed much greater enantioselectivity in the substrate recognition than their acyclic analogues. This gives an impression that restricting the degrees of freedom of the host molecule might be useful for enantio-differentiation of chiral anions as the interactions between host and guest would be more specific and well defined. Lin Pu further reported a modified bisbinaphthyl macrocycle that

exhibits an extremely high enantioselective fluorescent response in the emission from the monomer in the presence of mandelic acid.[36] They observed the highly enantioselective fluorescent recognition of mandelic acid by **(S)-14** with an average enhancement factor, ef~46. Furthermore, as this high enantioselectivity was observed at the emission of the **(S)-14** monomer, it decreased the working concentrations of the sensor and mandelic acid by one and two orders of magnitude, respectively. Even at the greatly decreased concentrations of both the sensor and substrate, the fluorescence enhancement of **(S)-14** in the presence of (S)-mandelic acid could be over 10- times greater than that of **(S)-12** in the presence of (S)- mandelic acid. Again the interesting fact is that the flexibility of the host is restricted by the introduction of more rigid bisamine cyclohexyl as the spacer group which results in better enantioselectivity.

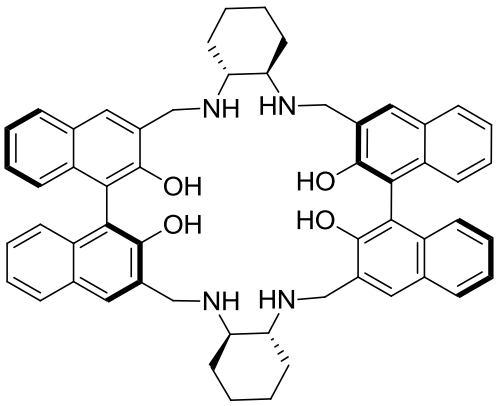

14

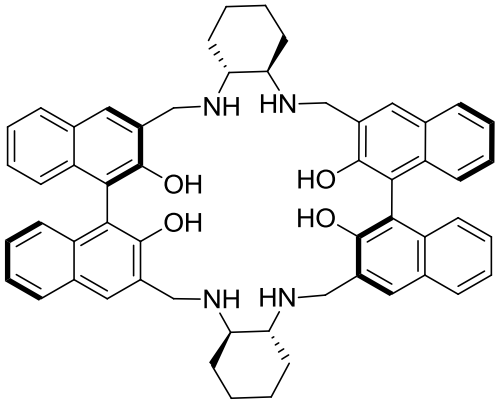

15

A new acyclic chiral sensor was reported that can be used to visually recognize the enantiomers of α-hydroxycarboxylic acids by enantioselective precipitation.[37] In addition, the enantioselective precipitation generated strongly fluorescent particles and provided an additional quantitative method for enantioselective discrimination. When (*S*)-mandelic acid ($\geq 3.0\times10^{-3}$ M) was added to a solution of host compound (*S*)-**16** (5.0×10^{-4} M) in benzene (containing 0.4 vol % dimethoxyethane, DME), the clear solution immediately turned into a white suspension. Under the same conditions, when (*R*)-mandelic acid was added to a solution of (*S*)-**16** in the concentration range of 1.0×10^{-3}–8.0×10^{-3} M, the solution remained clear. When the enantiomer (*R*)-**16** was used, precipitation with (*R*)-mandelic acid was observed, but not with (*S*)-mandelic acid. The complex formation of (*S*)-**16**-(*S*)-mandelic acid also showed strong fluorescense upon UV irradiation.

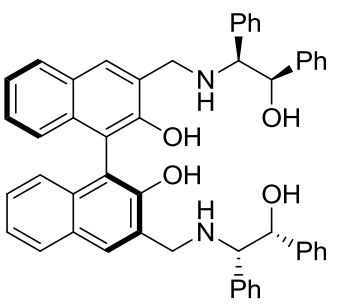

16

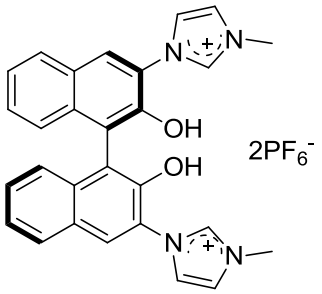

17

A novel imidazolium-functionalized BINOL fluorescent receptor **17** was developed as a multifunctional receptor for both chromogenic and chiral anion recognition by Yu and coworkers.[38] The association constants for **17** with L- and D- BOC alanine were calculated as 4.55×10^5 M^{-1} and 1.02×10^5 M^{-1} respectively, which shows an interesting enantioselectivity ($K_L/K_D = 4.5$). They also observed K_L/K_D ratio of 2.1, 3.9 and 1.7 for serine, leucine and phenyl alanine, respectively. Receptor **17** displays a remarkable binding ability for the *t*-Boc alanine anion, but the enantioselective discrimination was not as good for other amino acids. Recently, chiral discrimination of α-amino acids was realized by a C_2-symmetric homoditopic receptor, which was based on a binaphthyl chiral skeleton with 2,2′-diisopropoxy substituents and a common binding side arm, (*o*-carboxamido)-trifluoroacetophenone moiety, in the 3,3′-positions, which recognized α-amino acids as their amino carboxylate forms through formation of stabilized adducts.[39] The receptor **18** utilizes the o-(carboxamido)-trifluoroacetophenone motif for carboxylate as well as amine recognition, which recognizes both amine and carboxylate through the formation of stabilized and reversible covalent bonds. It shows very high enantioselectivity for L-isomers of alanine, serine, tryptophan and phenylalanine (almost 95%) and moderate selectivity for L-isomers of methionine, valine and leucine (almost 80%).

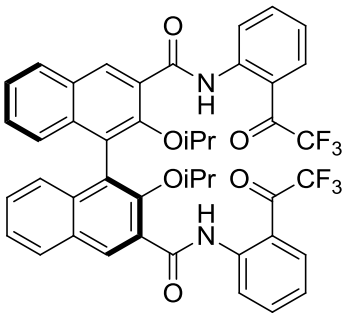

18

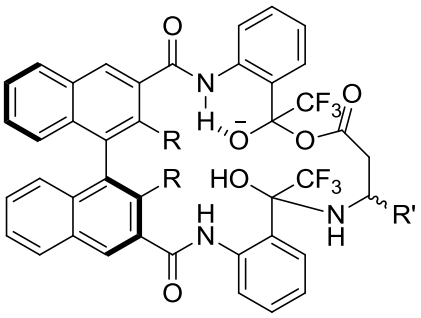

19

Wang et al. prepared four novel derivatives of 1,1'-bi-2-naphthol.[40] The enantioselective recognition of these sensors was studied by fluorescence titration and ^{1}H NMR spectroscopy. The sensors exhibited different chiral recognition abilities towards N-Boc-protected amino acid anions and formed 1:1 complexes between the host and the guest. Sensor (***S*)-20** exhibited enantiomeric recognition up to a factor of 5.5 ($K_{ass(S)}/K_{ass(R)}$) for alanine amino acid.

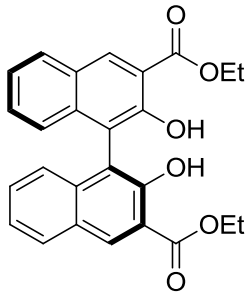

20

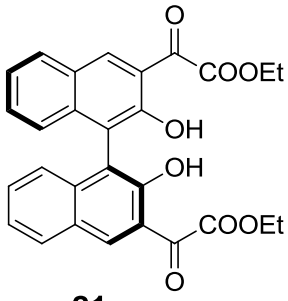

21

Four novel derivatives of BINOL bearing (*S*)-tryptophan unit (**22** and **23**) were prepared by Wang et al.[41] The enantioselective recognition of these receptors was studied by fluorescence titration and ^{1}H NMR spectroscopy. These receptors exhibit excellent enantioselective fluorescent recognition ability towards the amino acid derivatives. The maximum chiral recognition was achieved for phenyl alanine (factor ~5). Interestingly, ***S*-22** and ***S*-23** had greater affinity for the *S*-enantiomer and ***R*-22** and ***R*-23** had higher association constants for the *R*-isomer.

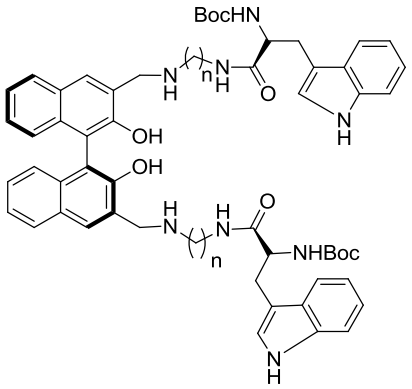

22a, n=2
22b, n=3

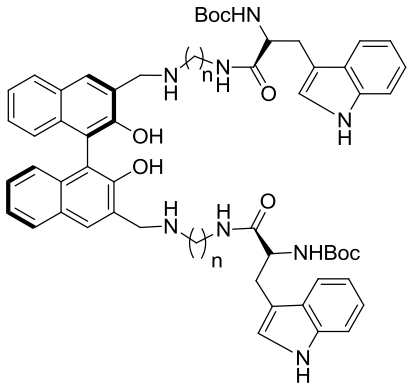

23a, n=2
23b, n=3

Two new binaphthyl derivatives **24** and **25** bearing two imidazolium, or bisurea groups were investigated as fluorescent chemosensors for the chiral anion recognition by Swamy et. al.[42] The association constants of host **24** with (*S*)-2-phenylbutyrate and (*R*)-2-phenylbutyrate in DMSO were calculated as 1570 and 340 M^{-1}, respectively. The chiral selectivity of host **24** (K_S/K_R) was found to be ~4.6. On the other hand, the open form host **25** displayed a mixed stoichiometry of 1:1, 1:2 and 1:3 with (*S*)-2-phenylbutyrate and (*R*)-2-phenylbutyrate in acetonitrile. A slight selectivity for (*S*)-2-phenylbutyrate was also observed by host **25**.

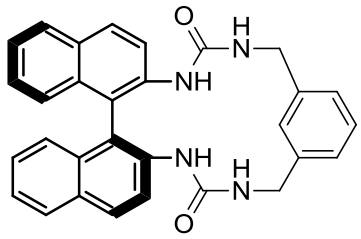

24

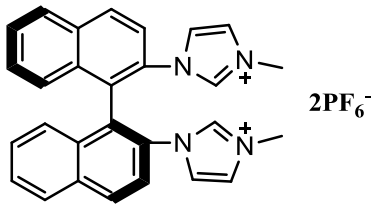

25

1.2.2 Other chiral host systems

James et al. reported chiral fluorescent boronic acid **26** which was found to be a highly enantioselective, chemoselective, and sensitive sensor for sugar acids.[43] At pH 7.0, the binding constants of *R,R*-**26** with the D- and L-tartaric acid were logK_D= 4.79 and logK_L= 2.07, and the binding constants of *S,S*-**26** with the D- and L-tartaric acid were log K_D= 2.09 and log K_L= 4.81. Hence, for this system, the enantioselectivity (K_D:K_L) is 490:1 for D-tartaric acid and 1:550 for L-tartaric acid. No enantioselective discrimination between D- and L-tartaric acid was observed

when the monoboronic acid sensors *R*-**27** and *S*-**27** were used instead of the diboronic acid sensors *R,R*-**26** and *S,S*-**26**. This result indicates that for enantioselective discrimination, 1:1 cyclic complexes must be formed between *R,R*-**26** and *S,S*-**26** and the sugar acids.

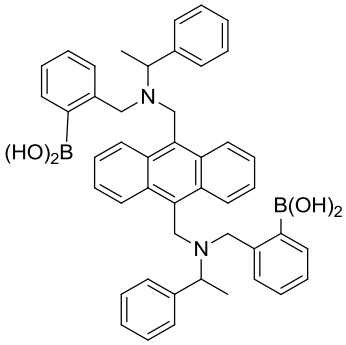

26

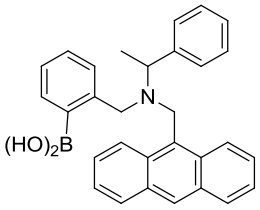

27

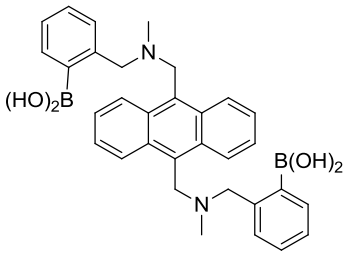

28

Kilburn et al. reported macrocyclic host **29** which favored the 1:1 binding of N-protected L-glutamate and aspartate, but favors 1:2 binding of the corresponding D-amino acids in polar solvents [44] (dimethyl sulfoxide and acetonitrile). The host gave 1:1 association constants ($K_a^{1:1}$) of 10,000 and 3,100 for N-Ac-L-Glu and N-Ac-D-Glu, respectively. On the other hand 1:2 (host:guest) binding constants ($K_a^{1:2}$) were observed to be 1,200 and 16,000 for L and D enantiomers, respectively. Later, the same group did a computational and experimental analysis of the enantioselective potential of a new macrocyclic receptor for N-protected α-amino acids.[45] This host represented the monomer analogue of receptor **29** and, thus, had the same structural characteristics, but a smaller cavity and reduced degrees of freedom, and was designed as a potential receptor for mono- rather than dicarboxylates. They observed a very modest enantioselectivity for N-Ac-L-phenylalanine ($K_a^{L/D}$= 1.6) by the host **30**. This could be due to the very small size of the cavity of the host molecule to accommodate the guest.

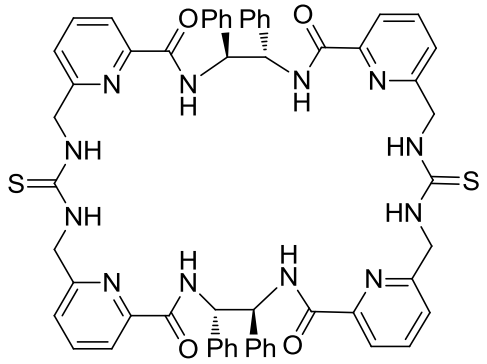

29

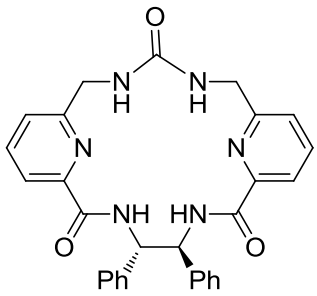

30

Caballero et al. reported a macrocyclic receptor based on a bis-chromenylurea and an α, α‘-(o,o’-dialkyl)diphenyl-p-xylylenediamine spacer which provided a C_2 chiral cavity to associate carboxylates by H-bonds.[46] The extent of the selectivity obtained for the racemic receptor **32** and enantiomerically pure (S)-naproxen was 7.2:1. Steric repulsions close to the cavity were decisive for the chiral selectivity.

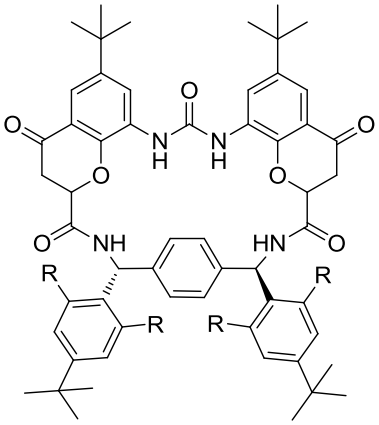

31, R=H
32, R=Me

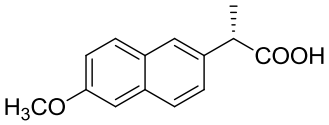

***S*-Naproxen**

Two anthracene thiourea derivatives, **33** and **34**, were investigated as fluorescent chemosensors for the chiral recognition of the two enantiomers of α-amino carboxylates by Hyun et al.[47] Especially, host **34** displayed K_L/K_D values as high as 10.4 with ^{t}Boc alanine. Furthermore, the D/L selectivity of hosts **33** and **34** was opposite, even though both hosts bear the same glucopyranosyl units. These intriguing opposite D/L binding affinities by **33** and **34** were obtained without/with hydrogen interaction between the anthrancene moiety and the methyl groups of the alanine moity, which were explained by extensive high-level theoretical calculations.

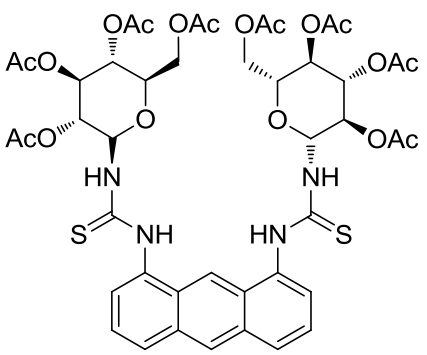

33

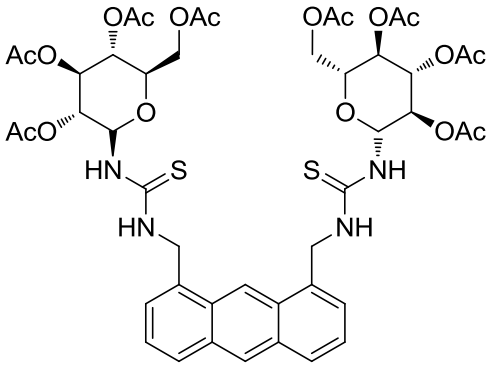

34

Two chiral fluorescent chemosensors **35** and **36** were synthesized by Hu et al.[48] Their recognition ability was studied in aqueous solution (Tris–HCl buffer pH 7.4, MeOH/H_2O = 1:1) through fluorescence spectra. The host **35-Cu^{2+}** complex showed a chiral recognition ability to mandelate anions with a preferable binding to L-mandelate than D-mandelate anions. The binding constant for L-mandelate was 576 M^{-1}, whereas that for D-mandelate was only 38 M^{-1}, which could be distinguished by the different change of fluorescence intensity.

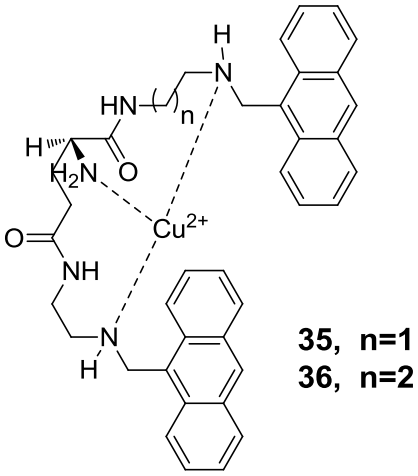

35, n=1
36, n=2

A neutral urea incorporated anion receptor **38** with a tripodal pseudocavity was synthesized by Vittal and coworkers.[50] The influence of preorganization and rigidity of the receptors towards anion recognition was evaluated using rigid (**38**) and flexible (**39**) receptors. Binding affinities were investigated using ^{1}H NMR and luminescence titration methods. Receptor **38** (K_{mes}= 20,800 M^{-1}, K_{phtha}= 22,600 M^{-1}) showed marginally higher binding affinities with 1:1 stoichiometry for carboxylate anions terephthalate and trimesylate in polar solvents in comparison to the receptor **39** (K_{mes}= 16,000 M^{-1}, K_{phtha}= 13,000 M^{-1}). The binding affinities are

marginally different from each other, but it gives a basic idea for the future design of the host molecules for carboxylate anions.

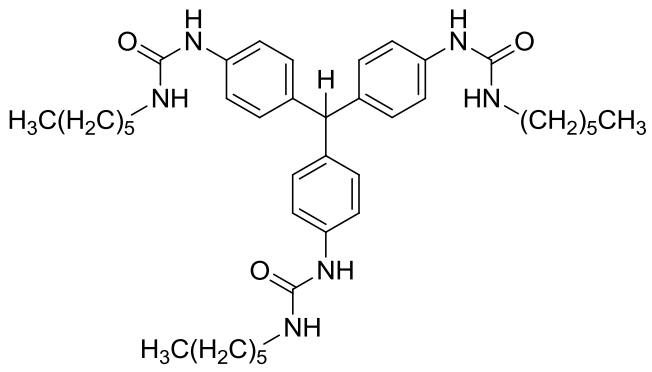

38

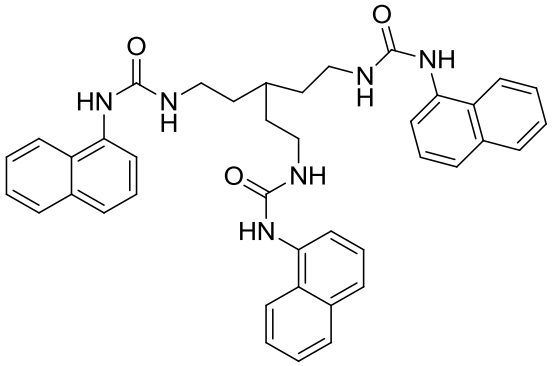

39

Steed et al. reported a chiral, tripodal anion hosts **40** derived from either *S*-phenylalanine or *S*-leucine which bound D-lactate enantioselectively.[51] The nature of the host–guest interaction was probed by solution NMR methods and by DFT calculations. The calculations suggested that the D-lactate may form an additional hydrogen bond in the host–guest complex while the L-lactate complex contains an intramolecular hydrogen bond. Both hosts provided selectivity by a factor of 3-6 in the binding constant for D-lactate. While not yet of the kind of selectivity required for resolution of chiral materials in a single step, this augurs well for future refinement of the design.

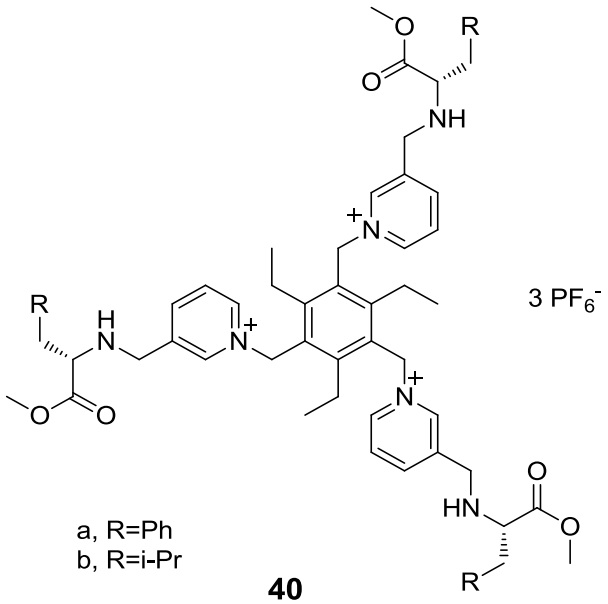

40

Wen-Yih Chen et al. did a comparative study of the DNA aptamer binding with L-argininamide (L-Arm) and its enantiomer (D-Arm) by spectroscopic and calorimetric methods.[52] An ITC study

revealed that both L-Arm and D-Arm binding with the aptamer were enthalpy driven and entropy cost processes. They did a comparative study of the DNA aptamer binding with L-argininamide (L-Arm) and its enantiomer (D-Arm) by spectroscopic and calorimetric methods. The ITC titrations derived K_d values are K_d(L-Arm) = 224.2 μM, and K_d(D-Arm) = 212.8 μM. Though, there was an insignificant enantio-recognition of the argininamide isomers, it was noted from the opposite behavior of the heat capacity change of the two enantiomers that L-Arm and D-Arm bind at different binding sites of the aptamer, resulting in different conformations of the binding complexes. Two kinds of novel chiral molecular tweezers containing imidazoliums were synthesized from L-alanine, L-phenylalanine, and L-glutamic acid by Rugang Xie et al.[53] The enantioselective recognition of L- and D-amino acid derivatives by these molecular tweezers was investigated by UV spectroscopic titration experiments and good enantioselectivities were obtained, which were highly sensitive to whether the spacer has the binding site and the pincers has the other aromatic rings besides imidazolium ring. The host molecule **42b** showed remarkable enantioselectivity for N-Boc protected histidine methyl ester, affording K_L/K_D of 5.10 in acetonitrile. **41b** showed an enantioselectivity of K_L/K_D= 4.07 for the same guest molecule.

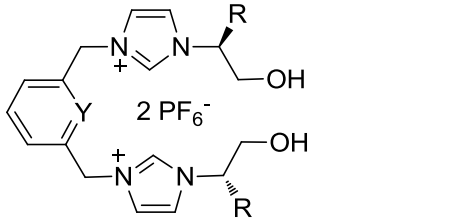

41 a-c, Y=CH **42** a-c, Y=N

a. R=CH_3 b. R=CH_2Ph c. R= $CH_2CH_2CH_2OH$

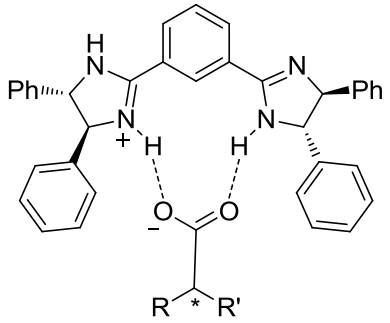

43

A bisimidazoline compound **43** was prepared by Kihang Choi as a new chiral solvating agent starting from isophthalaldehyde and (S,S)-1,2-diphenylethylenediamine.[54] In the presence of one equivalent of this reagent, carboxylic acid racemates show ^{1}H NMR chemical shift non-equivalences large enough for the discrimination of the enantiomers. In the presence of the chiral solvating agent, the α-hydrogens of the carboxylic acids (2-methyl butyric acid, methyl and bromo benzoic acid) racemates showed chemical shift non-equivalance up to ΔΔδ= 0.38. The chiral chemosensor **44**, based on a thiourea-activated phthalimide, was prepared by Griesbeck et.

al.[55] Moderate chiral recognition was observed for sodium D/L-lactate with $K_{ass}(D)/K_{ass}(L)$ = 1.93. The absorption spectra of sensor **44** in the presence of D- and L-lactate did not show significant changes. Only a weak increase of the absorption band at 373 nm was observed for L-lactate. This can be interpreted again as complex formation in the ground state. The analogous behaviour was obtained for D-lactate.

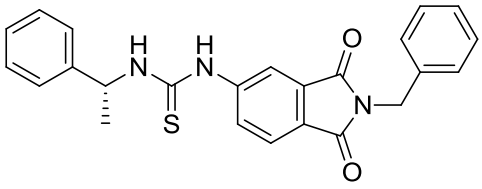

44

1.3 Equilibrium Ring Closing Metathesis (ERCM)

Ring-closing metathesis (RCM) of dienes is one of the most important methodologies now in use for the assembly of cyclic organic compounds. First employed by Villemin and by Tsuji nearly three decades ago,[56] the reaction has risen to astonishing prominence in organic synthesis over the past decade, owing largely to the development of easily handled catalysts that enable controlled reaction.[57] RCM represents a key step in many synthetic sequences: While the common rings of 5−7 members have historically been dominant, owing in part to their greater ease of access, important advances have been made in the synthesis of medium[58] and macrocyclic[59] targets. In the present work, open chain hosts were synthesized with the side arms possessing terminal double bonds and the RCM reaction was employed in order to form C-C bond between the terminal alkene groups to achieve cyclized hosts. It would be useful to understand the factors affecting the RCM reactions and the other processes which compete simultaneously with it.

Figure 1.3.1. Olefin metathesis catalysts cited in the following sections

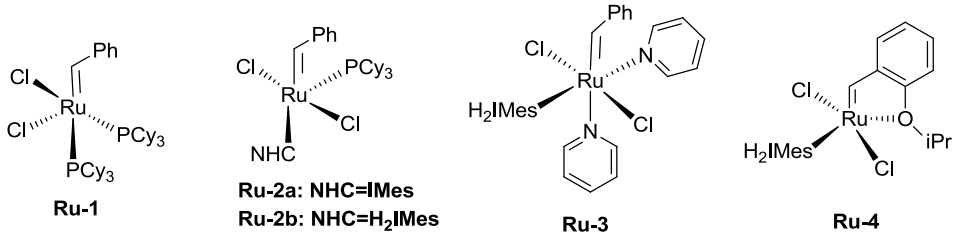

As with any other cyclization method, the synthetic efficiency of RCM is limited by the competition between intramolecular ring-closing and intermolecular oligomerization reactions.

In the standard depiction of figure (figure 1.3.2), olefin metathesis is represented as a fully reversible set of [2 + 2] cycloaddition−cycloreversion equilibria, implying a thermodynamic distribution of "living" metathesis products[60]. The extent of reversibility in the various reaction manifolds in fact varies considerably, depending on the nature of the substrate and the extruded olefin, the competence of the catalyst, and the experimental conditions.

Figure 1.3.2. Conventional representation of olefin metathesis pathways involving irreversible loss of ethylene.

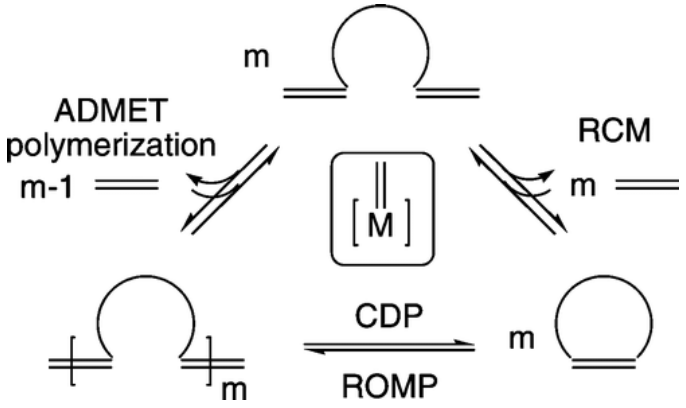

In ring opening metathesis polymerization (ROMP) applications, polymerization is typically driven by release of ring strain. Initiation of highly strained monomers is irreversible, though backbiting to form cyclic oligomers can occur. In RCM, no such enthalpic driver exists, barring strategies in which two reactions are coupled (e.g., ROM−RCM processes). RCM is thus entropy-driven, and the enthalpic costs that can be sustained are limited by the extent to which (in Gibbs−Helmholtz terms) the TΔS term can be maximized. The entropic benefit associated with release and volatilization of ethylene on metathesis of vinylic α,ω-dienes is powerful, but indiscriminate, driving both inter- and intramolecular reactions. There are different factors which affect equilibrium ring closing metathesis reaction. Over the years, scientists have tried different strategies to maximize the yield of the cyclic product in an ERCM reaction. A brief description of these factors will be given along with some recent examples in the following section.

1.3.1 Reaction Time:

To maximize yields of ERCM reactions, sufficient time must be allowed for the cyclodepolymerization (CDP) process to occur (presupposing operation in the appropriate concentration regime). The figure shown below (figure 1.3.1.1) depicts a representative plot

showing the evolution of products in an RCM macrolactonization.[61] While involatile oligomers dominated the product mixture at 15 min (ca. 70%), cyclodepolymerization was complete at 1 h using 5 mol % Ru-catalyst, at a maximum diene concentration of 5 mM (CH_2Cl_2, reflux).

Figure 1.3.1.1. Monitoring oligomerization and backbiting as a function of time.

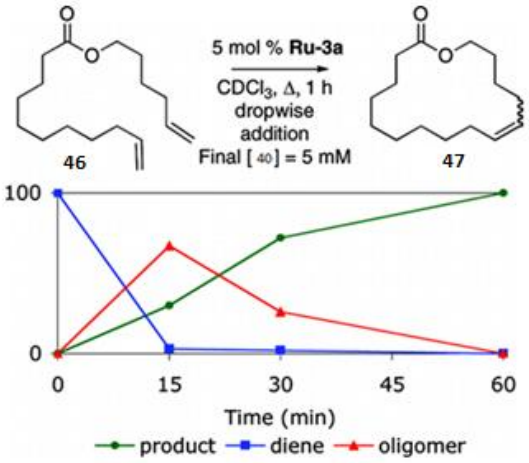

Cyclooligomerization of kinetically favored RCM products can also occur, at appropriate concentrations. During the synthesis of radicicol precursors, for example, Danishefsky and co-workers reported higher yields of the RCM product (**49**) when the reaction with **Ru-2b** was terminated after only 5−10 min. Longer reaction times resulted in formation of cyclic dimers through the ring-opening−ring-closing pathway.[62]

Figure 1.3.1.2.

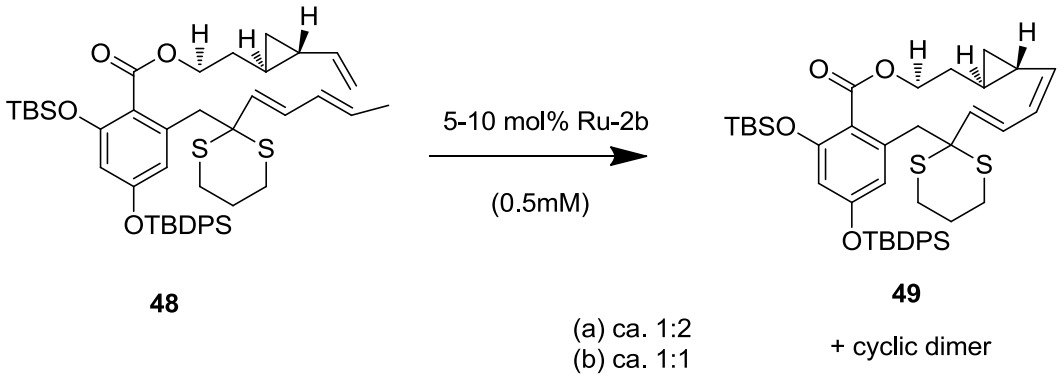

48

49

(a) ca. 1:2
(b) ca. 1:1

+ cyclic dimer

1.3.2 Temperature:

The elevated temperatures commonly employed in RCM (particularly in conjunction with second generation ruthenium catalysts), generally regarded as kinetic requirement, play an

additional thermodynamic role in ERCM. They favor cyclization by further reducing viscosity and maximizing thermal motion. They also serve to reinforce any entropic bias in the TΔS term. Danishefsky and co-workers[62] have commented on the potential to control product distributions in RCM macrocyclization reactions by increasing reaction temperature. In the reaction of figure 1.3.1.2, the relative proportions of the desired RCM product **49** vs the cyclic dimer were found to increase from ca. 1:2 at 40 °C, to 1:1 at 80 °C, at a constant dilution of 0.5 mM **48** in benzene or toluene, respectively. During the synthesis of 14-membered macrolactone **51**, Grubbs and co-workers observed that dimerization competed with RCM at room temperature at diene concentrations as low as 3 mM.[63] RCM of **50a−d** in refluxing CH_2Cl_2 enabled isolation of **51** in >75% yield, however. Reaction of hydroxyl derivative **50e**, in comparison, afforded only 23% **51**, though complete consumption of starting diene was noted. High proportions of oligomers were observed in the latter case, perhaps indicating deactivation of the catalyst by the α,β-unsaturated alcohol before significant cyclodepolymerization (CDP) can occur.

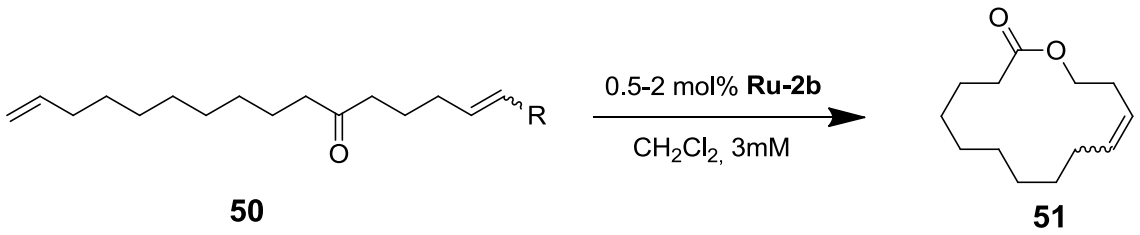

50 **51**

R=(a) H, (b) Et, (c) $(CH_2)_4CH_3$, (d) CH_2OAc, (e) CH_2OH

1.3.3 Concentration:

Concentration is one of the key experimental factors affecting ring−chain (ring−ring) equilibria in olefin metathesis, and one of the major tools available to manipulate product distributions in ERCM. It should be recognized, however, that high dilutions come at a cost. Indeed, from the industrial perspective,[64] high dilutions are not a viable solution to the challenges of ERCM, given the high direct costs of the large volumes of solvent required, and further costs associated with waste disposal, longer reaction times, and the problems of product purification that commonly result from high catalyst loadings. In an elegant exposition of the use of concentration effects to bias selectivity in the construction of topologically complex molecules, Leigh and co-workers described the conversion of cyclic **52** into catenated rings using **Ru-1**.[65] At a concentration of

200 mM, the [2]-catenane was obtained in >95% yield. Lowering the concentration increased the proportion of the noninterlocked, 29-membered macrocycle **53**. Above 200 mM, higher cyclic oligomers could also be detected by analytical HPLC and FAB-MS. The capacity of **Ru-1** to "unlock" the rings in **52** and **53** is noteworthy, given its relative inactivity toward 1,2-disubstituted olefins. The key to successful reaction presumably lies in the prolonged reaction times (up to five days), as well as the large difference in size between **52** and **53**.

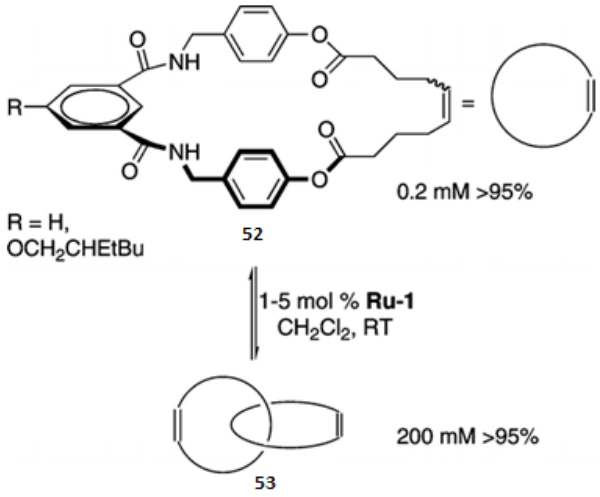

In a rare example of ERCM in formation of five-membered rings, the Grubbs group described a concentration-dependent cyclodimer−"cyclomonomer" equilibrium during RCM of a diene in which one of the olefinic sites was trisubstituted.[66] Using either **Ru-1** or **Mo-2b**, significant amounts of dimer were observed at 100 mM concentrations, but the equilibrium was shifted in favor of the smaller ring at 10 mM.

1.3.4 Addition of a more reactive catalyst:

Where modulation of time, temperature, and concentration fail to induce backbiting of oligomers to enable ERCM, addition of a second, more reactive catalyst can sometimes give access to the desired product. This strategy has been widely used to induce RCM of acyclic head-to-head dimers formed from unsymmetrically deactivated dienes.[67] Low catalyst activity inhibits metathesis at the internal, 1,2-disubstituted olefinic site. Hoveyda and co-workers reported that dimer **54** could not be induced to undergo backbiting with **Ru-5**, for example. In contrast, the Schrock catalyst **Mo-2b** was successful in converting **54** into the desired macrolactam **56**, after pretreatment of the Mo catalyst with ethylene to remove the unwanted alkylidene end group.[67b]

Isolated yields of **56** approached 60−65% over 12 h in benzene at 50 °C at a diene concentration of 10 mM.

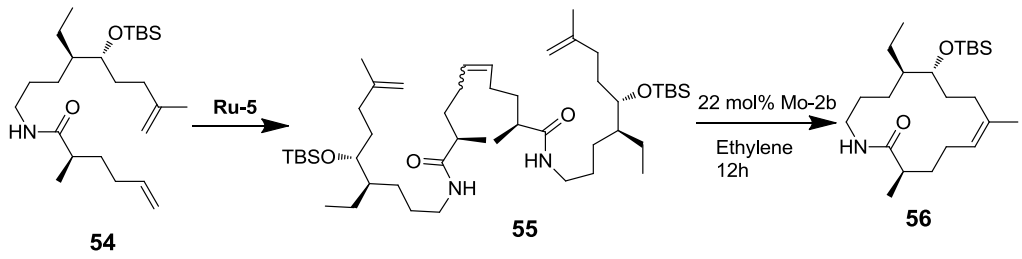

1.3.5 Perturbing Equilibria:

Two distinct strategies have been adopted, which we classify as templating or capping approaches, respectively. Templating agents (whether Lewis acids or bases) are used to bring together dienes separated by two or more donor or acceptor sites: these can act either to amplify a bias in ERCM or to inhibit oligomerization. Capping agents operate only in the latter mode: these are Lewis acids, used in conjunction with substrates containing an appropriately placed donor group, which act to block off one quadrant or hemisphere of the molecule, thus reducing the conformational flexibility of the substrate and hence the entropic penalty associated with cyclization. Examples of both strategies appear in the following sections.

Figure 1.3.5.1. Strategies used to favor RCM. Use of (a) templating agents or (b) bulky Lewis acid capping agents.

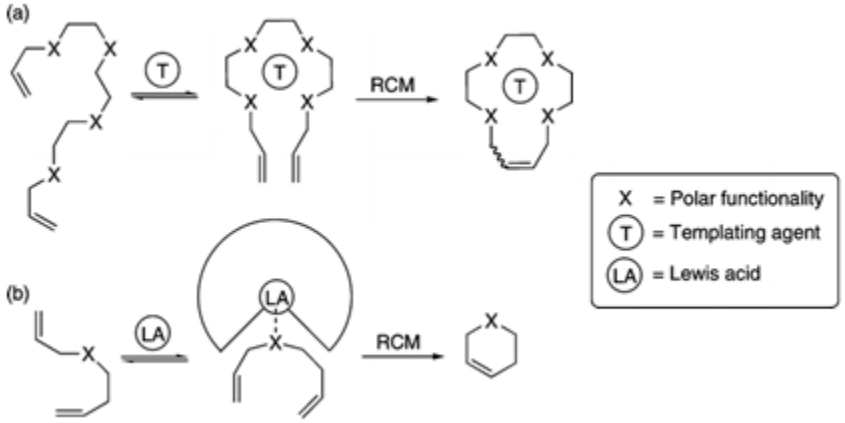

1.3.5.1 Use of Templating Agents:

Binding of the template to the polar site of the substrate increases the probability of intramolecular reaction by bringing the olefinic groups into close proximity. An added advantage can be the selective formation of *z*-olefin geometries.[68] Grubbs and co-workers described the **Ru-**

1-catalyzed synthesis of crown ether analogue **57** via a hydrogen-bonded [2]rotaxane assembly, in which the template is a dumbbell-shaped secondary ammonium ion **58**.[69] The rotaxane was also accessible in 95% yield starting from **57** itself, via a **Ru-2b** catalyzed magic ring synthesis involving ring-opening and ring-closing. In the case of the **Ru-1**-catalyzed reaction, the resistance of **57** to reopening limits the ability of the catalyst to correct the initial product distribution, and the bias exerted by the ammonium template is thus critical. Yields of ca. 70% were obtained at 100 mM, relative to ca. 50% at 5 mM for the untemplated reaction.[69]

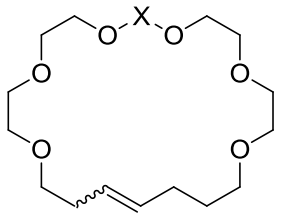

X=$(CH_2)_2$, 1,2-C_6H_4

57

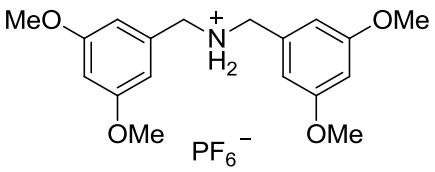

58

In another example demonstrating the synergy between equilibrium RCM and templating strategies, Sanders and co-workers described satisfactory yields of macrocycle **59** only in the presence of template **60**.[70] When a 10 mM mixture of diene and **60** (2:1 molar ratio) was reacted with **Ru-1** at room temperature for 3 days, catanene **59** was obtained in 50% yield. As evidence of the equilibrium pathway, these workers cited the near-identical yields of **59** obtained following deliberate oligomerization of the diene in the absence of **60**, followed by addition of the template and fresh **Ru-1**.

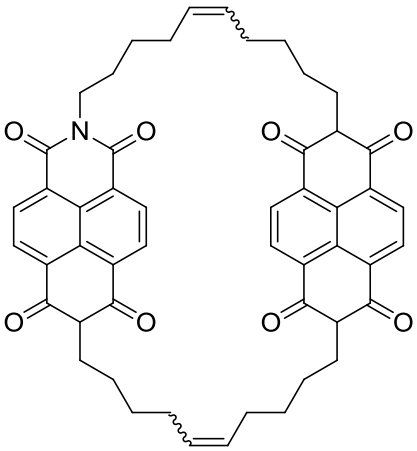

59

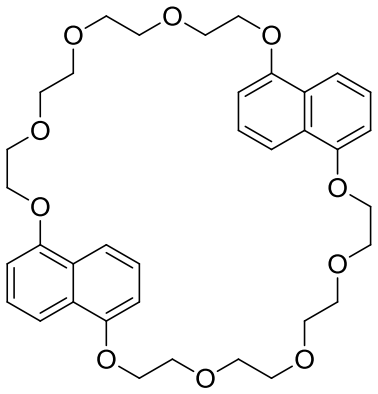

60

1.3.5.2 Perturbing Equilibria by reducing conformational Motion:

Most commonly used additive, $Ti(O^iPr)_{4,}$ was first shown by Fürstner and co-workers to facilitate formation of macrocyclic targets en route to (−)-gloeosporone.[71] The possibility of using Lewis acids to facilitate RCM by blocking the conformational mobility of the substrate is a strategy of more recent interest. The Percy group showed that $Ti(O^iPr)_4$ was effective in promoting RCM of a variety of eight-membered rings by **Ru-2b**, and they pointed out that use of the Lewis acid completely suppressed formation of oligomers.[72] The effective molarity (EM) of substrate **57** in the presence of 30 mol % $Ti(O^iPr)_4$ increased by 5-fold, as judged by ^{19}F and ^1H NMR analysis.

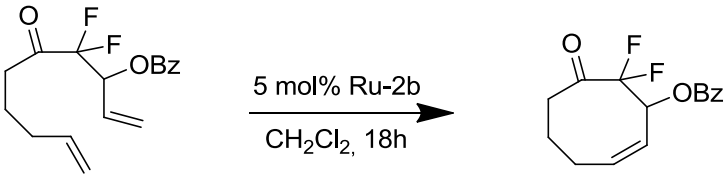

61 **62**

additive	EM (M)	
$Ti(O\text{-}^iPr)_4$	0.24	$EM= k_{intra}/k_{inter}$
none	0.48	

A related recent example from Nguyen and co-workers described the use of the bulky Lewis acid aluminum tris(2,6-diphenylphenoxide) (ATPH; **66**) to promote RCM of seven-membered prolactones such as **63**.[73] Formation of such essentially unsubstituted rings in high yields is particularly challenging, owing to the bias toward formation of the lower-strain cyclic dimers. In contrast to the Percy findings with **61**, RCM of **63** (20 mM, refluxing CH_2Cl_2, 10 mol % **Ru-2b**) resulted in sole formation of cyclodimer **65** in the presence of 1.05 equiv of $Ti(O^iPr)_4$. Use of **66**, in contrast, enabled formation of seven-membered **64** in 87% yield, under otherwise identical conditions.

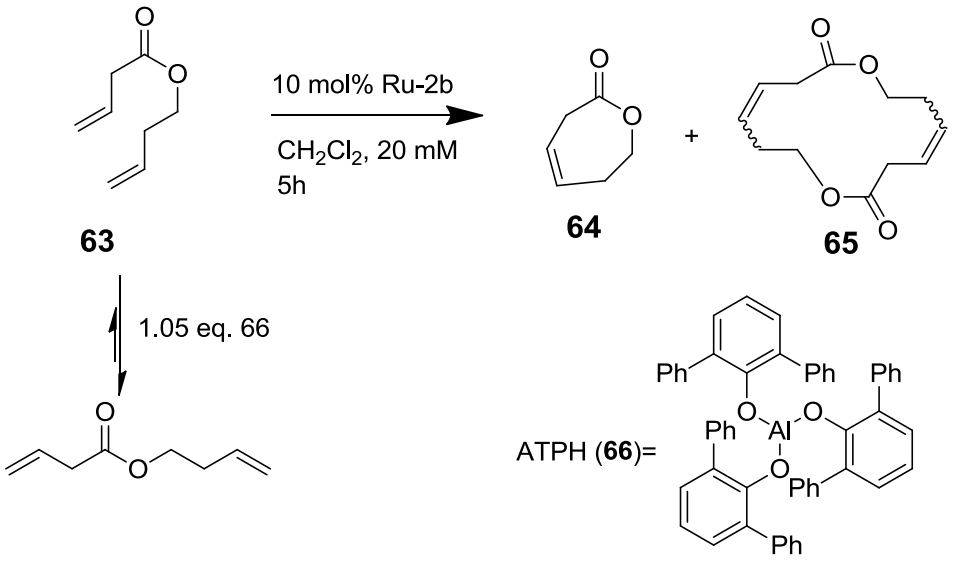

1.3.6 Microwave Assisted Ring Closing Metathesis:

In recent years, microwave (μW) irradiation has been proposed as a complementary activation mode for olefin metathesis. In many cases it has resulted in a dramatic shortening of reaction times and more importantly has allowed otherwise unproductive metathesis reactions. The first report on μW-assisted olefin metathesis appeared in 2000 and the method has gained increasing popularity since then.[74] Kiddle and co-workers reported a series of comparative RCM reactions for the formation of five-membered rings under thermal and μW conditions.[75] They studied the reaction in both the ionic liquid (1-Butyl-3-methylimidazolium (bmim)) BF_4 and in dichloromethane. Ionic liquids are indeed excellent solvents (or additives, see below) for μW-assisted chemistry as they couple with microwaves through a dielectric heating mechanism. A spectacular accelerating effect was observed under μW conditions with both solvents. From this study the authors concluded that the μW energy produces non-thermal effects that may involve direct coupling to one of the two or both reactants in this transformation.

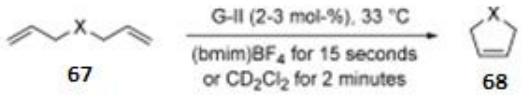

	Substrate	μW conditions (110 W)	thermal conditions
bmim	X = $C(CO_2Et)_2$	100%	3%
	X = N-Ts	100%	0%
CD_2Cl_2	X = $C(CO_2Et)_2$	100%	21%
	X = N-Ts	91%	45%

The domino RCM reaction (internal alkyne–olefin RCM, then bis-olefin RCM) of the Schiff base (shown below) could not be performed efficiently with the G-I catalyst and required 30 mol-% of the G-II catalyst added in three portions over 6 hours to go to completion under classical thermal conditions (toluene, 85 °C). These results were attributed to the fact that a relatively high temperature was used for several hours causing a gradual decomposition of the catalyst. This problem has been overcome by exposure of the reaction mixture to μW heating at a high temperature (160 °C) for a short time.[76] The authors argued that μW energy leads to extremely rapid heating by direct transfer of heat into the reaction medium in contrast to conventional heating in which the energy is transferred via the vessel wall. A thermally unstable catalyst may be expected to deteriorate more rapidly next to the hot vessel walls under conventional reaction conditions than in the uniformly heated interior of the μW-irradiated solution.

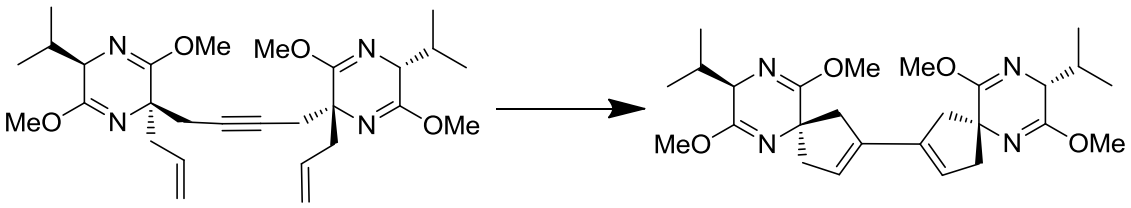

69 **70**

Thermal conditions: G-I (2x10 mol%), toluene, 85°C 2x5h, conversion a few %

MW conditions: G-I (14 mol%), toluene, 160 °C, 45 min, conversion 75%

Thermal conditions: G-II (3x10 mol%), toluene, 85 °C, 3x3h, conversion 92%

MW conditions: G-II (5 mol%), toluene, 160 °C, 10 min, conversion 100%

2. Aim of the work

Biological molecules have been the key motivation over decades behind the artificial supramolecular host or guest designs. In biological systems such as enzymes and antibodies, guanidinium groups present in the amino acid arginine forms strong non-covalent interactions with anionic groups like carboxylates, phosphates, sulphates and nitrates through hydrogen bonding and electrostatic interactions. They are also responsible for stabilization of protein tertiary structures via internal salt bridges mainly with carboxylates.[11] Owing to the significance of guanidinium functionality in biological systems, it is evident to find them in many drug substances as well as a binding motif in molecular recognition studies involving artificial receptors.[5]

Figure 1: Sketch of bicyclic guanidinium motif interacting with an oxoanion.

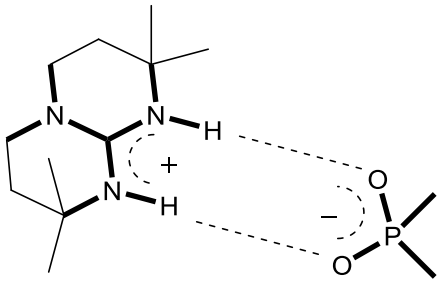

Bicyclic guanidines are different from their acyclic counterparts in physical, chemical and electronic properties. Here the hydrogen bond donors are properly aligned to interact with oxygen atoms from the carboxylates or phosphates and the guanidinium cation complements through electrostatic interactions with the anion (figure 1). The use of chiral bicyclic framework in anionic hosts can help in reducing the variety of binding modes possible with the oxoanionic guest and can act as a chiral binding motif for various chiral oxoanions. Substitution of this inbuilt chiral bicyclic guandine with various side chains can lead to the formation of chiral open chain hosts, as evident from the examples reported in the previous chapter. Further, conformationally more rigid macrocyclic hosts can be obtained by performing cyclization reactions (eg. ring closing metathesis) or by using spacer functional groups.

The present work is aimed at the elucidation of the energetics of:

a) enantiorecognition of carboxylate anions by guanidinium hosts.

b) the extent of structural rigidity that can make a difference in chiral recognition.

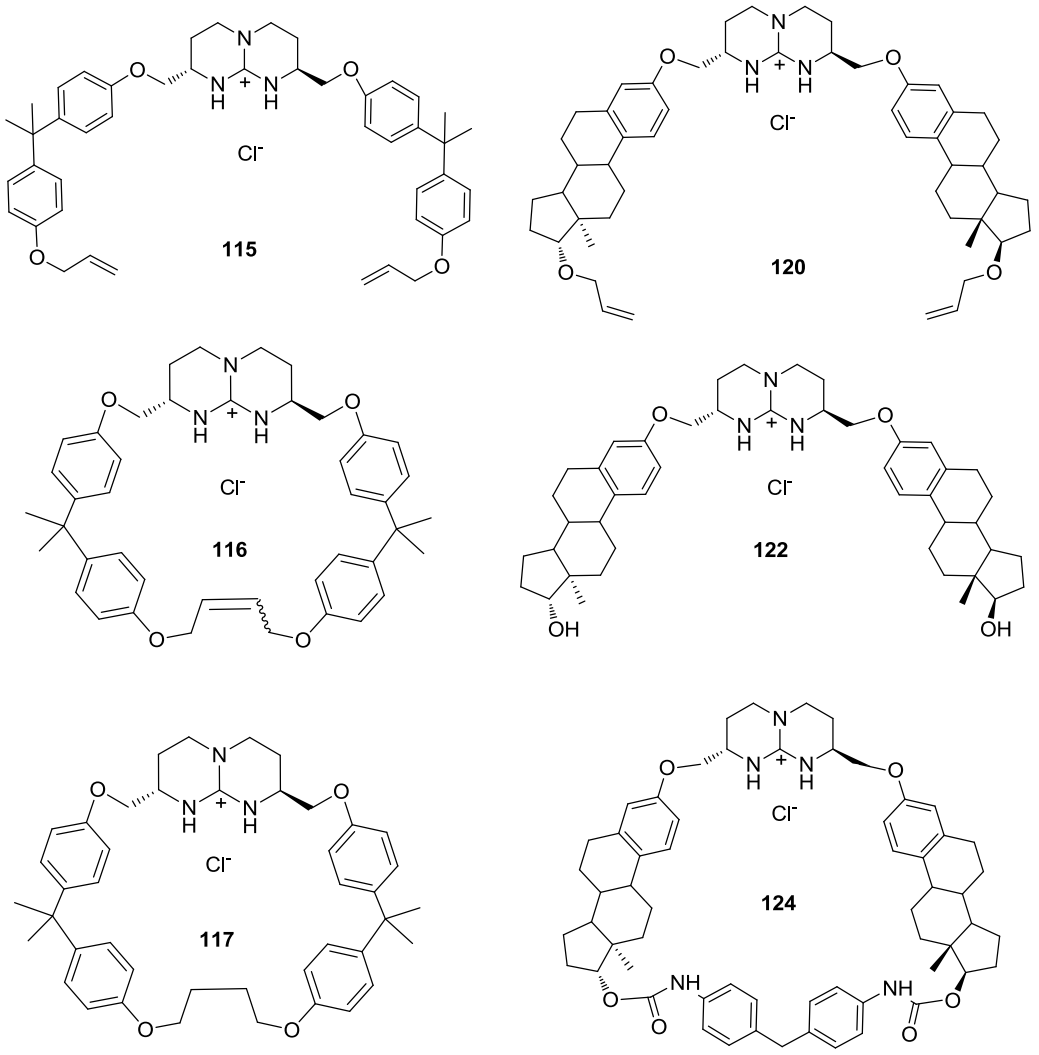

Chirally active guanidinium compounds were designed as target host molecules (**115, 116, 117, 120, 122** and **124**). In host **115**, guanidinium unit was substituted by mono allylated bis phenol A side arms. Host **115** had conformationally free side arms with unrestricted spatial movement. That does not help much in terms of having unique geometrical interaction between the host and the guest. It was desirable to obtain a cyclic derivative of **115** to analyse the effects of conformational restriction on the enantiorecognition potential of the guandinium hosts. Host **115** was designed such that it had terminal double bonds on the side chains which were later utilized for ring closing metathesis reaction to obtain the cyclized host **116**. Host **116** was reduced to obtain host **117** which has a less rigid cyclic framework than **116** but is still more rigid than host **115**. These cyclic structures, having confined number of degrees of conformational freedom,

could be exploited to get better enantiorecognition. Hosts **120** and **122** had more rigid steroid units as the side chains. In addition to the guanidine chiral centers, the steroid chain contains optically active centres which might add to the enantiospecific interaction and could be beneficial in enantiomeric recognition. Though, the side arms of host **120** and **122** are more rigid than the previous bisphenol host **115**, yet they are attached to the bicyclic guanidinium unit by a single bond which makes them again freely mobile in space. So, the macrocyclic host **124** was synthesized from **122** by the addition of bis(4-isocyanatophenyl) methane as linker group between two terminal hydroxyl functions.

3. Synthesis

3.1 Synthesis of the macrocyclic bisphenol guanidinium host 116

The synthetic strategy for the preparation of the macrocylic guanidinium host **116** is depicted in the scheme 3.1.1.

Scheme 3.1.1: Scheme of the synthetic strategy for the preparation of guanidinium macrocyclic hosts **116** and **117**

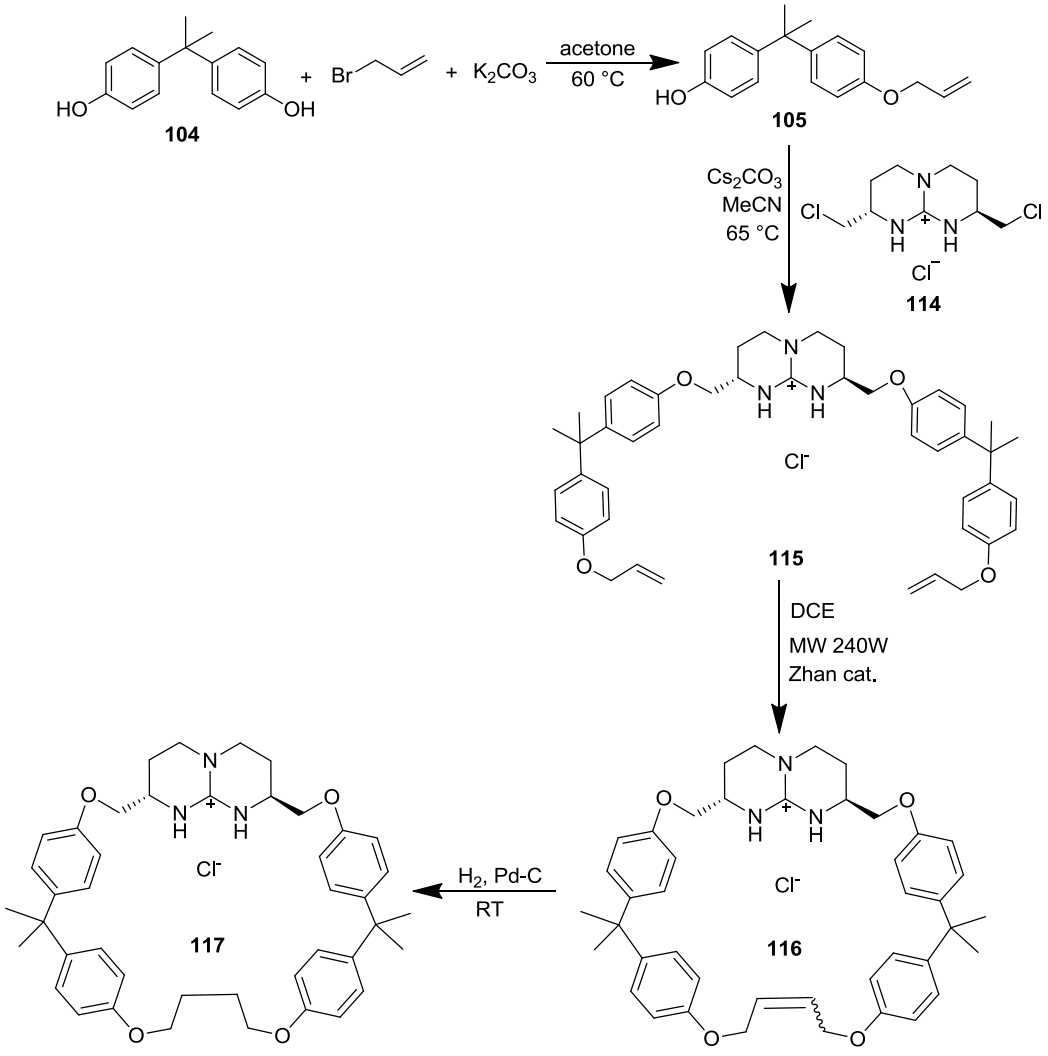

It was conceived that the preparation of the host **116** would start off with selective allylation of the commercially available bisphenol-A compound to introduce terminal double bonds in the open-chain host **115** to facilitate ring closing metathesis. A substitution reaction would be carried out between **105** and **114** under basic conditions to obtain the bis-substituted guanidinium

compound **115**. Subsequently, ring closing metathesis would be carried out on compound **115** to arrive at the macrocyclic host **116**. It was decided later on to hydrogenate the host **116** to the less rigid host molecule **117** in order to study the effects of structural rigidity of host molecules in enantiomeric recognition of chiral anions by comparison of the hosts **115**, **116** and **117** binding with different chiral oxoanions. Selective allylation of 4, 4'-methylenediphenol **101** was tried with different reagents under different reaction conditions (Scheme 3.1.2). The results are summarized in the table 3.1.1. No reaction was observed with sodium hydroxide on refluxing in benzene. Using sodium hydride in dimethylformamide at room temperature showed complete conversion of the starting compound, but did not result in good yields of the desired mono allylated compound **102**. Fortunately, employment of sodium carbonate as base at reflux temperature in water/toluene resulted in 70% conversion of starting material giving 100% yield of desired mono allylated product.

Scheme 3.1.2: Allylation of 4, 4'-methylenediphenol **101**

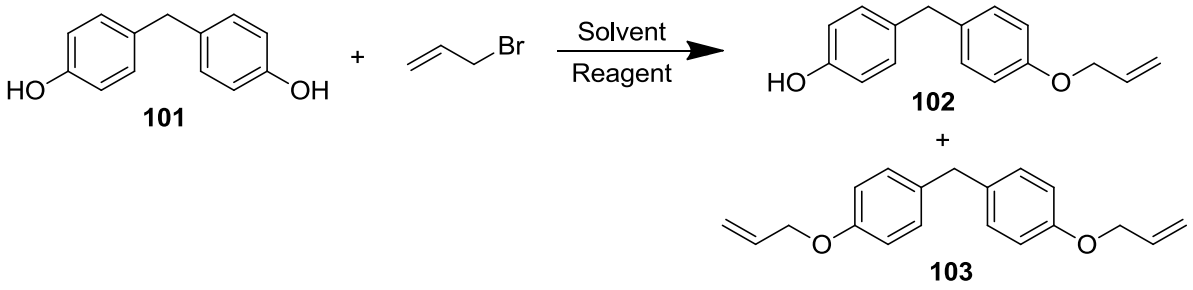

Table 3.1.1: Reaction between 4, 4'-methylenediphenol **101** and allyl bromide

entry	**solvent**	**Reagent**	**temperature/ time**	**conversion**	**mono product 102**	**bis product 103**
1	benzene	NaOH	reflux/ 2.5 hrs	no reaction	-	-
2	water/ether	Na_2CO_3	RT/ overnight	10%	100	-
3	DMF	NaH	RT/ 2.5 hrs	100%	40%	10%
4	water/toluene	Na_2CO_3	100 °C/ 4 hrs	70%	100%	-

Later on, the starting material was switched to bisphenol A **104** which was thought to be serving the purpose well and is commercially available (Scheme 3.1.3). Phenols are examples of bidentate nucleophiles, meaning that they can react at two positions: on the aromatic ring giving an aryl ketone via C-acylation, a Friedel-Crafts reaction or, on the phenolic oxygen giving an ester via O-acylation, an esterification. The product of C-acylation is more stable and predominates under conditions of thermodynamic control. On the other hand, the product of O-acylation forms faster and predominates under conditions of kinetic control. O-acylation can be promoted by either: acid catalysis via protonation of the acylating agent, increasing its electrophilicity or base catalysis via deprotonation of the phenol, increasing its nucleophilicity. Allylation of bisphenol A occurs via nucleophile formation at phenolic –OH. Selective allylation of bisphenol A **104** was carried out in a heterogeneous system consisting of potassium carbonate as the base in acetone. Refluxing under nitrogen atmosphere resulted in complete conversion of starting compound into a mixture of mono substituted **105** (60% yield) and bis substituted **106** (40% yield) allyl ether compounds. The pure mono allylated compound **105** was isolated as a gummy liquid by silica flash chromatography in petroleum ether and ethyl acetate (9:1) as eluent.

Scheme 3.1.3: Allylation of bisphenol A **104**

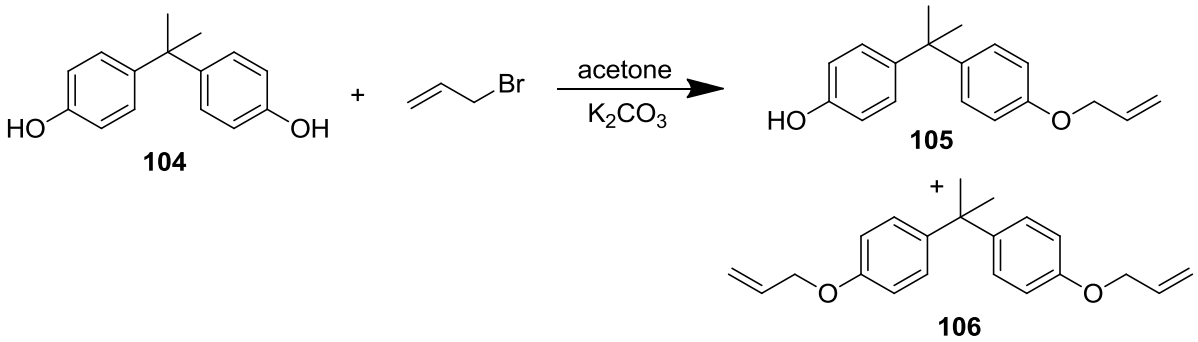

In parallel the preparation of the guanidinium building block was also attempted following the previously reported method [77] using L-methionine as the starting material (Scheme 3.1.4). In this synthesis, the guanidinium target compound **111** is constructed by virtue of an intramolecular two-step, one-pot, double-cyclization process of a linear, yet branched, guanidinium precursor. Coupling of **107** and **108** in presence of trifluoroacetic acid gives **109** in 70% yields. Thereafter, the bissulfonium compound **110** was obtained in quantitative yield by stirring the guanidinium

compound **109** in neat methyl iodide at room temperature overnight. To afford the final bicyclization step bis-sulfonium compound **110** was treated with 1,8-diazabicyclo(5,4)undec-7-en (DBU). This treatment expectedly resulted also in the formation of the undesired regioisomer **112** along with the desired target compound **111** in the ratio of (**111**/**112**) 60:40, respectively. Attempts to improve this ratio in favour of the desired product **111** were not successful. Finally, another method[78] which has already been reported, starting with L-asparagine, was adapted. The bicyclic guanidinium bishydroxy compound **113** was synthesized by previously reported method starting from L-methionine.[25] The conversion of **113** to the respective bischloride compound was carried out in neat thionyl chloride at 80 °C to give **114** in quantitative yield.

Scheme 3.1.4: Scheme of the synthesis of the bicyclic guanidinium building block

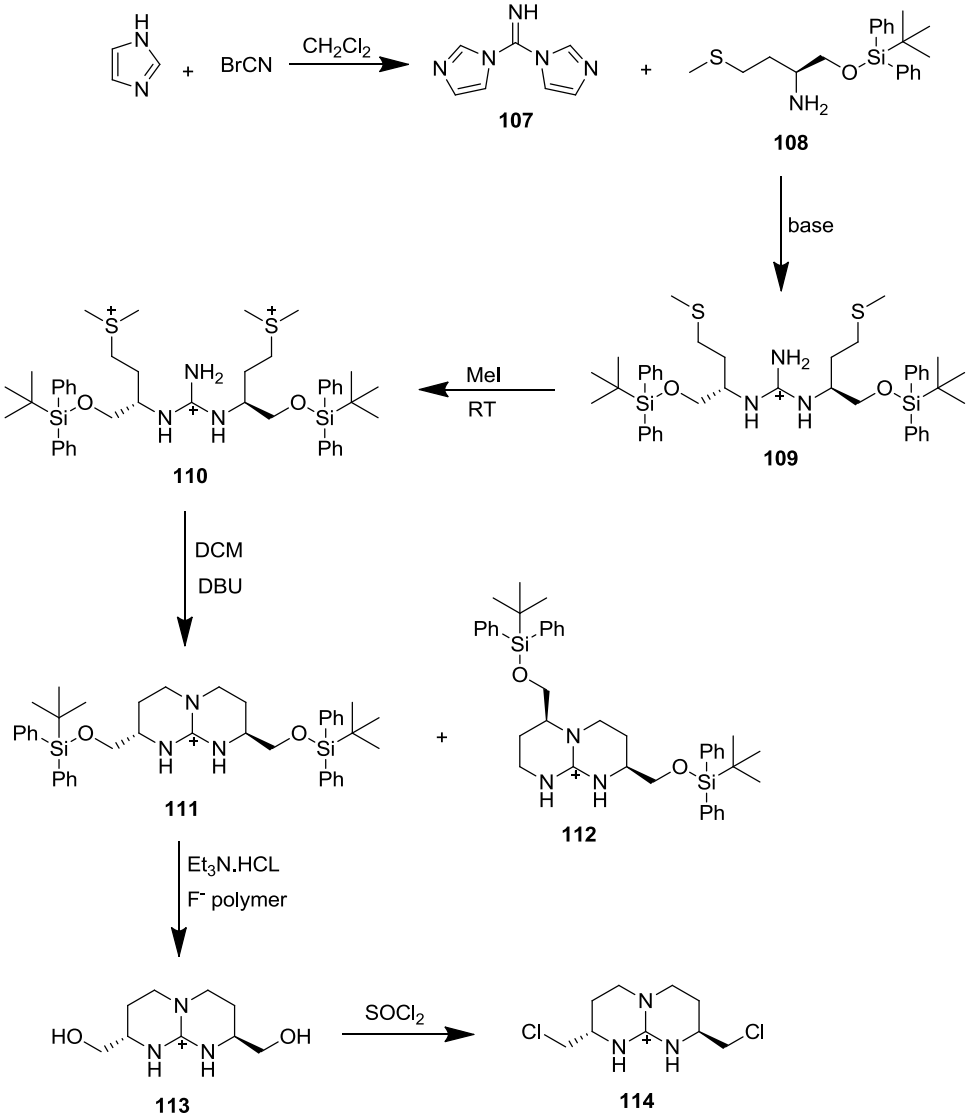

The nucleophilic substitution reaction on **114** by **105** was tried in different solvents and at different temperatures (Scheme 3.1.5, Table 3.1.2). The reaction in acetonitrile at 60 °C under basic condition gave almost 80% yield of the desired product **115**. At higher temperature (>80 °C), a by-product was also formed along with the formation of **115**. P1-^{t}Bu phosphazene base and cesium carbonate were used as alternative bases. Almost the same yield of the bis substituted compound was observed with both bases, though the reaction in presence of cesium carbonate took 4 hours for completion while P1-^{t}Bu base took almost 20 hours for complete conversion of guanidinium compound **114** into the final product.

Scheme 3.1.5: Substitution reaction between **105** and **114** to form host **115**

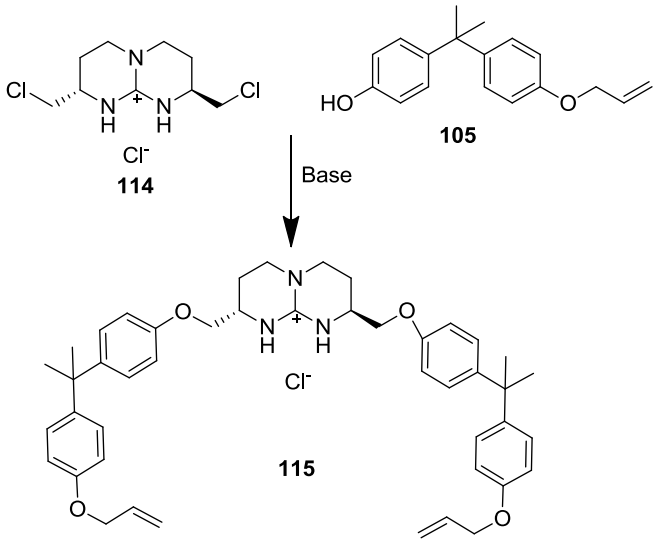

Compound **115** possesses flexible side chains which are free to move in the space. Thus the number of degrees of freedom of the host **115** is quite high. As a result, it lacks any conformational rigidity. It was also reflected in the ITC titrations performed on **115** with different chiral oxoanion guests. ITC titrations indicated that there was no significant enantiomeric preference shown by host **115**, so introducing more structural rigidity into the host molecule might be a profitable route for better enantiorecognition towards chiral anions. Molecular dynamics calculations were also performed on **115** and the macrocyclic compound **116** which was designed to spatially confine the number of degrees of freedom in the structure of molecule **115** (Sceheme 3.1.6) and the analysis of the MD simulation results indicated improved structural uniqueness in **116** in comparison to **115**.

Table 3.1.2: The catalogue of reaction conditions used to synthesize host **115** from the reaction between **105** and **114**.

entry	solvent	base	temperature	yield %
1	CH_3CN	P1-^{t}Bu	60 °C	80
2	CH_2Cl_2	P1-^{t}Bu	45 °C	20
3	DMF	P1-^{t}Bu	90 °C	30
4	DMF	Cs_2CO_3	100 °C	60
5	CH_3CN	Cs_2CO_3	65 °C	80
6	THF	Cs_2CO_3	65 °C	85

Scheme 3.1.6: Ring closing metathesis reaction to synthesize macrocyclic host **116** from acyclic **115**

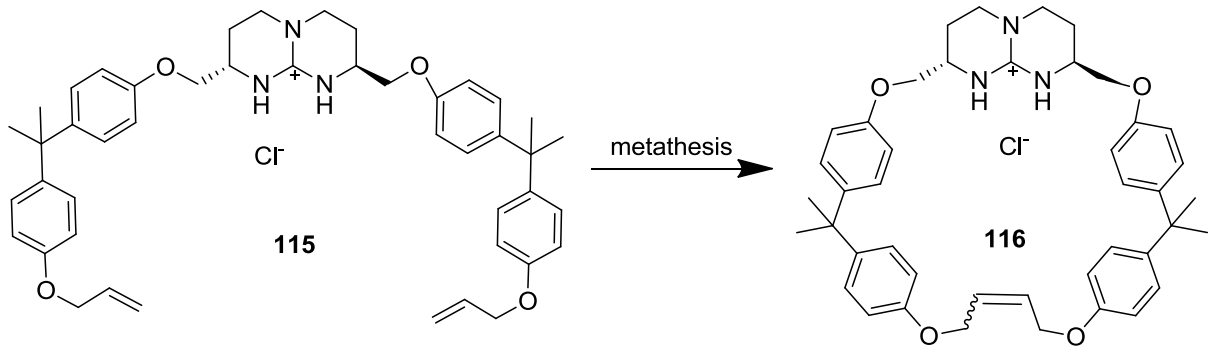

Two approaches were tried for the synthesis of macrocyclic compound **116**. In the first approach, homo cross metathesis of **105** was carried out with Grubbs first generation catalyst G(I) and then substitution reaction with **114** was done (Scheme 3.1.7). Homo cross metathesis with G(I) catalyst gives almost up to 80% yield of the dimerization product **105a** in DCM at 40°C. But the substitution reaction of the bisphenol product **105a** to **114** in acetonitrile at 70°C under basic conditions resulted in mono substitution as the major product and the macrocycle **116** was formed only in trace amounts. The reaction was also tried under high dilution at higher

temperature (90 °C) to foster formation of the cyclised product, but there was not much improvement in the yield of the desired compound.

Figure 3.1.1: Metathesis catalysts which have been used in this work

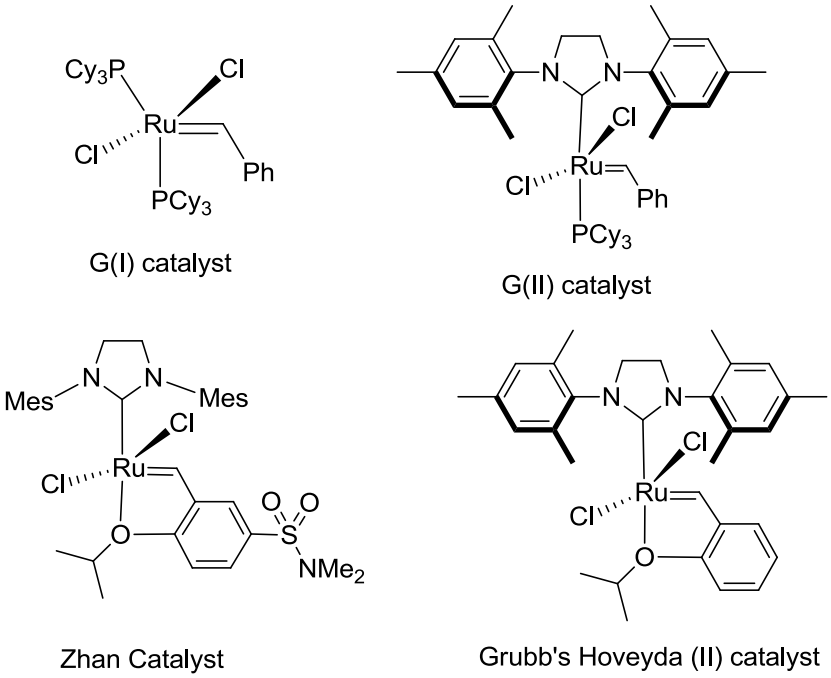

In the other approach, the ring closing metathesis (RCM) reaction was carried out on **115** with Grubb's second generation catalyst or Grubbs-Hoveyda catalyst. RCM reactions are generally entropy-driven, and the enthalpic costs that can be sustained are limited by the extent to which (in Gibbs- Helmholtz terms) the TΔS term can be maximized. The entropic benefit associated with release and volatilization of ethylene on metathesis of vinylic α,ω–dienes is powerful but indiscriminate, driving both inter- and intramolecular reactions. Different combinations of metathesis catalysts and solvents were tried under thermodynamic conditions (table 3.1.3), but the cyclized product **116** could not be obtained in appreciable yields. The reaction did not proceed to the desired product with Grubbs-Hoveyda catalyst. A similar outcome was seen in the reaction in DCM at 45 °C with Grubbs (II) catalyst resulting only in polymerization products. The cyclization was tried at higher temperatures also in dichloroethane, acetonitrile, DMF, methanol and chlorobenzene, still cross metathesis (i. e. polymerization) was the dominant reaction.

Scheme 3.1.7: Attempted synthesis of host **116** by cross metathesis followed by substitution

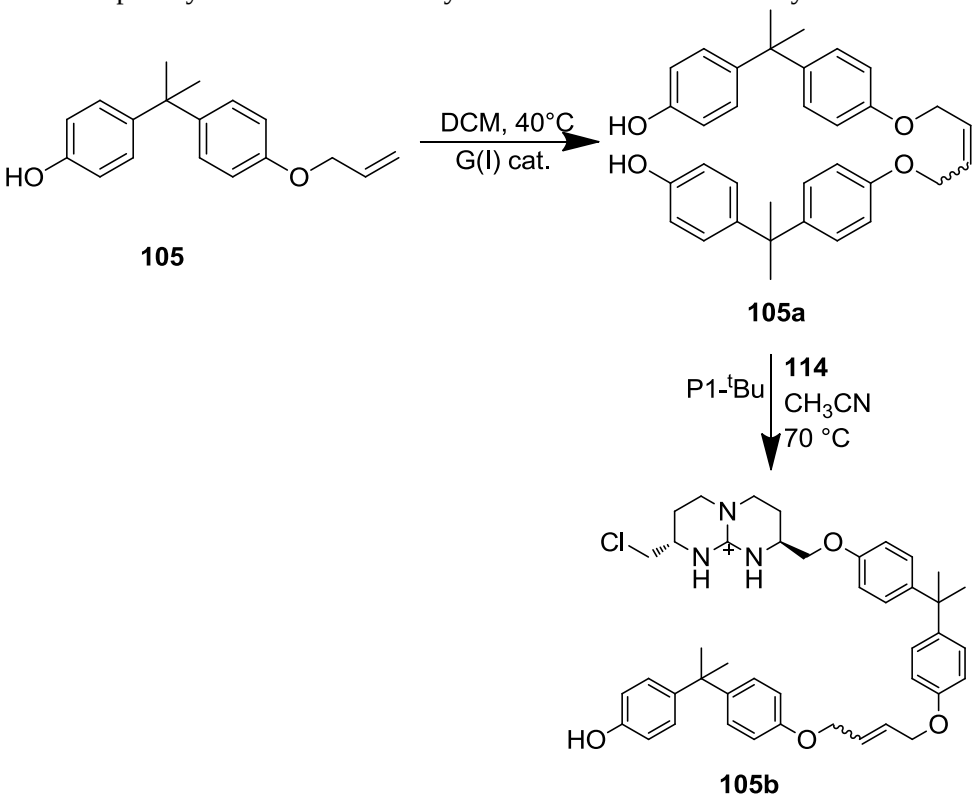

Table 3.1.3: Ring closing metathesis reactions attempted on **115** under various reaction conditions and with different metathesis catalysts.

entry	**solvent**	**metathesis catalyst**	**temperature**	**time**	**Result**
1	CH_2Cl_2	Grubbs (II)	45 °C	24 h	less than 10 % yield of **116**
2	MeOH	Grubbs (II)	65 °C	24 h	no reaction
3	PhCl	Grubbs (II)	80 °C	20 h	oligomerization
4	PhCl	Grubbs (II)	130 °C	21 h	oligomerization
4	MeCN	Grubbs (II)	80 °C	24h	no reaction

5	CH_2Cl_2	Grubbs-Hoveyda	45 °C	48 h	oligomerization
6	DCE	Grubbs (II)	60	20 h	oligomerization
7	DMF	Grubbs (II)	100 °C	21 h	no reaction

Adopting molecular dynamics calculation for inspiration, *S*- and *R*- binaphthyl phosphates (SBNP, RBNP) were also used as templating reagents to align the two terminal double bonds in the host compound **115** in close vicinity which might lead to the cyclization product (Figure 3.1.2). The reaction at 85°C in dichloroethane gave a better yield of the cyclised product, but again polymerization was the major deviation from the desired product (Table 3.1.4).

Figure 3.1.2: Binaphthyl phosphate complex used as templating reagent for RCM reaction.

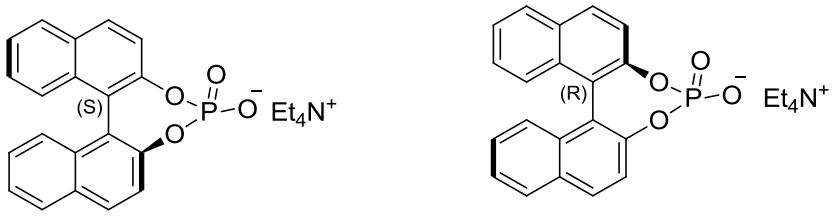

Table 3.1.4: Results of RCM reactions with templating reagent as analysed by HPLC analysis.

entry	solvent	template	temperature	time	result
1	DCM	SBNP	45 °C	18 h	< 10 % yield
2	DCE	SBNP	85 °C	6 h	10 % yield
3	DCE	RBNP	85 °C	24 h	10 % yield

In another approach the use of microwave irradiation conditions for ring closing metathesis of host **115** was considered. Microwave heating is an efficient method for the acceleration of ring closing metathesis reactions using ruthenium-based catalysts. The reaction can be conducted in either ionic liquids or in a microwave transparent solvent.[75, 79] In our concrete case microwave-

assisted ring closing metathesis gave much better results in terms of highly reduced reaction time as well as higher yields of the desired macrocyclic compound **116**. Reaction with Grubbs (II) catalyst under microwave condition gave up to 30% yield of the cyclised product. This yield was even further improved by the use of the more reactive Zhan-catalyst. The ring closing metathesis reaction with Zhan-catalyst under same condition gave almost 100% conversion of the starting compound and up to 40% yield of the desired macrocyclic product **116**. In ring closing metathesis, both cis- and trans-alkenes were formed which could be observed by HPLC analysis. It was also evident from the HPLC analysis that one of the isomers was formed in major quantity over the other one. The two isomers were isolated by chromatography; however, they could not be identified separately by NMR analysis due to the symmetry of the molecules. A small amount of compound was isolated as a singular pure alkene for ITC titrations and other analysis purposes. The rest of the mixture of cis- and trans-**116** was hydrogenated over Pd-C catalyst to obtain the structurally less rigid macrocyclic host **117** (Scheme 3.1.8).

Scheme 3.1.8: Hydrogenation of macrocyclic host **116**.

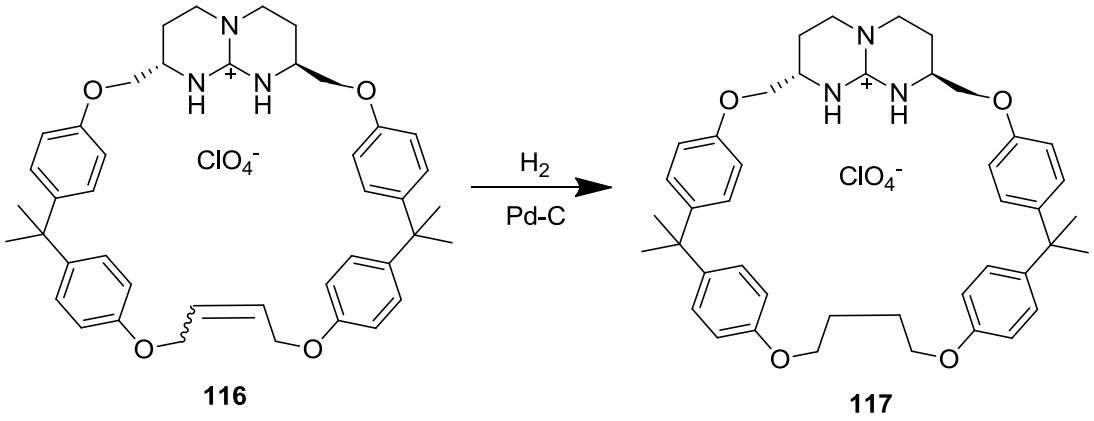

3.2 Synthesis of the macrocyclic estradiol guanidinium host 124

The synthetic strategy for the preparation of the macrocylic guanidinium host **124** is depicted in scheme 3.2.1.

The synthesis of the host **124** started off with the substitution reaction between the bicyclic guanidinium building block **114** and commercially available estradiol **121** to furnish the bis-substituted guanidinium host **122**. Cyclization was carried out by the means of an addition

reaction between bis(4-isocyanatophenyl)methane **123** and the open chain host **122** using the former as the linker group.

Scheme 3.2.1: Schematic representation of the synthetic strategy to form guanidinium macyrocylic host **124**

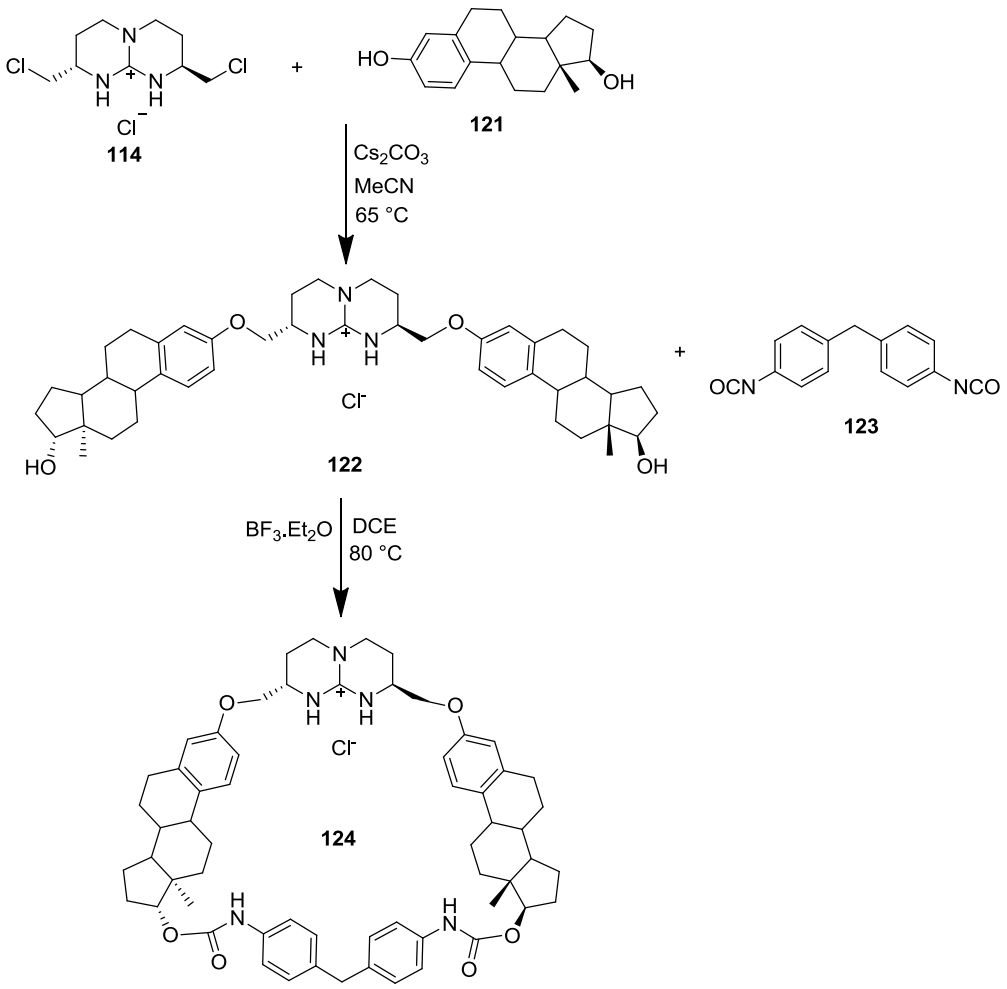

Host molecule **120** was synthesized from the estradiol benzoate **118.** Allylation of estradiol benzoate **118** was carried out with a ruthenium catalyst under acidic conditions followed by subsequent deprotection of the phenol function. The reaction yielded up to 70% of the allylated ether product **119** (Scheme 3.2.2).

Scheme 3.2.2: Allylation of estradiol benzoate followed by subsequent deprotection.

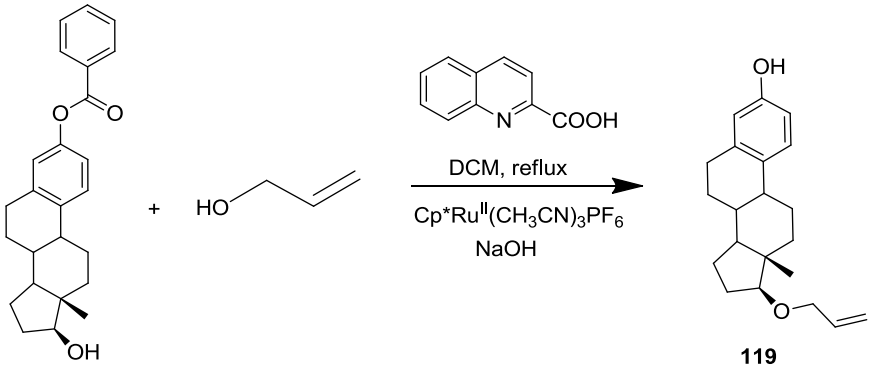

118 119

Substitution of **119** to the guanidinium unit **114** was done under basic conditions which gave the host molecule **120** in up to 80% yield (Scheme 3.2.3, table 3.2.1).

Scheme 3.2.3: Substitution reaction between **114** and **119** to synthesize host **120**.

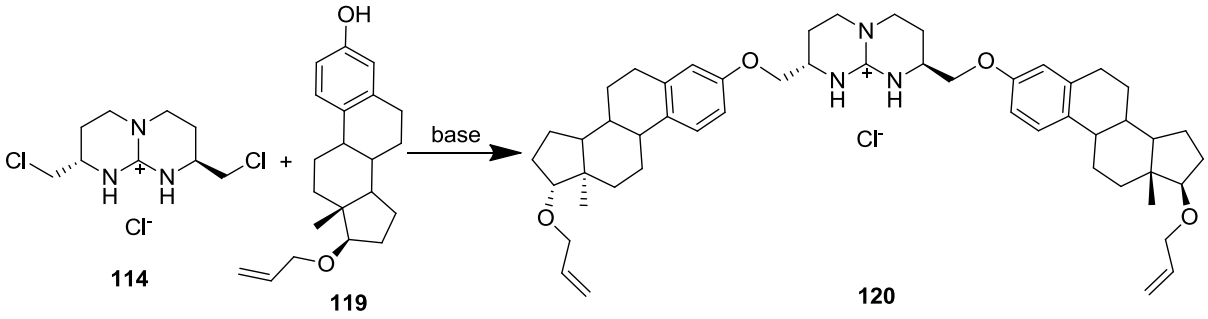

114 119 120

Table 3.2.1: Substitution reaction between **114** and **119** under different reaction conditions.

entry	solvent	base	temperature	yield %
1	MeCN	P1-^{t}Bu	60 °C	70
2	MeCN	Cs_2CO_3	65 °C	80
3	MeCN	KO^{t}Bu	65 °C	75
4	THF	Cs_2CO_3	65 °C	72

Ring closing metathesis reaction was implemented on **120** to form the cyclized host in the same way as exercised in the case of the bisphenol macrocycle **116** (Scheme 3.2.4). The RCM reaction was done under conventional thermodynamic conditions as well as using microwave irradiation. At lower temperature in DCM, intermolecular olefin metathesis was observed resulting in polymerization of guanidinium host **120**. Ring closing metathesis reaction in DCE with Grubbs

second generation catalyst G(II) and Zhan catalyst under microwave irradiation resulted in the cleavage of the allyl ether bond which was confirmed by HPLC and mass spectra. Metathesis reaction at 80 °C under nitrogen atmosphere gave again the cleaved allyl ether product. Grubbs first generation catalyst and Grubbs- Hoveyda catalyst were also tried in THF under microwave conditions, but no metathesis reaction was observed in either case. Even on using high intensity microwave irradiation at 480 W, no conversion of starting material was observed. The reaction was attempted at higher temperature in DMF with Grubbs (II) catalyst and Zhan catalyst, but the desired cyclized product was not formed. Benzoquinone was used as templating agent in DMF at 170 °C, again the cleavage of allyl ether group was observed. The observations are summarized in table 3.2.2. The steroid side arms are connected to the guanidinium unit by a single bond. As a result, these arms are free to move in the space, but the steroid unit is conformationally quite rigid in itself. It might be that the two terminal double bonds on steroid cannot approach each other in close proximity and also the terminal double bonds are sterically more hindered in comparison to bisphenol host **115**.

Scheme 3.2.4: Attempted ring closing metathesis on host **120**

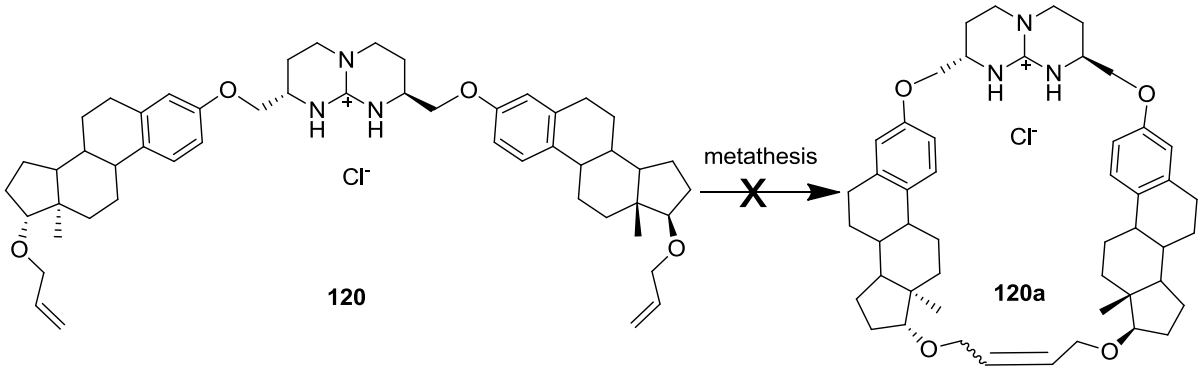

Table 3.2.2: Attempted ring closing metathesis on host **120** with different metathesis catalysts

entry	solvent	metathesis catalyst	temperature	time	Result
1	DCM	Grubbs (II)	45 °C	21 h	Oligomerization
2	DCE	Grubbs (II)	MW- 480 W	8 min	no metathesis
3	THF	Grubbs (I)	MW- 480 W	4 min	no reaction
4	THF	Grubbs-Hoveyda	MW-480 W	4 min	no reaction
5[a]	EtOH	G(I), G (II),	MW- 320 W	6 min	no metathesis
6[a]	EtOH	Grubbs Hoveyda	MW- 320 W	6 min	no metathesis
8	DCE	Zhan Cat.	MW- 480 W	12 min	no metathesis
9	DCE	Grubbs (II)	80 °C	20 h	no metathesis
10	DCE	Zhan cat.	80 °C	15 h	no metathesis
11	DMF	Grubbs (II)	160 °C	3 h	no metathesis
12	DMF	Zhan cat.	160 °C	overnight	no metathesis
13[b]	DMF	Zhan cat.	170 °C	overnight	no metathesis
14[b]	DMF	Grubbs (II)	170 °C	overnight	no metathesis
15	DMSO	Grubbs (II)	190 °C	5 h	no metathesis

a) Sodium benzoate was used as templating agent; b) Benzoquinone was used as templating agent.

Alternatively, the rigid (3,6)-hexahydrofuro-furan dithiol linker group was tried to ring-close two steroid arms. Photochemically and/or thermally-induced thiol-ene coupling reaction (TEC) proceeds by a radical mechanism to give an anti-Markovnikov-type thioether.[80] Over the years, the TEC reaction has been extensively exploited in polymer chemistry.[81] The reaction between the bis-thiol linker and the open chain compound 120 was carried out at room temperature by UV irradiation (λ= 254 nm). Unexpectedly, the photo induced reaction furnished only polymerization products as confirmed by HPLC and mass spectroscopy (Scheme 3.2.5).

After failed attempts to obtain the cyclized product from **120** by the means of ring closing metathesis, an alternative strategy was followed to synthesize the estradiol side chain containing

macrocyclic host **124**. Bicyclic guanidinium chloride **114** was substituted with the commercially available estradiol building block **121** under basic conditions to obtain host **122** (Scheme 3.2.6).

Scheme 3.2.5: Attempted synthesis to form cyclized product from **120** using a linker group

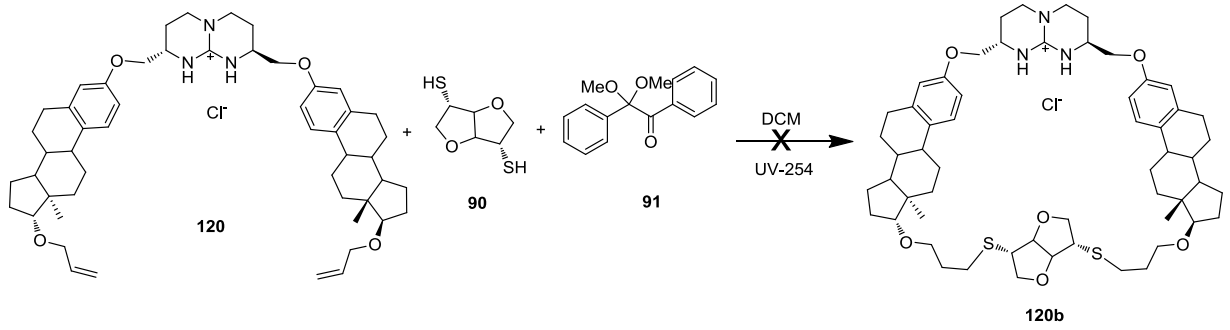

Scheme 3.2.6: Substitution reaction between estradiol **121** and **114** to synthesize host **122**

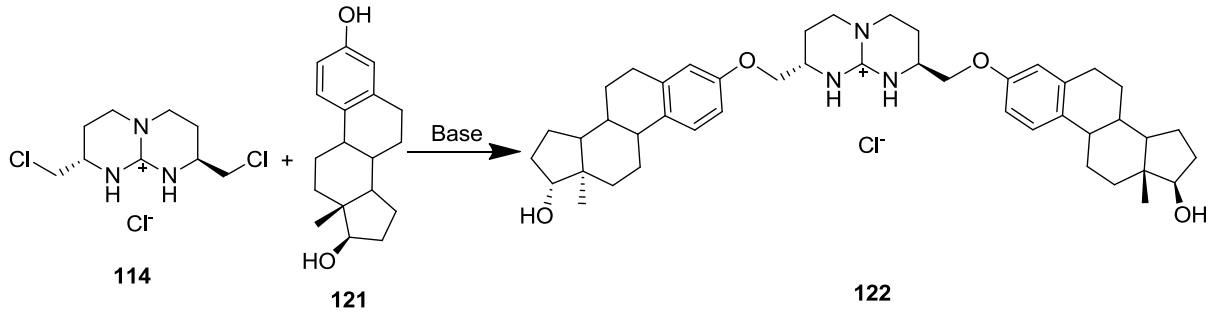

Then, bis(4-isocyanatophenyl) methane **123** was introduced as the spacer group to synthesize macrocyclic host **124** (Scheme 3.2.7). The addition reaction in DCE at 80 °C in the presence of trifluoroboron etherate finally gave the desired macrocylic host compound **124** as was corroborated by the mass spectroscopy. But as this is a double addition reaction, the mass of the mono addition product would also be the same as the macrocylic compound **124**. Infrared spectroscopy was performed on the product to see if there was any isocyanate peak. No peak was observed in the isocaynate stretching frequency region in IR spectrum which confirms that both isocyanate functions reacted with the starting compound **122**. The symmetry observed in the NMR spectrum again confirmed the identity of the macrocyclic compound **124**. The integration of the aromatic and methylene unit of isocyanate peaks in the ^{1}H NMR shows 1:1 ratio of the compound **122** and **123** in the final cyclized product **124**.

Scheme 3.2.7: Cyclization of host **122** using bis(4-isocyanatophenyl)methane **123** as linker group to synthesize macrocyclic host **124**

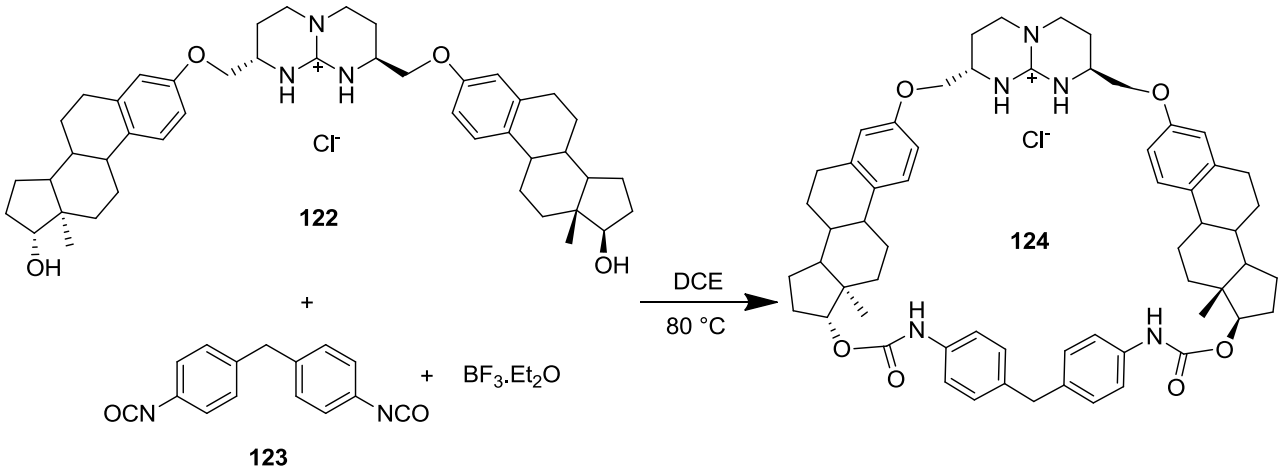

4. Results and discussions of binding studies

The experimental observations from isothermal calorimetric titrations (ITC) are discussed in this section which were performed on the specially designed hosts and different chiral oxoanion guests in acetonitrile and 1,2-dichloroethane. The complexation of host-guest ion pairs could be better understood if we dissect the free energy of binding (ΔG) into its corresponding enthalpy (ΔH) and entropy (ΔS) parts. It was proved earlier that enthalpy and entropy could compensate each other [27, 82], hence it is necessary to measure the magnitude of each component individually. Complexation studies were performed using a standard isothermal titration microcalorimeter (MCS-ITC, Microcal, USA) and employed carefully degassed and filtered (0.2 mm Teflon syringe filter) solutions of the host and the guest compounds in absolute acetonitrile and 1,2-dichloroethane. This technique provides a measure of association strength, stoichiometry of binding as well as thermodynamic parameters of association (enthalpy ΔH°, entropy ΔS° and free energy ΔG°) from a single experiment. Data analysis relied upon Origin 5.0 software supplied by the instrument manufacturer. The choice of the binding model and the subsequent fit procedure used various (commonly 15-20) different starting parameter sets to raise the probability of finding the global error minimum.

The report of a typical ITC plot (ref. figure 4.1.1) from a titration consists of two panels- an upper panel corresponds to the heat (absorbed or released) pulses over time and the lower panel indicates the binding isotherm generated by integration of each peak plotted versus mol ratio. The titration curve gives the molar enthalpy ΔH° as the step height and the free energy ΔG° from the slope of the curve in the inflection point. The molar entropy ΔS° could be easily calculated from the Gibb's-Helmholtz equation and the stoichiometry *n* is derived from the curve fit as an independent parameter.

The ITC titrations discussed in the following sections focus on the following studies:

i. Enantiomeric recognition of oxoanions by chiral bicyclic guanidinium hosts
ii. Size compatibility between host and guest
iii. Enthalpy-entropy compensation in host-guest binding
iv. Effect of the structural confinement on the enantio-recognition of oxoanions

Scheme 4.1: Different oxoanion salts used for complexation with the hosts in the following sections.

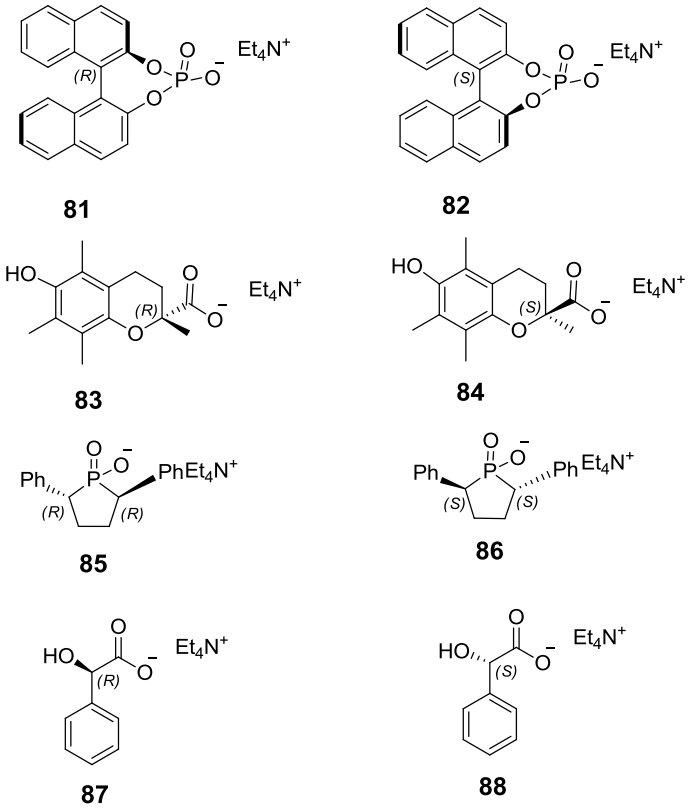

ITC titrations were performed with two series of guanidinium hosts to study their supramolecular interactions with different chiral oxoanions. One series contains the allylated bisphenol A as a side arm to the chiral bicyclic guanidinium building block. In the group, the host **115** is an open chain compound with no constraint on its degrees of freedom. The macrocyclic host **116** in contrast is derived from **115** by cyclization through ring closing metathesis of the terminal alkene bonds in compound **115**. Host **116** is quite restricted in its conformational freedom which was evident from CPK model and molecular dynamics simulations. Host **117** is synthesized from **116** by reducing the double bond, making it more flexible than **116**, but still more structured than the host **115**.

Host **116,** which is a pure geometrical isomer and, thus, has the most rigid conformational structure among all the three hosts analysed, shows the best enantio-recognition of the enantiomeric guests **85** and **86.** In fact, this host binds **85** preferentially over **86** by a factor of 360 (entry# 9, 10). Interestingly, host **117** obtained by reduction of the double bond in compound

116 does not give equally good enantio-differentiation. The binding constant of **85** is 16 times higher than that of **86** with host **117** (entry# 17, 18). This might be due to the loss of conformational rigidity in the macyrocyclic structure, as a single bond is more flexible than the double bond. Expectedly, host **115** gives insignificant enantiodifferentiation between two enantiomers **85** and **86**. The two bisphenol arms in the host **115** are completely free to move in space. This suggests that there is no specific geometric interaction between the host **115** and the diphenylphosphinate guests.

Scheme 4.2: Different guanidinium hosts used for complexation with the oxoanion guests.

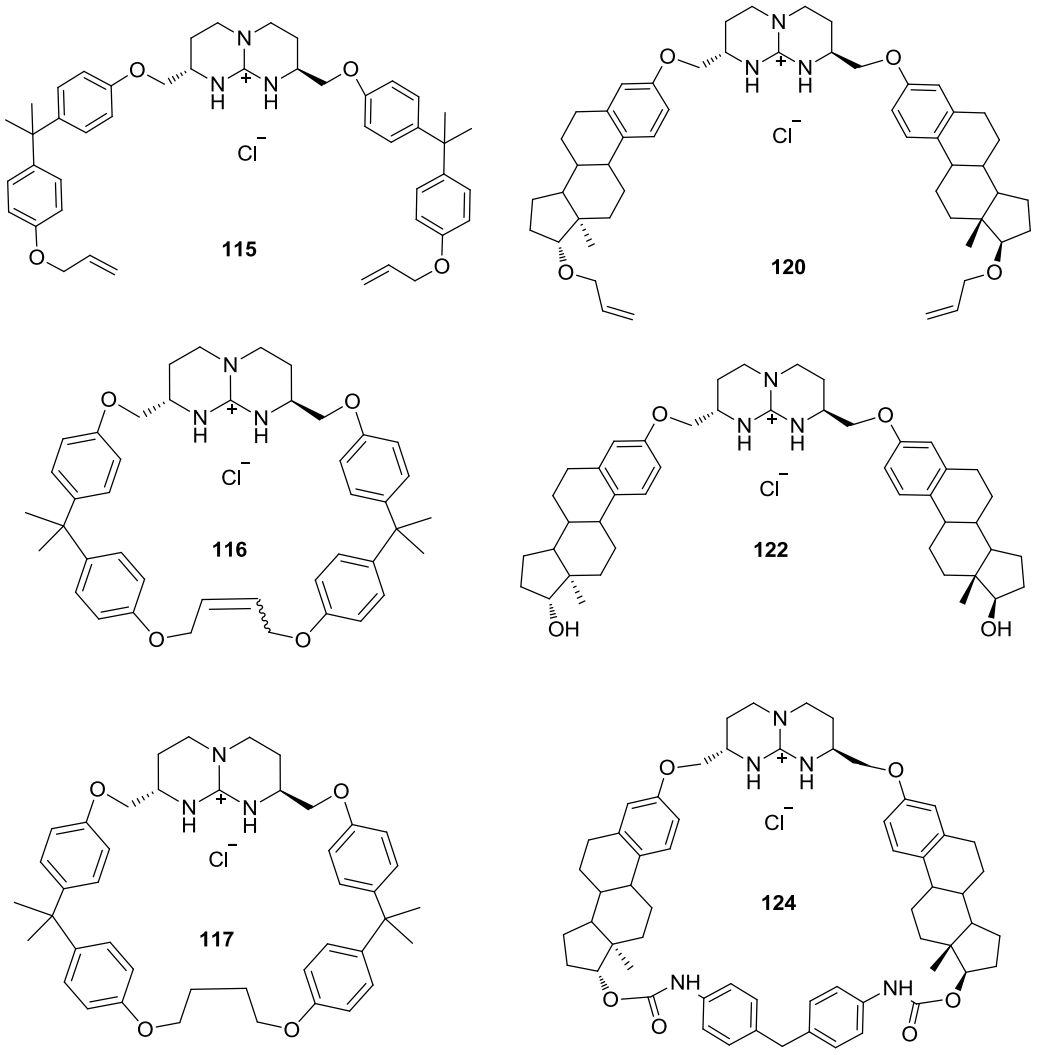

Table 4.1: Association constants (K_{ass} (M^{-1})) obtained from ITC titrations of various host guest ion pairs in acetonitrile at 303 K.

entry	titrated	titrand	n	K_{ass} (M^{-1})	$-\Delta H°$ (kcal mol^{-1})	$T\Delta S°$ (kcal mol^{-1})	$-\Delta G°$ [a] (kcal mol^{-1})
1	**81**	**115**	1.0	2.5 E3	6.7	-2.0	4.7
2	**82**	**115**	1.0	2.5 E3	4.0	0.7	4.7
3	**85**	**115**	1.0	7.7 E3	6.2	-0.8	5.4
4	**86**	**115**	2.0	4.5 E3	4.2	0.8	5.1
5	**81**	**116**	1.4	1.0 E3	2.9	1.3	4.2
6	**82**	**116**	1.2	1.1 E3	2.9	1.3	4.2
7	**83**	**116**	0.5	7.7 E4	4.6	2.2	6.8
8	**84**	**116**	0.8	3.1 E4	4.1	2.1	6.2
9	**85**	**116**	0.5	4.0 E5	5.9	1.8	7.8
10	**86**	**116**	0.4	1.1 E3	7.1	-2.8	4.2
11	**87**	**116**	1.3	5.2 E3	2.6	2.5	5.2
12	**88**	**116**	1.4	9.4 E3	2.6	2.9	5.5
13	**81**	**117**	1.5	1.4 E3	2.4	1.9	4.4
14	**82**	**117**	1.1	0.9 E3	3.0	1.1	4.1
15	**83**	**117**	1.0	1.9 E4	3.6	2.4	6.0
16	**84**	**117**	1.0	9.2 E3	3.8	1.7	5.5
17	**85**	**117**	1.3	2.6 E4	3.4	2.7	6.1
18	**86**	**117**	2.0	1.6 E3	4.1	1.3	5.4
19	**87**	**117**	1.3	6.2 E3	2.6	2.6	5.3
20	**88**	**117**	1.4	9.3 E3	2.7	2.8	5.5
21	**81**	**120**	1.0	3.6 E4	5.7	0.7	6.3
22	**82**	**120**	1.0	9.8 E3	5.0	0.5	5.5
23	**85**	**120**	1.0	8.8 E3	8.5	-3.0	5.5
24	**86**	**120**	1.0	1.4 E4	7.7	-1.9	5.7
25	**81**	**122**	1.0	5.9 E3	7.4	-2.1	5.2
26	**82**	**122**	0.9	7.5 E3	7.2	-1.9	5.4
27	**83**	**122**	1.1	1.8 E4	3.8	2.2	5.9
28	**84**	**122**	1.0	2.6 E4	2.4	3.6	6.1
29	**85**	**122**	0.7	2.4 E4	2.4	3.7	6.1
30	**86**	**122**	0.8	2.2 E4	2.4	3.6	6.0
31	**124**	**81**	0.7	1.2 E4	2.9	2.8	5.7
32	**124**	**82**	0.5	1.8 E4	2.5	3.4	5.9
33	**83**	**124**	1.9	1.1 E4	3.0	2.6	5.6
34	**84**	**124**	2.0	5.6 E3	2.4	2.8	5.2
35	**124**	**85**	0.7	3.2 E4	6.3	-0.04	6.3
36	**124**	**86**	0.7	3.5 E4	5.3	1.0	6.3
37[b]	**81**	**124**	1.4	4.6 E3	3.8	1.4	5.1
38[b]	**82**	**124**	1.0	1.7 E4	1.7	4.2	5.9
39[b]	**85**	**124**	1.0	1.4 E3	3.0	1.4	4.4
40[b]	**86**	**124**	0.7	7.8 E3	1.2	4.2	5.4

a) $-\Delta G = RT \ln K_{ass}$ ($R=1.99$ cal $K^{-1}mol^{-1}$, $T= 303$ K), b) titrations were done in DCE

It was observed that the macrocyclic hosts **116** and **117** give moderate enantiodifferentiation between trolox enantiomers **83** and **84**, and very little enantiorecognition for mandelate **87** and **88**, and binaphthylphosphate guests **81** and **82** (entry# 5-20, table 4.1). This trend suggests that the size relation between hosts and guests might play an important role in the supramolecular interactions between the two species. The size of the cavity of the hosts **116** and **117** is almost same. As a result, the enantio-recognition trends with respect to the various guests are quite similar in both cases. Binaphthylphosphate is too big to enter into the cavity of the host, as observed in the CPK model and MD simulations, which means that there is little interaction based on supramolecular geometric fit between the host and the guest. The association constant is predominantly driven by the electrostatic interaction between two oppositely charged entities. On the other hand, the mandelate anion is too small in comparison to the cavity size of the hosts. The size of the trolox and diphenylphosphinate guests is suited to the host cavity which results in better supramolecular interactions. The molecular dynamic simulations suggest the possibility of π-π interactions between host **116** and guest **85**, which explains the high association constant in this host-guest pair. It is very important for understanding the origin of any supramolecular interaction to consider enthalpy and entropy separately rather than just going by the total free energy in designing host guest systems. ITC titration is the most effective method to dissect the total free energy into its originating factors as this method provides all these values in a single experiment. An enthalpy-entropy compensation effect was observed in many of the ITC titrations. For example, host **115** gives identical association constants for both enantiomers of binaphthylphosphate guest **81** and **82** (entry# 1-4, table 4.1). But, their energy signatures are totally different from each other which suggest two different modes of binding. The interaction between host **115** and guest **81** is much exothermic than for guest **82** which indicates a stronger binding for **81**, but the positive entropy released in the process of complexation between guest **82** and host **115** compensates for the lack in enthalpy. These two compensating factors result in an almost similar free energy for the two enantiomers.

The other series of hosts is constituted of the bicyclic guanidinium unit as a building block and estradiol forming the side arms. Hosts **120** and **122** are open chain species **120** having additional terminal allyl bonds. Macrocyclic host **124** was synthesized from **122** by addition to bis(4-isocyanatophenyl) methane as the linker group.

Figure 4.1: Depiction of the binding affinities (log K_{ass}) of hosts **115**, **116** and **117** with different oxoanions.

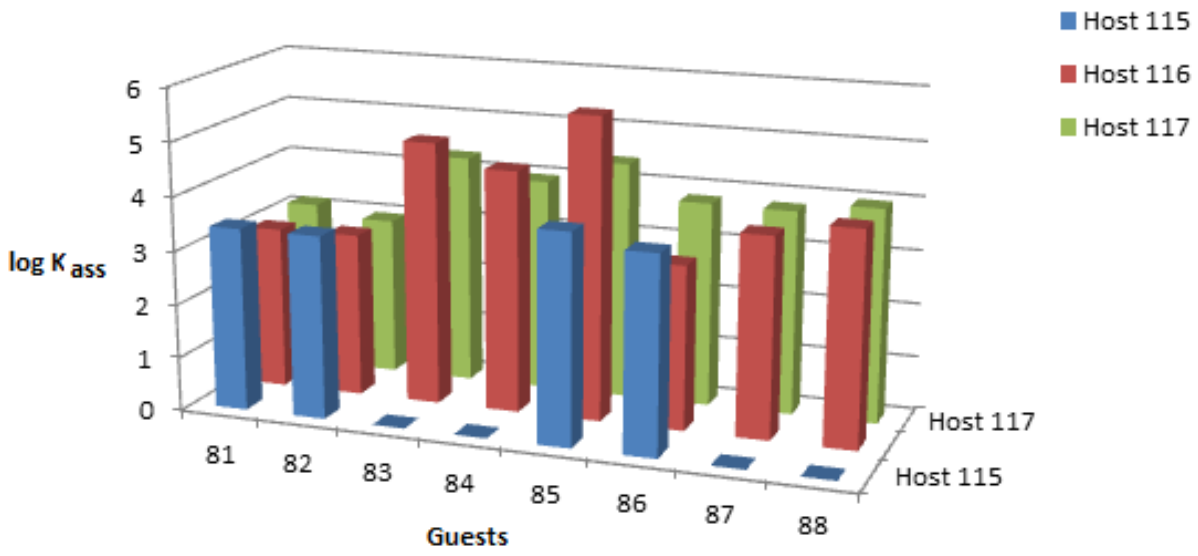

Though the steroid arms are conformationally rigid, they are still free to move in the space by means of rotaion around single bonds connecting them to the guanidinium unit.Thus, it is less of a surprise that hosts **120** and **122** do not give any specific interaction with either of the guests **85** and **86**. The host **124** does not show any enantio-differentiation in acetonitrile for any of the guests, but a moderate enantio-differentiation was observed in 1,2-dichloroethane between enantiomers of the binaphthyl phosphate guest **81** and **82**.

Interestingly, in the case of guests **81** and **82**, host **116** (entry# 5, 6) does not differentiate between two enantiomers. The guests are bound very weakly with host **116** and the association constants are almost same for both enantiomers, **81** and **82**. On the contrary, hosts **120** (entry# 21, 22) and **124** (entry# 37, 38) give a moderate enantiorecognition with the guests **81** and **82**. The association constant is almost 4 times higher for **81** than **82** with host **120** and enantiomeric preference is just reversed in the case of host **124**. The size of the cavity of the host **124** is bigger in comparison to **116** owing to the spacer group used to synthesize macrocyclic host **124** which might be fitting well to the big size of the guests **81** and **82**.

Figure 4.2: Depiction of the binding affinities (log K_{ass}) of hosts **120**, **122** and **124** with different oxoanions.

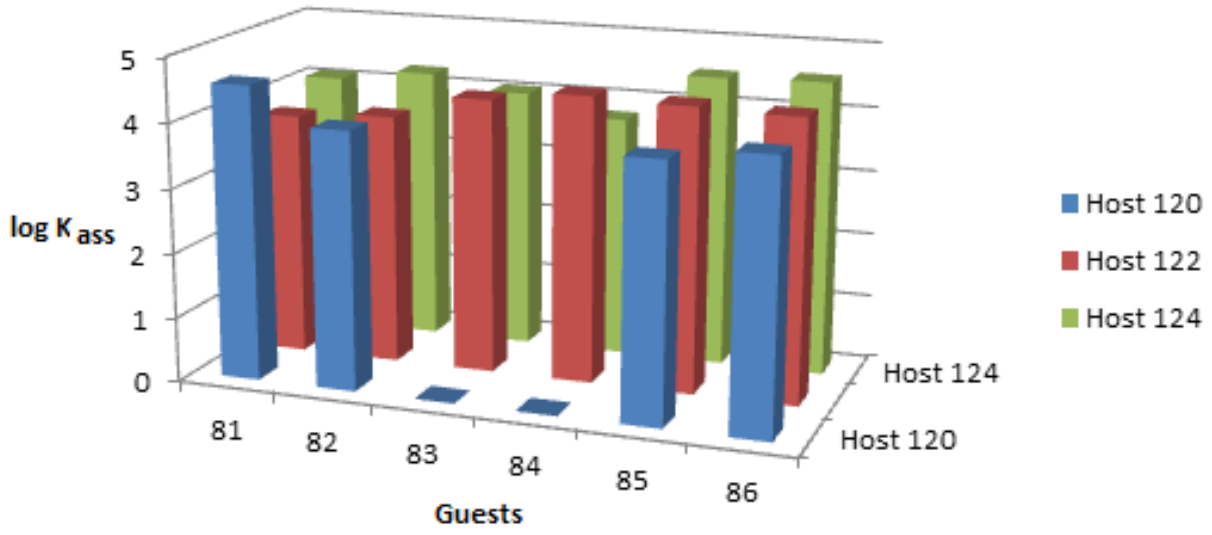

4.1 ITC titration of host 115 with different chiral oxoanions

The ITC titrations of the host **115** into the bisnaphthylphosphate enantiomers (**81** and **82**) displayed monotonous exothermic processes (figure 4.1.1). The OSB model curve fits quite well with the titration data and indicates 1:1 binding between the host and the guests for both enantiomers. The association constant was observed to be, K_{ass}= 2,500 M^{-1} ($\Delta H°$= -6.69 kcal mol^{-1}, $\Delta S°$= -6.5 e.u.) for **81** and K_{ass}= 2,500 M^{-1} ($\Delta H°$= -3.99 kcal mol^{-1}, $\Delta S°$= +2.4 e.u.) for **82**. Again, the total free energy is similar in both cases despite very different energy signatures owing to the compensation between enthalpy and entropy.

The titration data of the host **115** with tetraethylammonium salts of enantiomers of trolox anion **83** and **84** are represented in the figure 4.1.2. The depiction clearly indicates that this host-guest complexation cannot be represented by a simple 1on1 binding scheme, but must involve higher order process. However, all attempts to deconvolute the obvious complexity in this system failed.

Figure 4.1.1: ITC-traces of the titration of the host **115** (9.88 mM) into the guest **81** (0.51 mM) and the guest **82** (0.33 mM) solution in acetonitrile at 303 K.

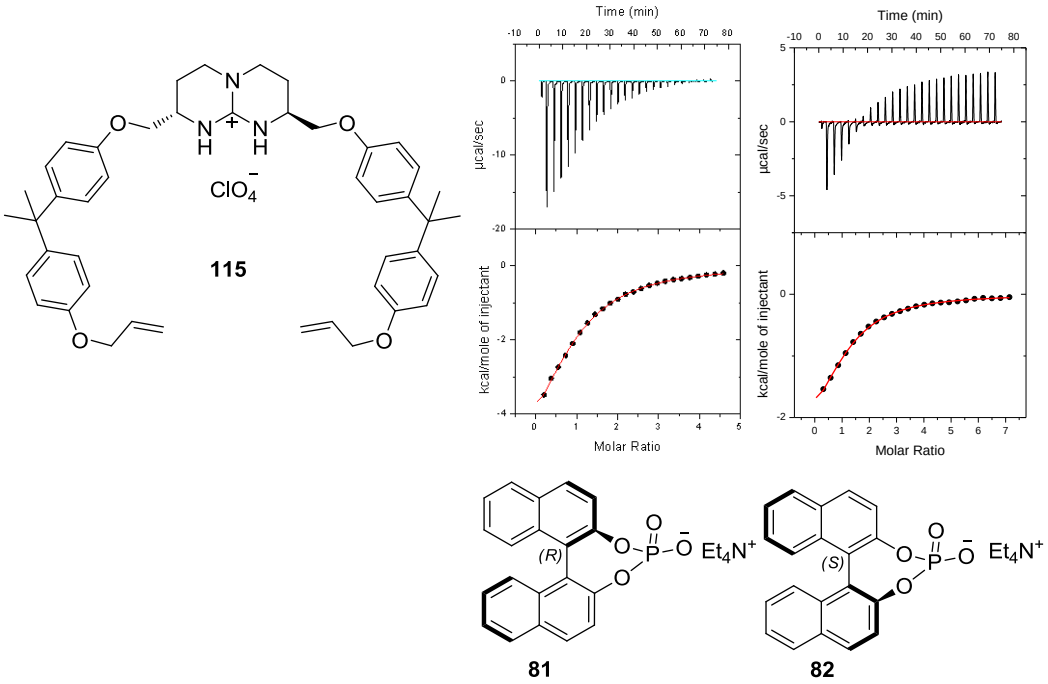

The titrations of the open chain guanidinium host **115** into the solutions of tetraethylammonium salts of *R*- and *S*- diphenyl phosphinate guests (**85** and **86**) in acetonitrile at 303 K are presented in figure 4.1.3. Both complexation processes are exothermic, but the entropy is positive in the case of **86** while it is negative for **85**. The one-site-binding model gives an association constant of K_{ass}= 7,750 M^{-1} ($\Delta H°$= -6.18 kcal mol^{-1}, $\Delta S°$= -2.6 e.u.) for **85** and K_{ass}= 4,500 M^{-1} ($\Delta H°$= -4.2 kcal mol^{-1}, $\Delta S°$= +2.8 e.u.) for **86** and with a stoichiometry (guest to host) of 2 and 1 for **86** and **85**, respectively. The reason behind the stoichiometry of **86** could be an error while making the guest solution. As the solution was quite dilute, even a small error in weighing of the compound can result in considerably different concentration. The binding constants of both enantiomers differ by a factor of 1.7 only, but the energetic signatures are totally different from each other. The interaction between host **115** and the guest **85** is much more exothermic than for guest **86** which indicates a stronger binding for *R*-enantiomer, but the entropy released in the complexation of guest **86** is much more positive which compensating for the inferior enthalpy. These two compensating factors combine to an almost similar free energy for the two enantiomers. This supports the concept that the total free energy cannot be considered as the only

criterium for an effective design of the host-guest system. Rather the enthalpy and entropy components should be also taken into the consideration.

Figure 4.1.2: ITC-traces of the titration of the host **115** (9.88 mM) into the guest **83** (0.33 mM) and the guest **84** (o.32 mM) solution in acetonitrile at 303 K.

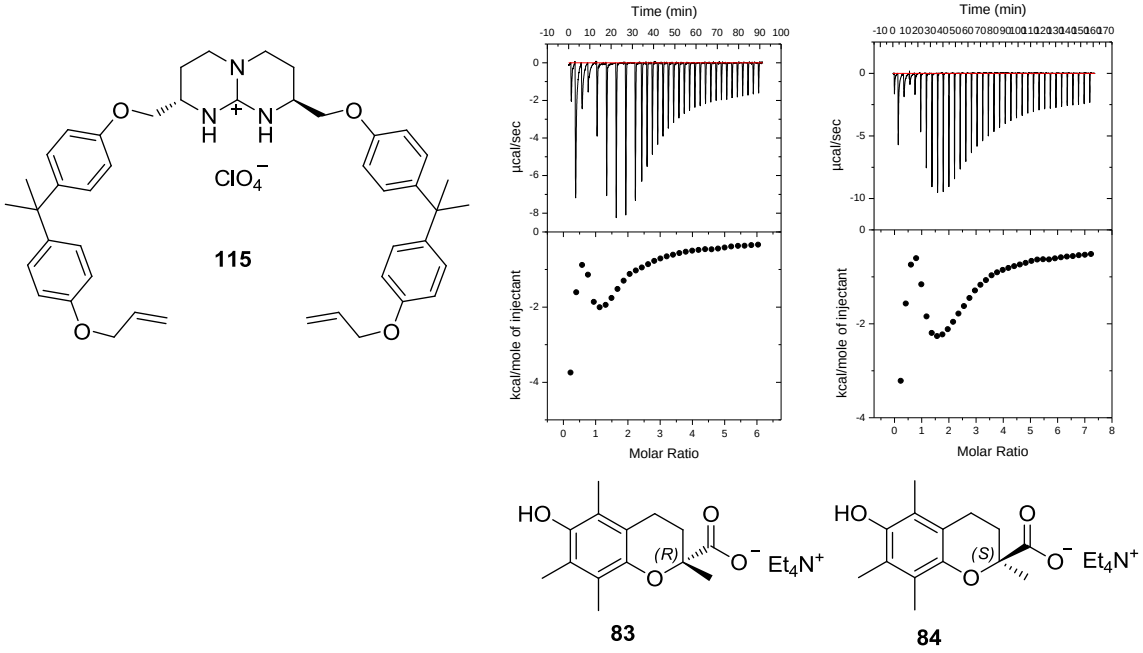

Figure 4.1.3: ITC-traces of the titration of the host **115** (13.14 mM) into the guest **85** (0.50 mM) and of the host **115** (11.61 mM) into the guest **86** (0.58 mM) solution in acetonitrile at 303 K.

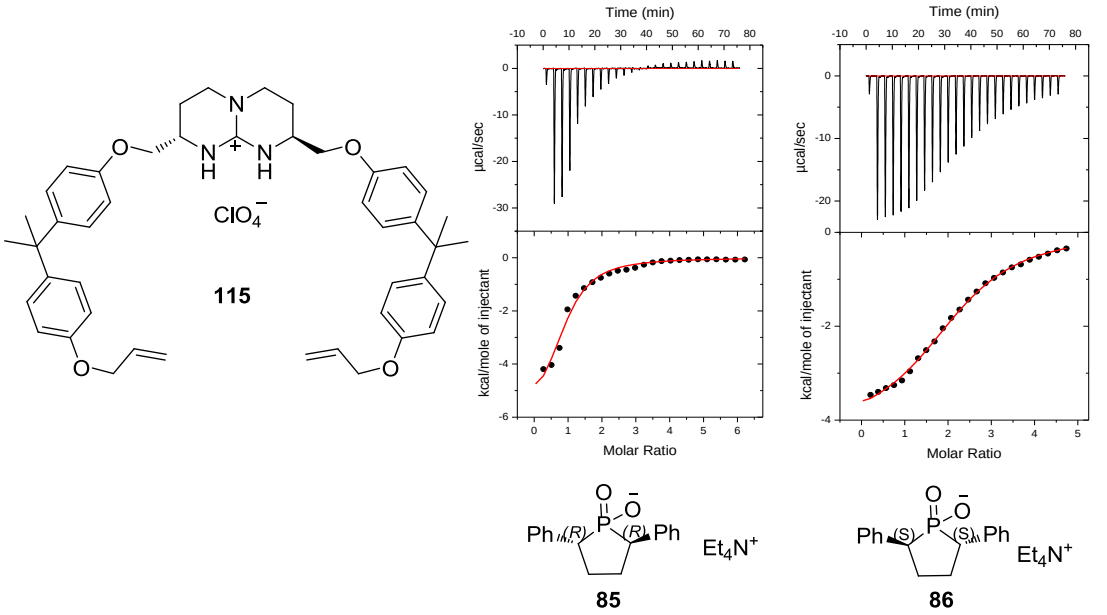

4.2 ITC Titrations of the host 116 with different chiral oxoanions

The ITC traces from the titration of macrocyclic host **116** into the *R*- and *S*- enantiomers of binaphthyl phosphate guests (**81** and **82**) are represented in figures 4.2.1. The complexation of both enantiomers with the host **116** indicate exothermic processes. The heat signatures of the complexations are similar to each other, resulting in quite comparable association constants. The one site binding model gives an association constant, K_{ass}= 1,100 M^{-1} for *S*-isomer ($\Delta H°$= -2.89 kcal mol^{-1}, $\Delta S°$= +4.4 e.u.) and K_{ass}= 1,050 $M^{-1}$for *R*-enantiomer ($\Delta H°$= -2.9 kcal mol^{-1}, $\Delta S°$= +4.2 e.u.) with a stoichiometry (host to guest) of 1.4 and 1.2 for **81** and **82**, respectively. The titration curves of both guests were quite monotonous and OSB model fitting was not exactly matching the titration curve which can be the reason for stoichiometry being slightly different from 1.

There is not any significant difference in the values of the enthalpy and entropy of complexation of these two enantiomers on interaction with the macrocyclic host. The reason might be the small size of cavity of the host molecule in comparison to the guest size as observed in the CPK model and the MD simulations which suggest that there might be very little geometric interaction between the host and either of the enantiomers and the association between the host and the guests is majorly contributed by the electrostatic interaction between the oppositely charged entities.

The titrations of tetraethylammonium salts of *R*- and *S*-Trolox (**83** and **84**) into the host **116** give very nice curves which fit well into the one-site binding model (figure 4.2.2). The complexation is exothermic with 1:1 stoichiometry between host and guest for both enantiomers. The interaction between host and guest is driven by favourable enthalpy and entropy changes in both cases. It gives an association constant, K_{ass}= 4.2x10^4 M^{-1} ($\Delta H°$= -4.21 kcal mol^{-1}, $\Delta S°$= +7.27 e.u.) for **83** and K_{ass}= 4.5x10^4 M^{-1} ($\Delta H°$= -3.11 kcal mol^{-1}, $\Delta S°$= +11.06 e.u.) for **84**.

Though, the binding constants are the same for both isomers **83** and **84**, there is a significant difference in their binding patterns. The complexation of the host **116** with *R*-isomer is highly exothermic which indicates towards strong supramolecular binding interactions. On the other hand, the binding between **116** and **84** is not as much exothermic, but this difference is compensated in the free energy by the more positive entropy released during the formation of

complex between the *S*- isomer and the host, in the end, furnishing the same free energy change for both enantiomers.

Figure 4.2.1: ITC-traces of the titration of the host **116** (19.5 mM) into the guests **81** (1.93 mM) and **82** (2 mM) solution in acetonitrile at 303 K.

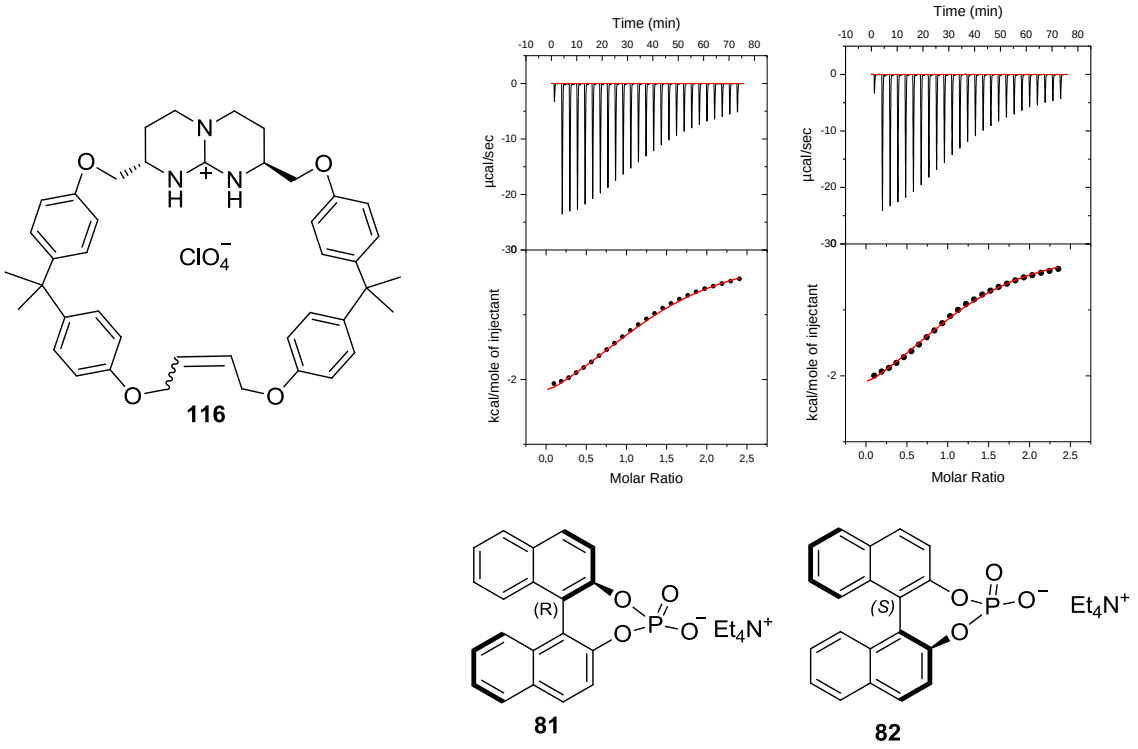

Reverse titrations were also carried out to see the effect of addition of host into the guest. Again, the basic nature of the binding isotherm remained the same giving exothermic complexation for both enantiomers of Trolox guests. In this case, one-site-binding model gives a binding constant, K_{ass}= 7.7x10^4 M^{-1} ($\Delta H°$= -4.57 kcal/mol, $\Delta S°$= +7.3 e.u.) for **83** and K_{ass}= 3.1x10^4 M^{-1} ($\Delta H°$= -4.14 kcal/mol, $\Delta S°$= +6.9 e.u.) for **84** with stoichiometry (host to guest) of 0.5 and 0.8 for **83** and **84**, respectively. The complexation of **83** with host **116** is favoured by a larger heat released and more positive entropy in comparison to the **84** which results in higher association constant for *R*-isomer than *S*-isomer by a factor of 2.5.

Figure 4.2.2: ITC-traces of the titration of the guest **83** (14.88 mM) and **84** (10.98 mM) into the host **116** (1.01 mM) solution in acetonitrile at 303 K.

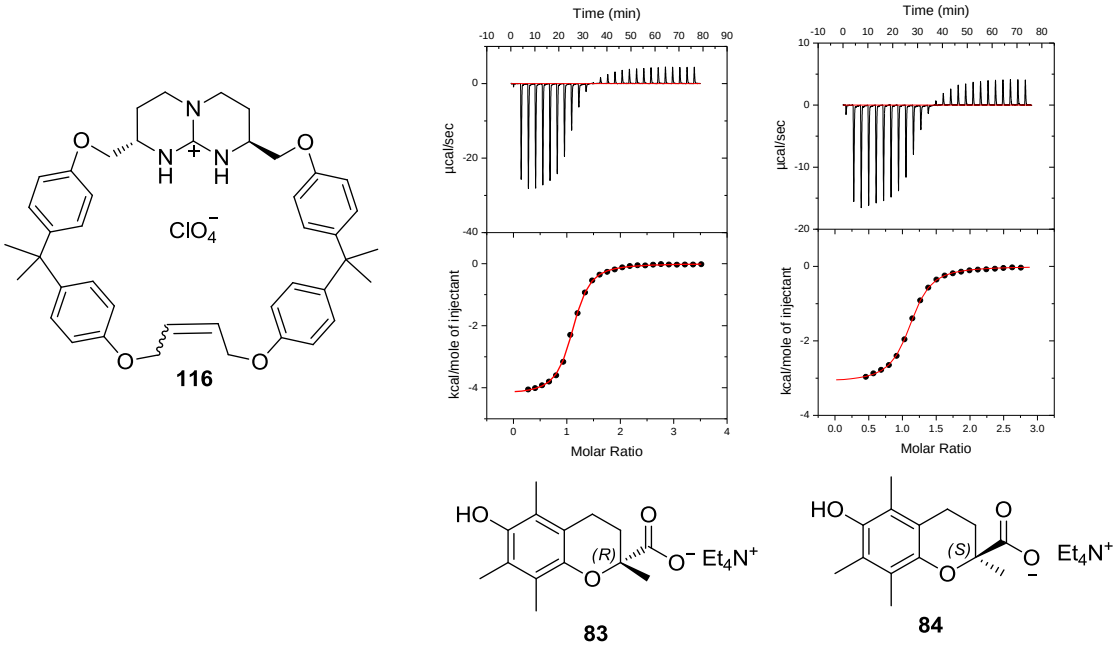

The ITC traces from the titration of macrocyclic host **116** into the *R*- and *S*- enantiomers of diphenyl phosphinate (**85** and **86**) are represented in figure 4.2.3. The complexation of *R*-enantiomer **85** with the host **116** is an exothermic process with favourable positive entropy of binding. On the other hand, titration of the host **116** into the *S*-diphenyl phosphinate anion **86** resulted in a highly exothermic process, but overall free energy was balanced by an equally high negative entropy component. The negative change in enthalpy as well as in entropy indicates formation of a highly structured complex. This difference in binding pattern of the two enantiomers surfaces this time in their association constants. The one-site-binding model gives an association constant, K_{ass}= 3.97x10^5 M^{-1} ($\Delta H°$= -5.94 kcal mol^{-1}, $\Delta S°$= +6.0 e.u.) for **85** and K_{ass}= 1,100 M^{-1} ($\Delta H°$= -7.07 kcal mol^{-1}, $\Delta S°$= -9.4 e.u.) for **86**.

Figure 4.2.3: ITC-traces of the titration of the host **116** (1.04 mM) into the guest **85** (0.11 mM) and the host **116** (19.52 mM) into the guest **86** (2.03 mM) solution in acetonitrile at 303 K.

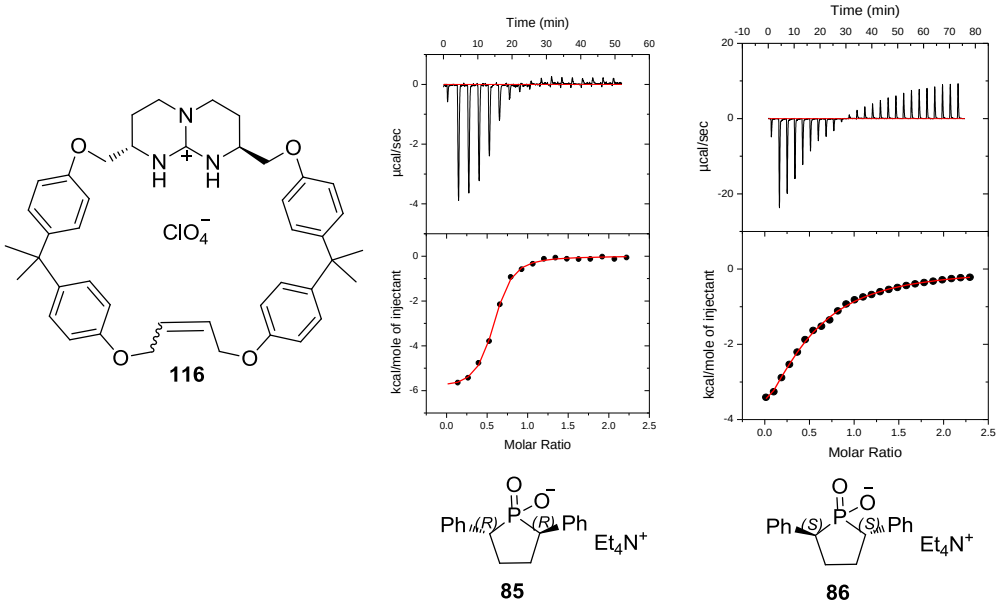

Figure 4.2.4: ITC-traces of the titration of the host **116** (9.75 mM) into the guest **87** (1.00 mM) and the guest **88** (0.69 mM) solution in acetonitrile at 303 K.

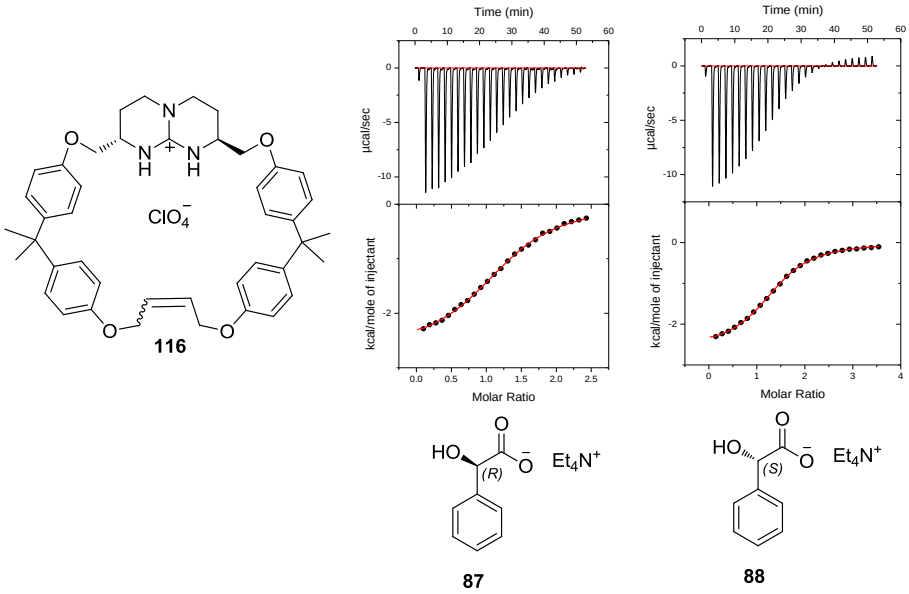

The ITC titrations of host **116** into the acetonitrile solutions of *R*- and *S*- enantiomers of mandelic acid (**107** and **108**) showed exothermic complexation processes and the supramolecular

interaction between host and guest gave rise to a positive entropy for both enantiomers (figure 4.2.4). The curves obtained from the titrations adhered quite well to the one-site-binding model, though the stoichiometries obtained were a bit off the mark from 1:1 binding. The one site binding model fitting curve revealed an association constant, K_{ass}= 5,200 M^{-1} ($\Delta H°$= -2.64 kcal mol^{-1}, $\Delta S°$= +8.3 e.u.) for **87** and K_{ass}= 9,400 M^{-1} ($\Delta H°$= -2.58 kcal mol^{-1}, $\Delta S°$= +9.7 e.u.) for **88**.

The binding affinity is relatively weak for mandelate anion in comparison to diphenyl phosphinate and Trolox anions. Such an outcome could be due to the small size of mandelate which does not fit so well in the cavity of the host compound. The binding affinity for **88** is 1.8 times higher than the **87** owing solely to the favourable positive entropy released in the complexation process.

4.3 ITC titration of Host 117 with different chiral oxoanions

The titration of host **117** into the acetonitrile solutions of enantiomers of binaphthylphosphate (**81** and **82**) gave monotonous exothermic titration curves (figure 4.3.1). The complexation between the host and the guest was very weak as was evident from the slope of the curve. The OSM curve fitting rendered an association constant, K_{ass}= 1,400 M^{-1} ($\Delta H°$= -2.42 kcal mol^{-1}, $\Delta S°$= +6.4 e.u.) for **81** and K_{ass}= 900 M^{-1} ($\Delta H°$= -3.01 kcal mol^{-1}, $\Delta S°$= +3.6 e.u.) for **82**.

The association constants for both enantiomers are quite comparable to each other. The difference in the free energy comes from the positive entropy of complexation between the host **117** and the *R*-enantiomer.

The ITC traces from the titration of guanidinium host **117** into the *R*- and *S*- enantiomers (**83** and **84**) of trolox anion are represented in figure 4.3.2. The OSM clearly indicates a stoichiometry of almost 1 for both the enantiomeric guest complexes and curve fitting gives a binding constant, K_{ass}= 1.94x10^4 M^{-1} ($\Delta H°$= -3.6 kcal mol^{-1}, $\Delta S°$= +7.9 e.u.) for **83** and K_{ass}= 9150 M^{-1} ($\Delta H°$= -3.8 kcal mol^{-1}, $\Delta S°$= +5.6 e.u.) for **84**. The association constant is mainly driven by highly negative enthalpy values.

Figure 4.3.1: ITC-traces of the titration of host **117** (10.02 mM) into the guest **81** (0.51 mM) and the guest **82** (0.33 mM) solution in acetonitrile at 303 K.

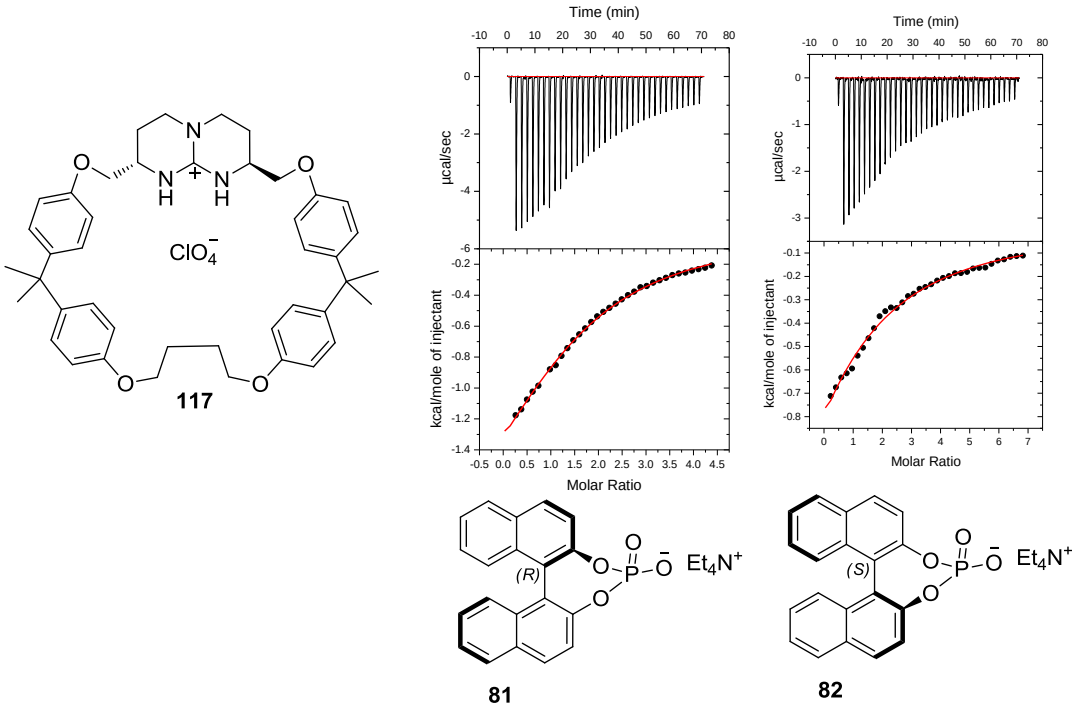

Figure 4.3.2: ITC-traces of the titration of host **117** (9.84 mM) into the guest **83** (0.33 mM) and the guest **84** (0.32 mM) solution in acetonitrile at 303 K.

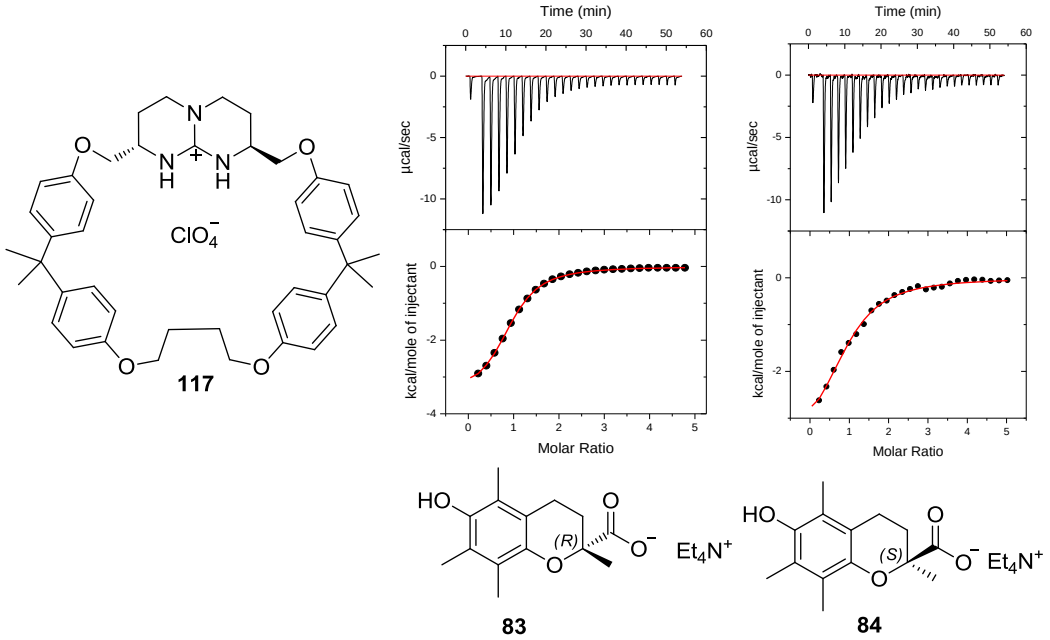

The binding constant for the complexation of **83** is just twofold higher than that of the **84**. This is also a very good example of entropy-driven enantio-differentiation. The enthalpy change on binding of **83** (-3559 cal) is insignificantly less negative than for **84** (-3793 cal), but is compensated and even further made favourable by the more positive entropy of binding (+7.9 versus +5.6, respectively, for **83** and **84**) which gives rise to a significant difference in the total free energy of complexation.

Macrocyclic host **117** was titrated into the acetonitrile solutions of *R*- and *S*- enantiomers of diphenylphosphinate guests (**85** and **86**) (figure 4.3.3). Both complexation processes were exothermic and favoured by positive entropies. The OSM model fitting curve furnished an association constant, K_{ass}= 2.6x10^4 M^{-1} ($\Delta H°$= -3.4 kcal mol^{-1}, $\Delta S°$= +8.9 e.u.) for **85** and K_{ass}= 1,600 M^{-1} ($\Delta H°$= -4.07 kcal mol^{-1}, $\Delta S°$= +1.3 e.u.) for **86**. The host to guest stoichiometry was observed to be 1.3 and 0.8 for **85** and **86**, respectively.

Figure 4.3.3: ITC-traces of the titration of host **117** (9.84 mM) into the guest **85** (0.53 mM) and the guest **86** (0.51 mM) solution in acetonitrile at 303 K.

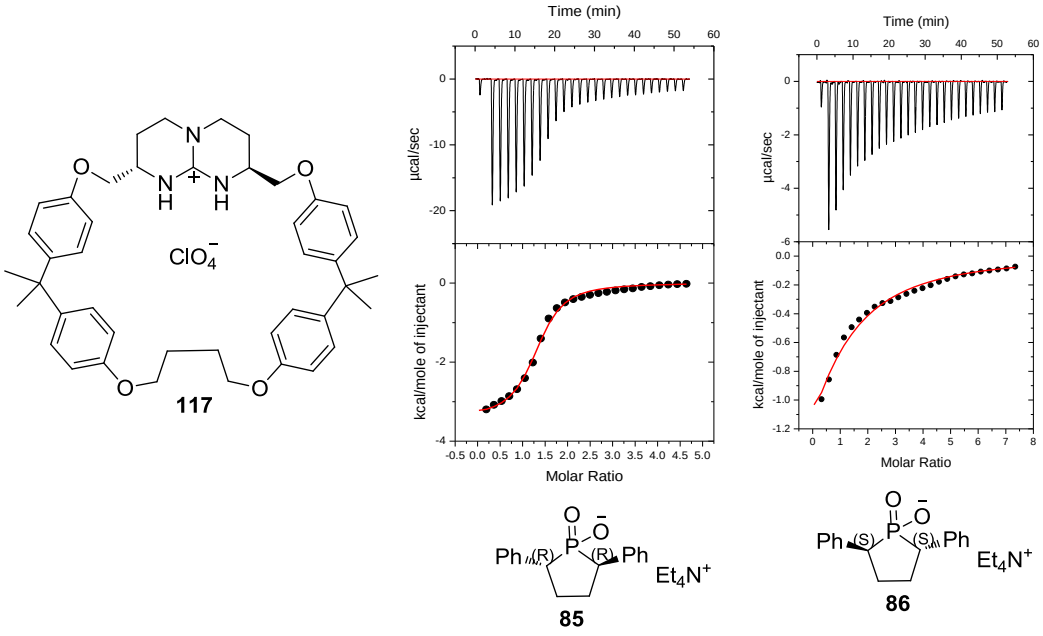

The complexation is driven by the highly positive entropy between guest **85** and host **117**. The association constant for **85** is higher than the **86** by a factor of almost 16. Though the released enthalpy of complexation between *R*-diphenylphosphinate and the host **117** is less than that of *S*-isomer, but it is over compensated by the highly positive entropy of binding between **117** and **85**.

The titration of guanidinium host into the solutions of tetraethylammonium salts of mandelate enantiomers in acetonitrile at 303 K are depicted in figure 4.3.4. The OSB model curve fits quite well with the titration curve and gives an association constant, K_{ass}= 6,200 M^{-1} ($\Delta H°$= -2.64 Kcal mol^{-1}, $\Delta S°$= +8.6 e.u.) for *R*-enantiomer and K_{ass}= 9,250 M^{-1} ($\Delta H°$= -2.68 Kcal mol^{-1}, $\Delta S°$= +9.3 e.u.) for the *S*-enantiomer with a host to guest stoichiometry of almost 1.4 for both guests **87** and **88**.

The binding constants of **87** and **88** differ by a factor of 1.5. The enthalpy and entropy both are slightly more favourable for the *R*-mandelate than the *S*-mandelate. The enantiomeric discrimination is not so prolific for practical purposes, but it gives an idea of size compatibility between the host and the guest.

Figure 4.3.4: ITC-traces of the titration of host **117** (9.84 mM) into the guest **87** (0.61 mM) and the guest **88** (0.67 mM) solution in acetonitrile at 303 K.

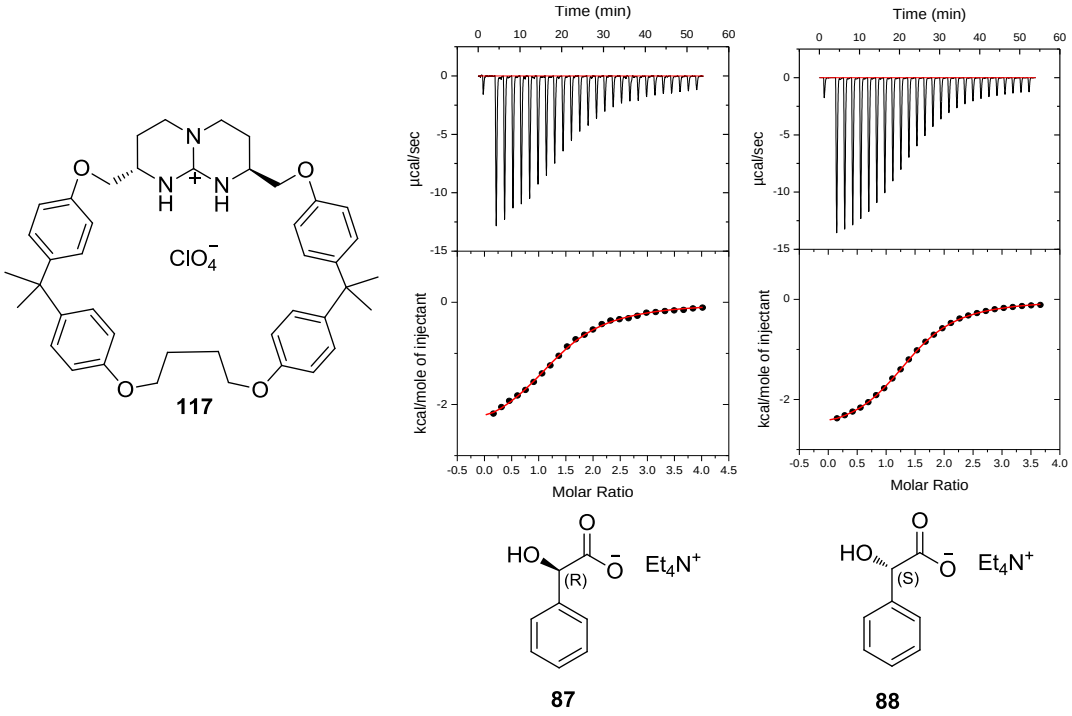

4.4 ITC titration of host 120 with different chiral oxoanions

The ITC traces from the titration of the steroid host **120** into the *R*- and *S*- enantiomers of binapthyl phosphate (**81** and **82**) are represented in figure 4.4.1. Complexation of both the enantiomers results in exothermic processes. The one site binding model fitting curve gives a

binding constant, K_{ass}= 9,850 M^{-1} (ΔH°= -5.05 kcal mol^{-1}, ΔS°= +1.6 e.u.) for the *S*- enantiomer and K_{ass}= $3.6x10^4$ M^{-1} (ΔH°= -5.67 kcal mol^{-1}, ΔS°= +2.2 e.u.) for the *R*-isomer with a stoichiometry of almost 1 for both the enantiomeric guest complexes.

The association constant for **81** is higher than the **82** by a factor of almost 3.6. This differentiation is favoured by both enthalpy as well as entropy. The strong complex formation leads to more negative enthalpy change in case of *R*- isomer and slightly more positive entropy also helps in arising a substantial difference in the total free energy.

Figure 4.4.1: ITC-traces of the titration of the host **120** (4.49 mM) into the guest **81** (0.51 mM) and the host **120** (10.28 mM) into the guest **82** (0.96 mM) solution in acetonitrile at 303 K.

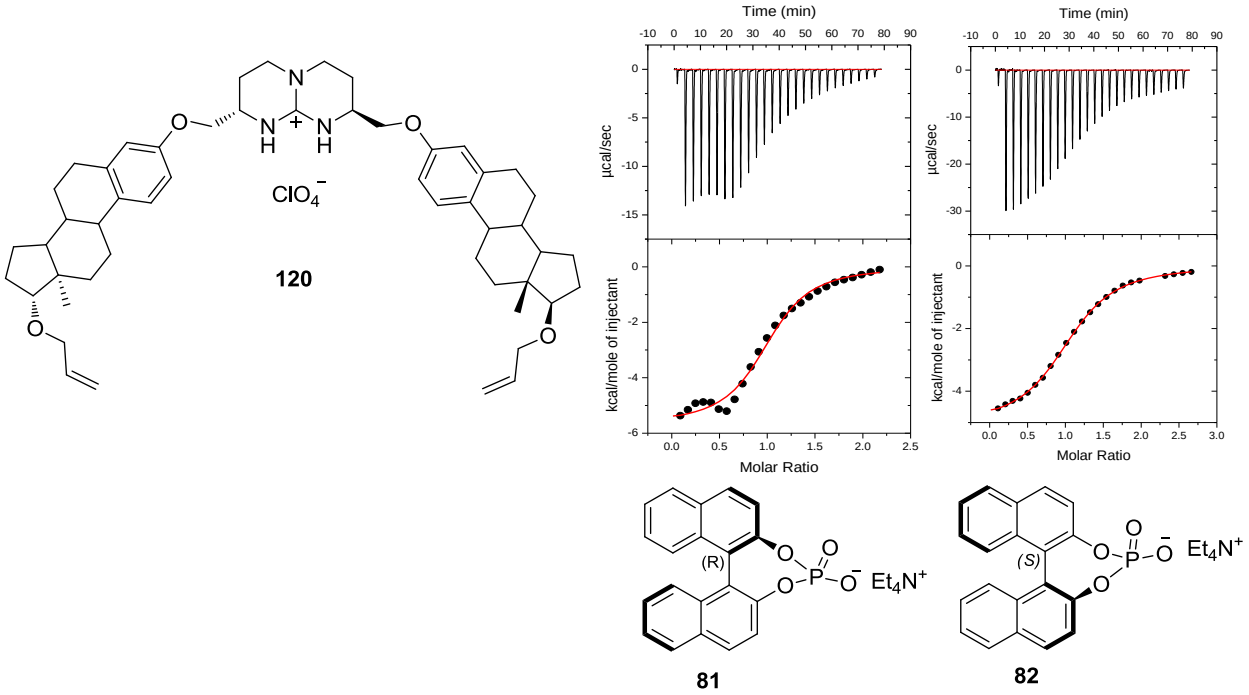

The titration data of the host **120** with tetraethylammonium salts of enantiomers of trolox anion **83** and **84** are represented in the figure 4.4.2. The host guest system proved too complicated for deconvolution. Precipitation was observed after titration of host into the guest for both trolox enantiomers.

Figure 4.4.2: ITC-traces of the titration of host **120** (4.49 mM) into the guest **83** (0.21 mM) and the guest **84** (0.21 mM) solution in acetonitrile at 303 K.

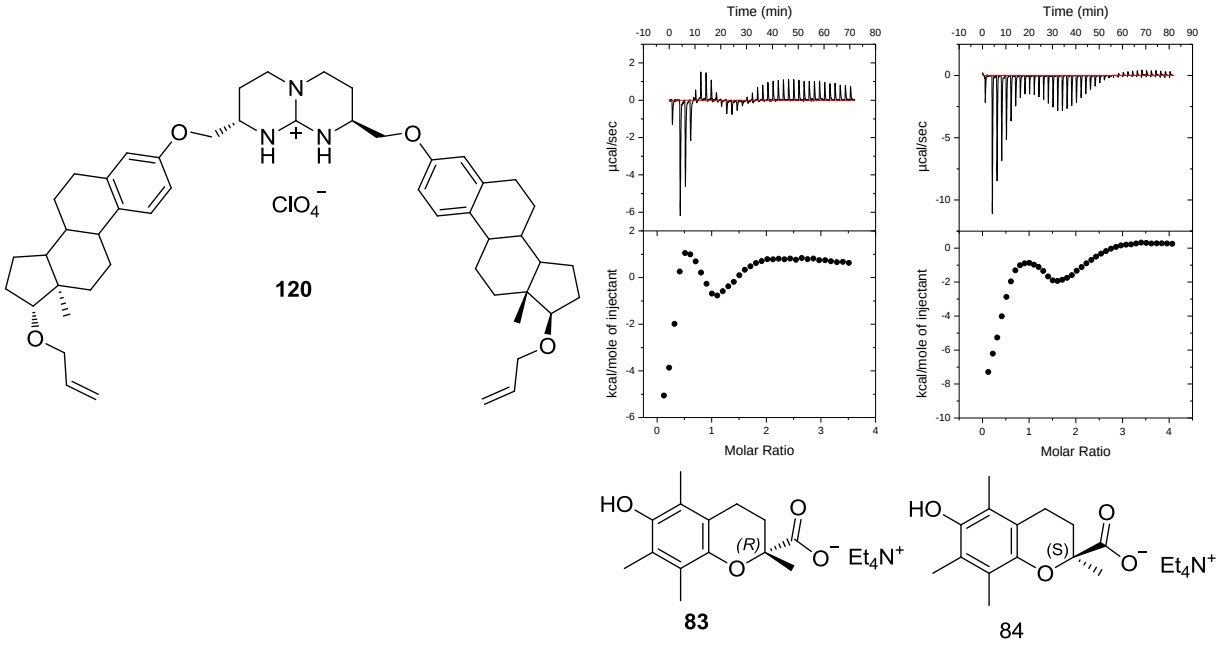

An acetonitrile solution of open-chain steroid host **120** was titrated into solutions of guests **85** and **86** at 303 K (figure 4.4.3). The OSB model curve indicated 1:1 binding between the host and either guest. The association constants were derived as, K_{ass}= 8,820 M^{-1} ($\Delta H°$= -8.5 kcal mol^{-1}, $\Delta S°$= -10.0 e.u.) for the *R*-diphenylphosphinate guest **85** and K_{ass}= 13,600 M^{-1} ($\Delta H°$= -7.7 kcal mol^{-1}, $\Delta S°$= -6.4 e.u.) for the *S*-enantiomer.

The complexation is driven by strong attraction of both the guests towards the host molecule as indicated by highly negative enthalpy values. Formation of a precipitate was observed in both titrations. A highly structured complexation is also indicated by the negative entropy values.

The binding constant for **86** is marginally higher than the guest **85** by a factor of 1.5. This is also a very good example of entropy-driven enantio-differentiation. Though, the enthalpy change is less negative in the case of **86**, it is supported by a less negative entropy value and, in the end, gives a higher total free energy than in the case of **85**.

Figure 4.4.3: ITC-traces of the titration of host **120** (10.284 mM) into the guest **85** (1.07 mM) and the guest **86** (1.12 mM) solution in acetonitrile at 303 K.

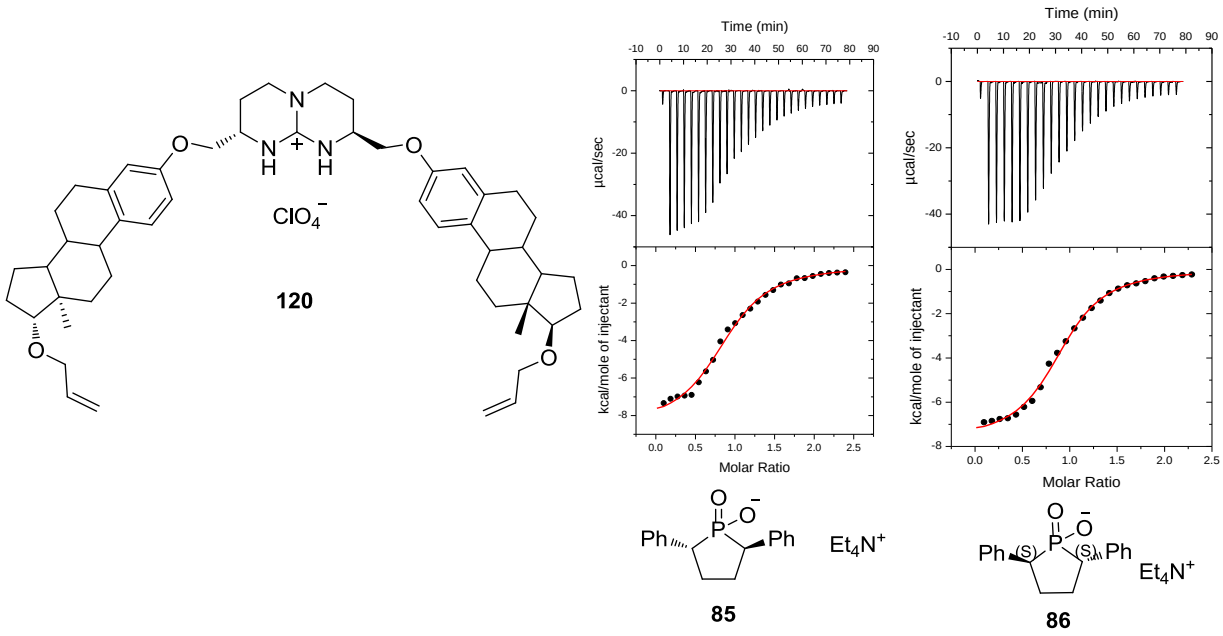

4.5 ITC titration of host 122 with different chiral oxoanions

The titration of host **122** into the acetonitrile solutions of enantiomers of binaphthyl phosphate anion **81** and **82** showed 1:1 binding between the host and either guest (figure 4.5.1). The complexation between host and both guests was highly exothermic suffering compensation by negative entropy contribution. The titration curve fits quite well with the OSB model giving an association constant of K_{ass}= 5,900 M^{-1} ($\Delta H°$= -7.36 kcal mol^{-1}, $\Delta S°$= -7.0 e.u.) for **81** and K_{ass}= 7,500 M^{-1} ($\Delta H°$= -7.25 kcal mol^{-1}, $\Delta S°$= -6.2 e.u.) for **82**. Precipitation was observed following the titrations with both enantiomers at 10 mM host concentration. The mode of binding of both enantiomers to the host molecule **120** appears quite similar resulting in strong well-structured complexation.

The ITC titrations of host **122** into tetraethylammonium salts of *R*- and *S*-trolox (**83** and **84**) anion gave very good fit to the one site binding model (figure 4.5.2). The host formed 1:1 complexes with both enantiomers. Both complexation processes were exothermic. The association constant were obtained as, K_{ass}= 1.8×10^4 M^{-1} ($\Delta H°$= -3.75 kcal mol^{-1}, $\Delta S°$= +7.2 e.u.) for the *R*- trolox and K_{ass}= 2.64×10^4 M^{-1} ($\Delta H°$= -2.45 kcal mol^{-1}, $\Delta S°$= +11.80 e.u.) for the *S*-

isomer. There was a minor enantio-differentiation between **83** and **84** (factor of 1.5) by host **122** which was driven mainly by a positive entropy of association between **84** and host **122**.

Figure 4.5.1: ITC-traces of the titration of host **122** (9.96 mM) into the guest **81** (1.02 mM) anf the guest **82** (1.05 mM) solution in acetonitrile at 303 K.

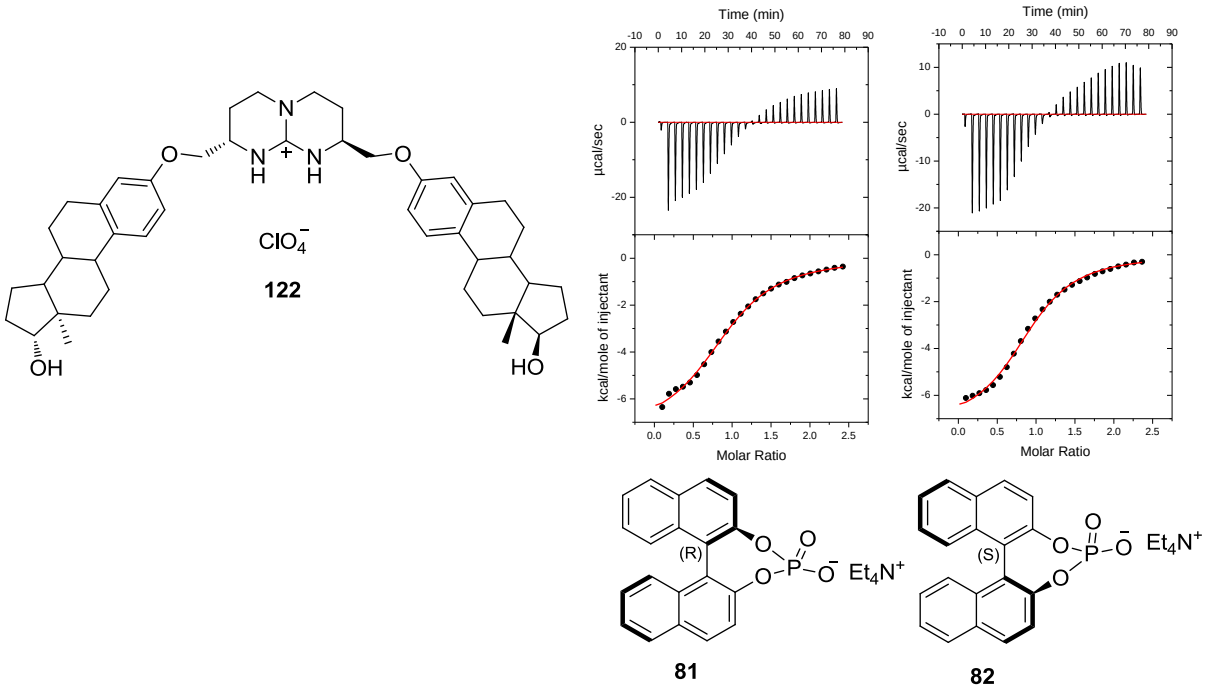

The solution of the open chain steroid host **122** was titrated into solutions of the guests **85** and **86** in acetonitrile at 303 K (figure 4.5.3). 20 µl of the host was titrated into the guest solution over a period of 50 seconds in every injection because the system took a long time to come to equilibrium after each injection. This is evident from broad peaks observed in the ITC traces. The titrations were done in dilute solutions due to the low solubility of the host in acetonitrile. The complexation of both enantiomers of diphenylphosphinate guest displayed favourable enthalpy as well as positive entropy. Analysis by the one site binding model revealed, K_{ass}= 2.4×10^4 M^{-1} ($\Delta H°$= -2.37 kcal mol^{-1}, $\Delta S°$= +12.2 e.u.) for the **85** and K_{ass}= 2.2×10^4 M^{-1} ($\Delta H°$= -2.45 kcal mol^{-1}, $\Delta S°$= +11.8 e.u.) for **86**. There was no enantio-differentiation observed by the host **122** in ITC titrations.

Figure 4.5.2: ITC-traces of the titration of host **122** (2.39 mM) into the guest **83** (0.21 mM) and the guest **84** (0.22 mM) solution in acetonitrile at 303 K.

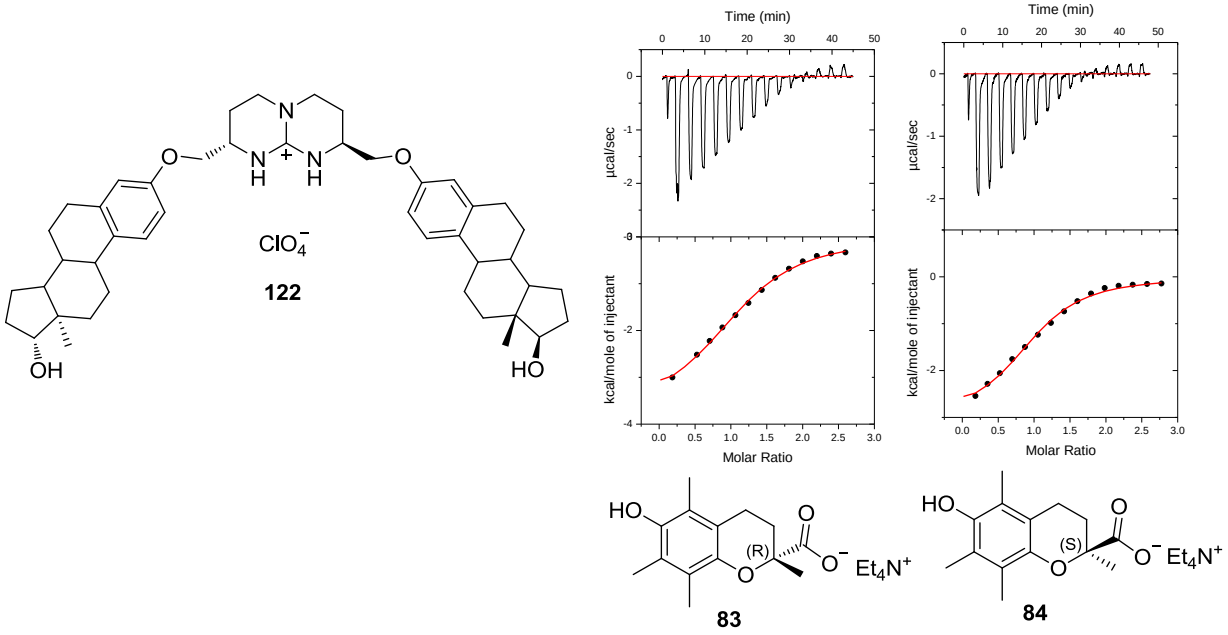

Figure 4.5.3: ITC-traces of the titration of host **122** (2.39 mM) into the guest **85** (0.21 mM) and the guest **86** (0.21 mM) solution in acetonitrile at 303 K.

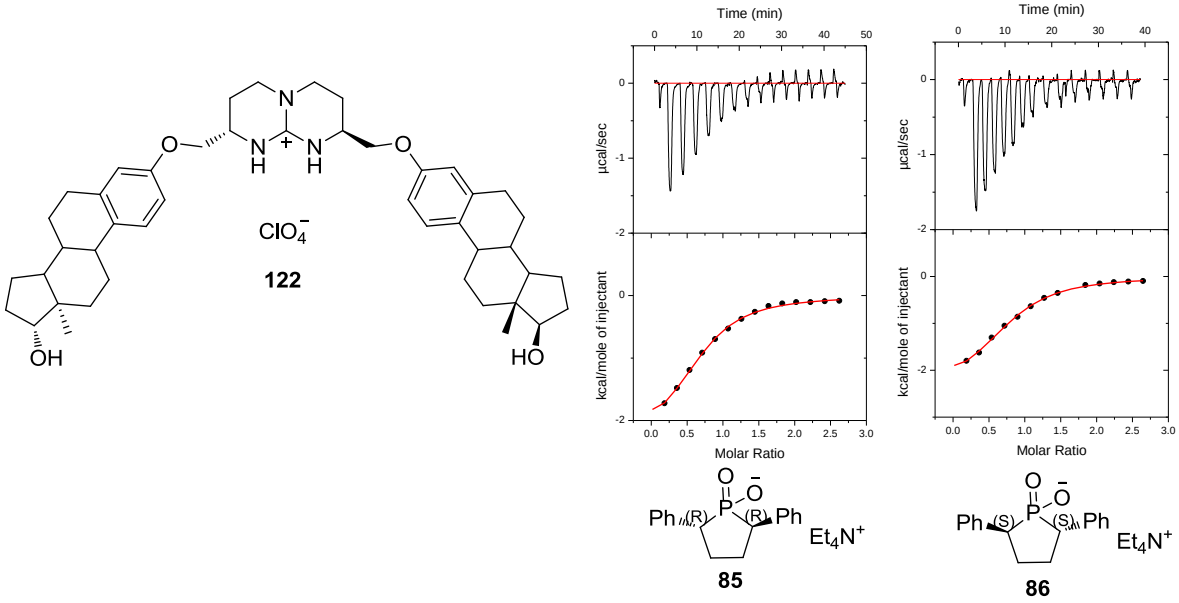

4.6 ITC titration of host 124 with different chiral oxoanions

4.6.1 ITC titrations in acetonitrile

The titrations of tetraethylammonium salts of binaphthylphosphate enantiomers **81** and **82** into the host **124** indicate exothermic complexation (figure 4.6.1.1). The one-site-binding model curve fitting gave the association constants as K_{ass}= 1.21×10^4 M^{-1} (ΔH°= -2.87 kcal mol^{-1}, ΔS°= +9.2 e.u.) for the *R*-binaphthylphosphate and K_{ass}= 1.82×10^4 M^{-1} (ΔH°= -2.53 kcal mol^{-1}, ΔS°= +11.1 e.u.) for the *S*-isomer. The binding affinity between **82** and the host is 1.5 fold higher than between the host and **81**, driven predominantly by the difference in entropy of binding of the two guests.

Figure 4.6.1.1: ITC-traces of the titration of the guest **81** (2.08 mM) and the guest **82** (2.52 mM) into the host **124** (0.11 mM) solution in acetonitrile at 303 K.

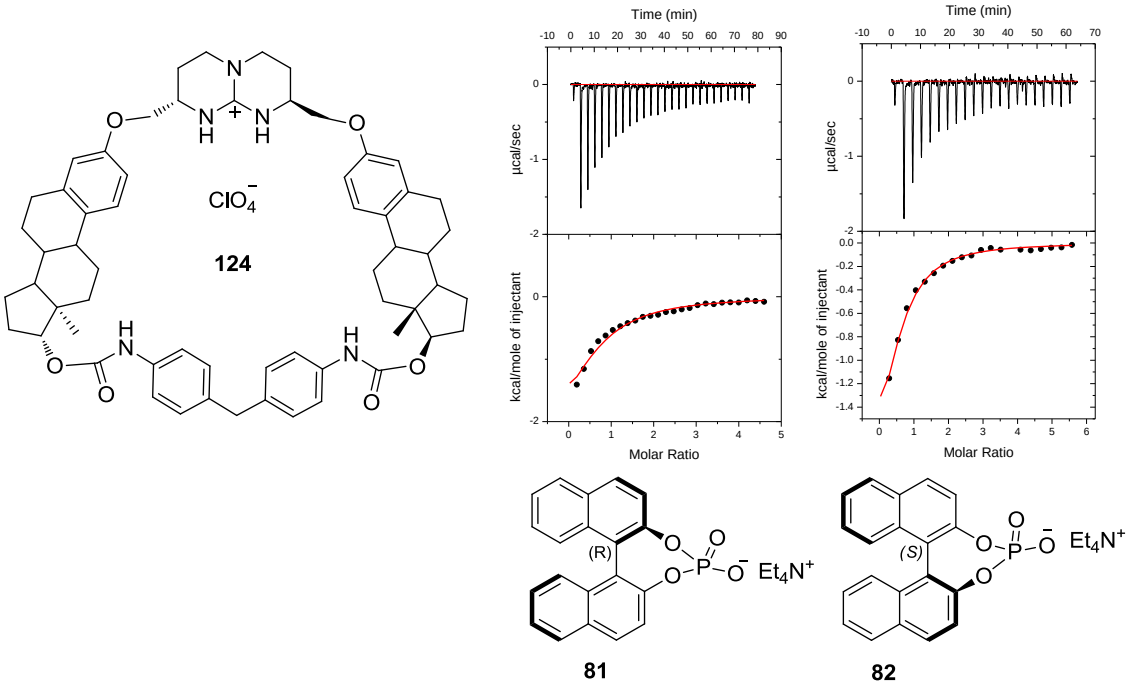

The macrocyclic host **124** was titrated into the acetonitrile solution of tetraethylammonium salts of *R*- and *S*-trolox (figure 4.6.1.1 and 4.6.1.2). The initial part of the titration curve was exothermic. The one-site-binding model curve indicated 1:2 binding between the guest and the host, respectively for both enantiomers. This unexpected stoichiometry could be due to the self-assembly of the host compound or significant amount of impurities. The association constants

were obtained as, K_{ass}= 1.13×10^4 M^{-1} (ΔH°= -3.01 kcal mol^{-1}, ΔS°= +8.6 e.u.) for the *R*- trolox and K_{ass}= 5,600 M^{-1} (ΔH°= -2.39 kcal mol^{-1}, ΔS°= +9.3 e.u.) for the *S*-isomer.

Figure 4.6.1.2: ITC-traces of the titration of host **124** (7.61 mM) into the guest **83** (0.40 mM) and the guest **84** (0.31 mM) solution in acetonitrile at 303 K.

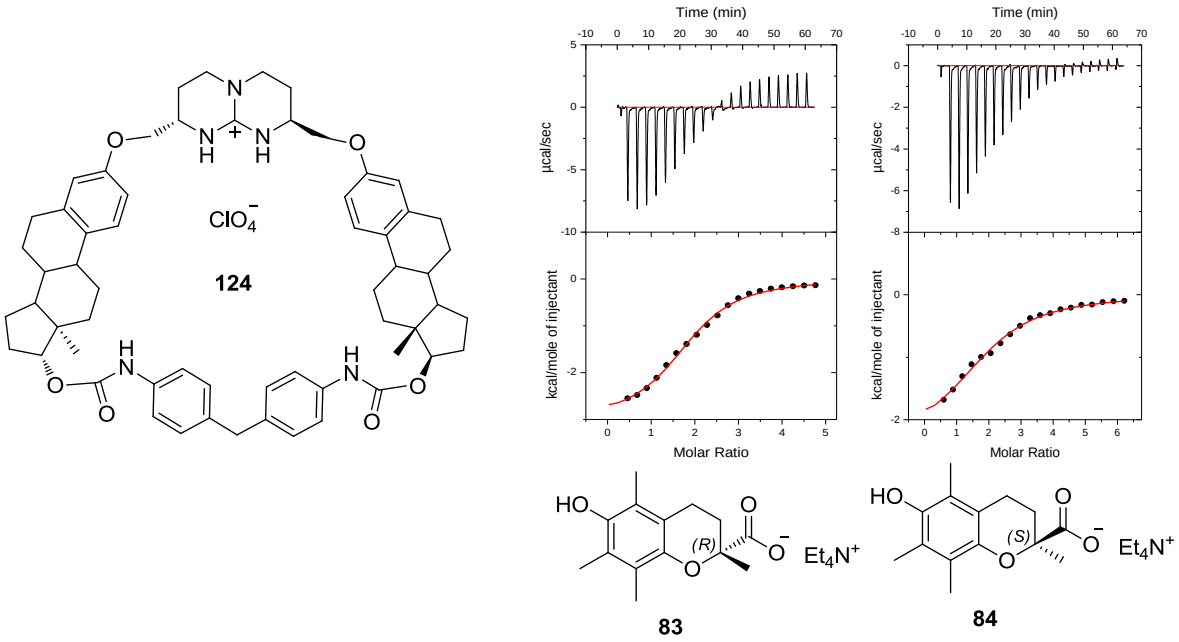

The association constant between the host **124** and **83** is twofold higher than between **124** and **84**. The difference in the binding affinities is predominantly driven by the difference between the enthalpy of complexation of the two enantiomers with the host.

The host **124** had low solubility in acetonitrile and precipitation was observed in the case of titration with Trolox anion. Thus, a dilute solution of the host was prepared and the guests were titrated into the host. The ITC traces from titration of enantiomers of diphenylphosphinate guest **85** and **86** into the host **124** are shown in figure 4.6.1.3. Both complexations were of exothermic nature. The one-site-binding model fitted quite well with the titration curve and allowed elucidation of association constants, K_{ass}= 3.2×10^4 M^{-1} (ΔH°= -6.29 kcal mol^{-1}, ΔS°= -0.1 e.u.) for the *R*-diphenylphosphinate and K_{ass}= 3.5×10^4 M^{-1} (ΔH°= -5.3 kcal mol^{-1}, ΔS°= +3.3 e.u.) for the *S*-isomer. The stoichiometry of complexation was again off the mark and the ratio between guest and host was 0.7 in both cases pointing to insufficient purity of the macrocyclic host.

Figure 4.6.1.3: ITC-traces of the titration of the guest **85** (2.14 mM) and the guest **86** (2.32 mM) into the host **124** (0.11 mM) solution in acetonitrile at 303 K.

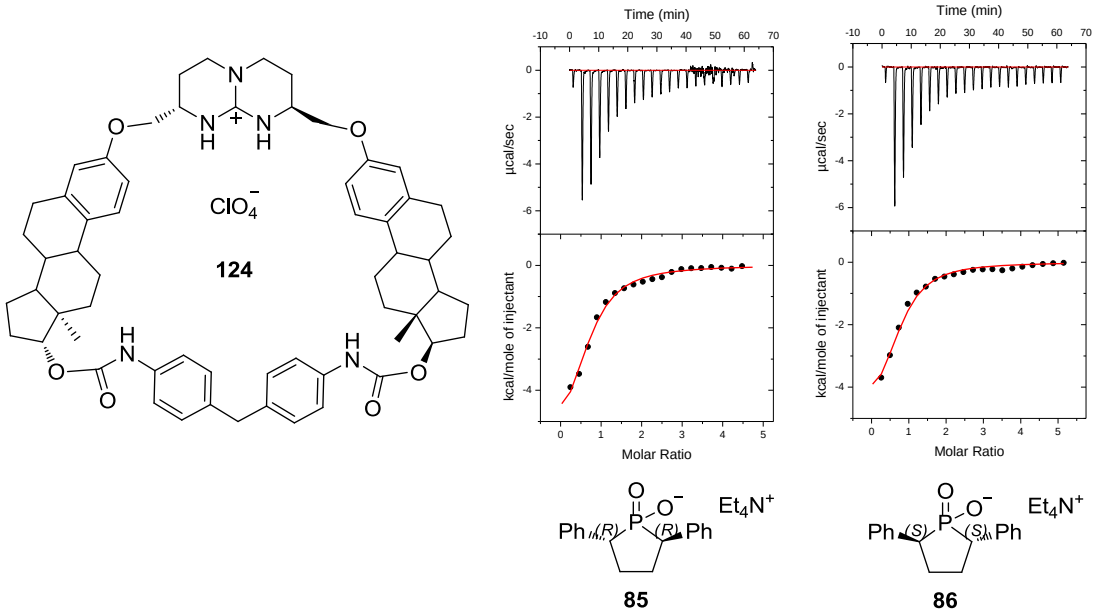

There is no sign of enantio-recognition by host **124** using *R*- and *S*-diphenylphosphinate guests probing. The association constants are identical for both isomers, yet the binding pattern is very different from each other. Binding constant is totally driven by a highly favourable enthalpy for **85**. On the other hand, **86** features less favourable enthalpy, but scores by a positive entropy of association.

4.6.2 ITC titrations in 1,2-dichloroethane

The ITC titrations with macrocyclic host **124** were tried in 1,2-dichloroethane following its low solubility in acetonitrile. The titrations of host **124** into the dichloroethane solution of *R*- and *S*-binaphthylphosphate **81** and **82** resulted in exothermic complexation (figure 4.6.2.1). The titration curves were not so well fit with the one-site-binding model due to the noise in the titration peaks. The association constants were obtained as K_{ass}= 4,600 M^{-1} ($\Delta H°$= -3.76 kcal mol^{-1}, $\Delta S°$= +4.6 e.u.) for the *R*-bisnaphthylphosphate and K_{ass}= 1.68×10^4 M^{-1} ($\Delta H°$= -1.67 kcal mol^{-1}, $\Delta S°$= +13.8 e.u.) for the *S*-isomer.

The association constant for **82** is 3.5 times higher than that of **81**. The respectiveenantio-differentiation is driven predominantly by the change in entropy. Though, the complexation

between the host **124** and **82** is less exothermic than between **124** and **81**, but it is positively compensated by change in entropy.

Figure 4.6.2.1: ITC-traces of the titration of the host **124** (3.78 mM) into the guest **81** (0.22 mM) and the guest **82** (0.2 mM) solution in 1,2-dichloroethane at 308 K.

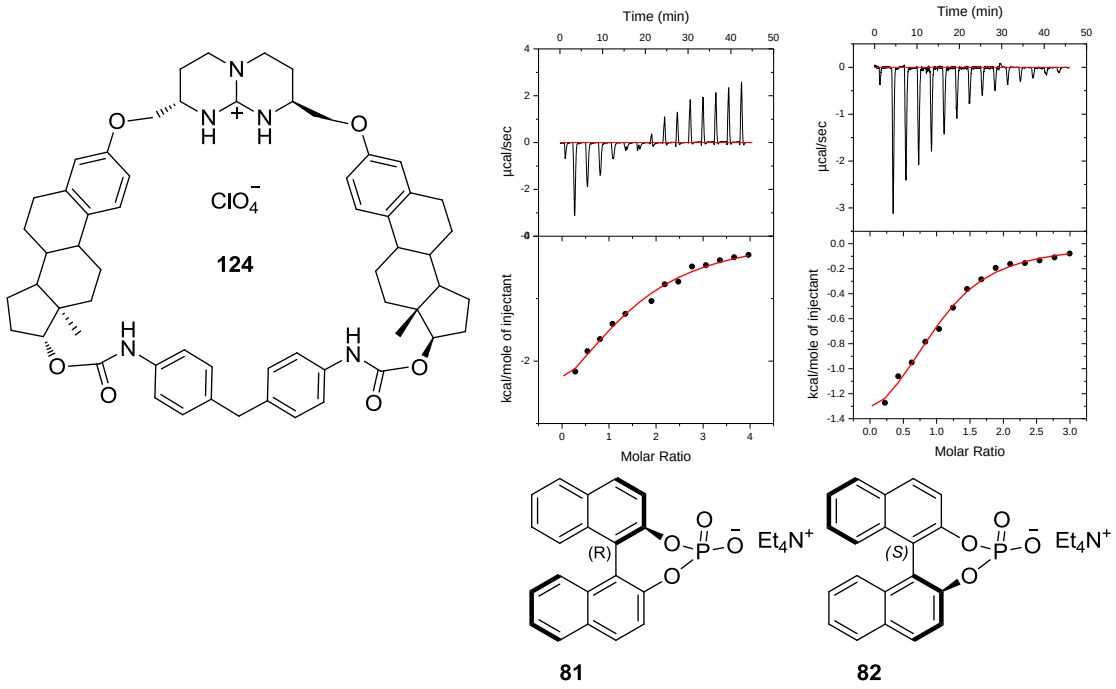

The ITC traces of titration of **124** into the tetraethylammonium salts of diphenylphosphinate enantiomers (**85** and **86**) are shown in figure 4.6.2.2. The one-site-binding model curve fitting indicates 1:1 binding between host **124** and either guest. The association constants were determined as K_{ass}= 1,400 M^{-1} ($\Delta H°$= -3.00 kcal mol^{-1}, $\Delta S°$= +4.5 e.u.) for **85** and K_{ass}= 7,750 M^{-1} ($\Delta H°$= -1.2 kcal mol^{-1}, ΔS= +13.8 e.u.) for **86**.

The binding affinity for *S*-diphenylphosphinate **86** is 5.5 times higher than for the *R*-enantiomer **85**. Interestingly, it is entirely driven by a significantly more positive entropy of association taking **86** as the guest. As can be observed, the titration curves are not exactly reliable due to the noise in the baseline. It might be due to some mechanical error in the measurements or due to the insufficient purity of the compound.

Figure 4.6.2.2: ITC-traces of the titration of the host **124** (3.78 mM) into the guest **85** (0.26 mM) and the host **124** (9.56 mM) into the guest **86** (0.96 mM) solution in 1,2-dichloroethane at 308 K.

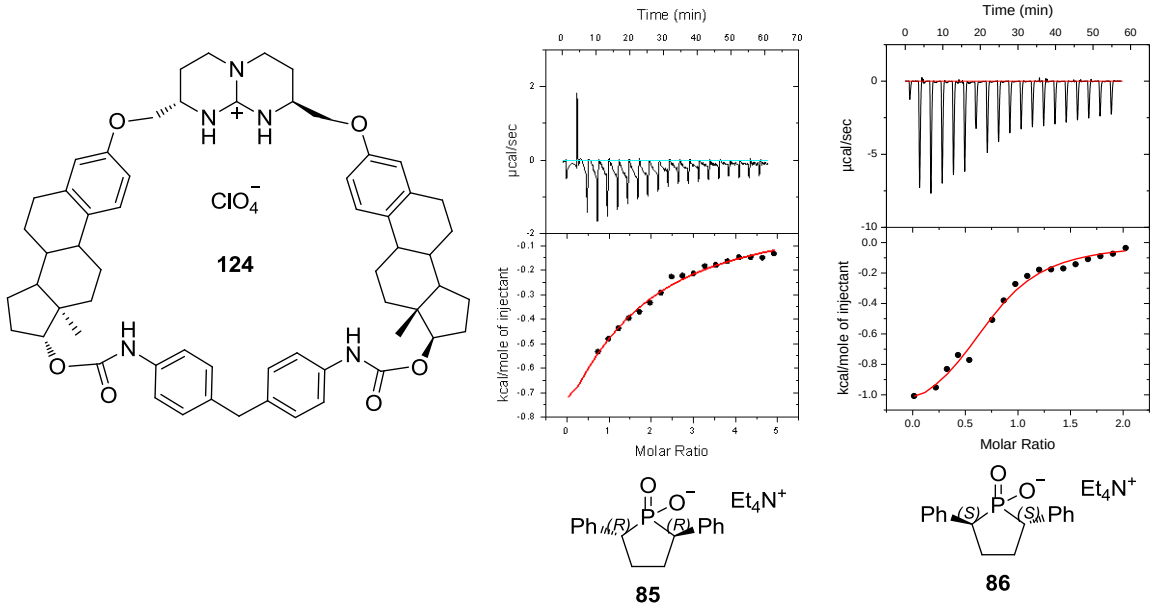

4.7 Molecular Dynamics Simulations

Computation based on molecular models is playing an increasingly important role in biology, biological chemistry, and biophysics. Since only a very limited number of properties of biomolecular systems are actually accessible to measurement by experimental means, computer simulation can complement experiment by providing not only averages, but also distributions and time series of any definable quantity, for example, conformational distributions or interactions between parts of systems.[83] As such, it is an indispensable tool to interpret experimental data. Moreover, it can be used to predict properties under environmental conditions that are difficult or expensive to realize. It also provides an understanding of the relation between microscopic properties and macroscopic behavior. Under favorable conditions computer simulation can be used to obtain quantitative estimates of the quantities like binding constants of ligand to receptors,[84] NMR data of biomolecules,[85] protein folding[86] etc.

Chemical systems are generally too inhomogeneous and complex to be treated by analytical theoretical methods. The treatment of molecular systems in the gas phase by quantum mechanical methods is straightforward; if a classical statistical mechanical approximation is permitted the problem becomes even trivial. This is due to the possibility of reducing the many-

particle problem to a few-particle one based on the low density of a system in the gas phase. In the crystalline solid state, treatment by quantum mechanical or classical mechanical methods is made possible by a reduction of the many-particle problem to a few-(quasi)particle problem based on symmetry properties of the solid state. Between these two extremes, that is, for liquids, macromolecules, solutions, amorphous solids, etc., one is faced with an *essentially* many-particle system. No simple reduction to a few degrees of freedom is possible, and a full treatment of many degrees of freedom is required in order to adequately describe the properties of molecular systems in the fluid-like state.[87] This state of affairs has two direct consequences when treating fluid-like systems.

1. One has to resort to numerical *simulation* of the behavior of the molecular system on a computer, which

2. produces a *statistical ensemble* of configurations representing the state of the system.

If one is only interested in static equilibrium properties, it suffices to generate an ensemble of equilibrium states, which may lack any temporal correlations. To obtain dynamic and non-equilibrium properties dynamic simulation methods that produce trajectories in phase space are to be used. The connection between the microscopic behavior and macroscopic properties of the molecular system is governed by the laws of statistical mechanics.

A biomolecular force field generally consists of potential energy terms representing covalent interactions between atoms (such as bond-stretching, bond-angle bending, improper and proper dihedral-angle torsion) on the one hand and non-bonded interactions on the other hand between atoms in different molecules and between atoms in a molecule that are separated by more than two or three covalent bonds.[88] Since non-bonded interactions govern the thermodynamic equilibria and processes of interest (complexation, protein folding etc.), MD simulations focus on the formulation and parametrization of these potential-energy terms. Furthermore, we are not interested in biomolecular systems at a temperature of 0 K, we have to consider the contribution of entropy S to the free energy F=U-TS of the system of interest. It is well known that entropy plays an essential role in all complexation processes. Changes in free energy that drive processes may result from changes in internal energy (U) or in entropy (S), which may work together or against each other depending on the relative strengths of the non-bonded interactions between the various components (atoms, molecules) of the system.[89]

In MD simulations, mainly atomic and molecular degrees of freedom are considered with the corresponding classical force fields and classical Newtonian dynamics to sample the degrees of freedom. System sizes, which includes explicit solvent molecules, that can be considered range up to 10^5 or 10^6 atoms or particles, which is still very small compared to Avogadro's number, that is, macroscopic sizes. For such small systems, the modeling of the boundary or surface will have a large effect on the calculated properties. Such surface effects can be minimized by using periodic boundary conditions, where the box that contains the molecular system is surrounded by an infinite number of copies of itself (Figure 4.7.1). This avoids surface effects at the expense of introducing periodicity artefacts. Thus, GROMOS MD simulation can be beneficial in addressing the following aspects of theoretical calculations

i) Calculations are done in the presence of explicit solvent molecules which can duplicate the experimental host-guest system quite well.

ii) Periodic boundary conditions can avoid the surface effects.

iii) Force field which addresses bonded as well as non-bonded interaction between host and guest. It takes into account both, enthalpy and entropy, factor of the free energy.

Figure 4.7.1: Three types of spatial boundary conditions used in molecular simulation.

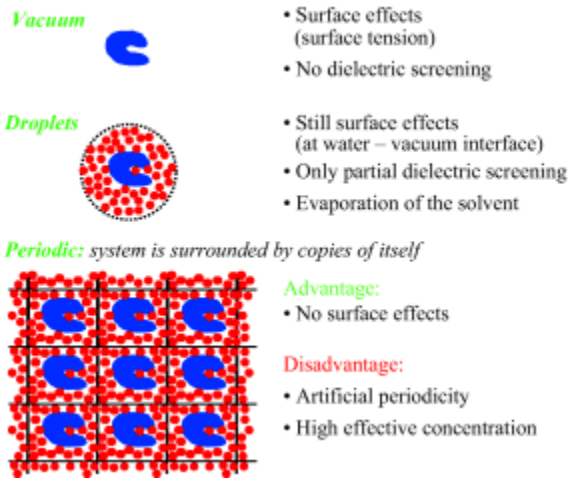

MD simulations were performed using GROningen MOlecular Simulation program package GROMOS'96[90] software and Pentium PC's. GROMOS'96 was developed for the dynamic modelling of (bio)molecules using the methods of molecular dynamics, stochastic dynamics, and energy minimization as well as the path-integral formalism. It has been widely used for small molecules having peptide residues like arginine with its guanidine side chain. Owing to the

similarities between acyclic guanidine and the bicyclic guanidines it is easier to employ this software for present calculations. GROMOS not only offers force field 45a4 ‘’united atom’’ but also a software package for analysis of the resulting data.

Simulations were carried out in chloroform at 300 K to study the complexation between host-guest ion pairs as presented in table 4.7.1.1. The molecular modelling studies were carried out in explicit solvent on open chain hosts **115** and **120** and macrocyclic host **116** with enantiomers of binaphthyl phosphate (**81**, **82**), diphenylphosphinate (**85**, **86**) anions and mandelate (**87**, **88**).

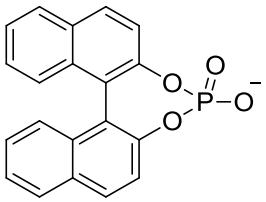

81 and **82** **85** and **86**

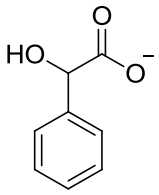

87 and **88**

The MD simulations were successfully run by GROMOS’96 program using two different sets of files – the topology files and the coordinate files. The topology files for host and guest were constructed according to the rules described in the GROMOS manual. [90] The partial charges for phosphorus atom and bond parameters for the C-P bond in the guest molecules **85** and **86** were adapted from the literature.[91] The combined coordinate file was prepared by first drawing the structures of the respective host and guest molecule in the ChemSketch (ACD/Labs Release: 12.0) program (drawn close enough but separate structures as the initial conformation of the plausible complex) and then the combined structure was saved as 3D coordinate file (*.mol). Using the Openbabel (version 2.2.1) program, the 3D coordinate file was converted into the GROMOS file (*.gr96). Then the respective host and guest topology files were combined along with the 3D coordinates followed by the energy minimization in vacuum using the GROMOS’96 program. The MD simulations can be run in vacuum or in a solvent. The boundary conditions (the box size and shape) and the solvents were decided prior to the energy minimiation. The truncated octahedron box was chosen for all the MD simulation studies as it offers the spherical surrounding which bear a resemblance to the natural system.

The energy-minimised structures were placed into the pre-equilibrated box filled with the explicit solvent molecules. The MD simulations were performed in chloroform at 300k

temperature for a period of 10 nano seconds. The results obtained from the MD simulations were analysed using the provided software. The non-bonded interactions or energies found and the H-bond analysis from the MD simulations between different host-guest pairs is discussed in the following sections.

4.7.1 MD simulations of host 116 with phosphate guests (81 and 82)

The MD simulations were run on host **116** and guests **81** and **82** in explicit chloroform solvent at 300 K. The supramolecular complex formed between host **116** and enantiomeric guests **81** and **82** was stabilized by the electrostatic interaction between guanidinium and the phosphate units. The boundary conditions applied in the individual runs for all the host-guest pairs are shown in the table 4.7.1.1.

Table 4.7.1.1: All simulations in this table were carried out in chloroform at 300 K.

host	guest	edge size [Å]	No. of solvent molecules
116	**81**	41.8	261
116	**82**	42.5	276
116	**85**	42.4	273
116	**86**	42.9	286
116	**87**	41.6	264
116	**88**	42.6	277
120	**81**	49.2	435
120	**82**	49.3	430

Cluster analysis was performed to examine the favourable conformation of the host-guest pair over the period of the MD simulation. First, the atom-positional root-mean-square deviation (RMSD) between all pair of structures in a given trajectory file was calculated for the cluster analysis. For this, atom names were defined in the input file which were used for least square translational and rotational fitting of the atom positions for the calculation of the RMSD. We took only heavy atoms (N, C and O) for all the MD runs. Then, the cluster analysis was run using this RMSD output file as the input file. A cut off value was set to specify the similarity criterion for two structures. This analysis gave most abundant cluster structures of the host-guest complex with their size as the number of similar conformations in the particular cluster.

The cluster analysis of the molecular dynamics simulations between **116** and **81** showed that there were three major conformations of the supramolecular complex formed between the host **116** and the guest **81** (figure 4.7.1.1). It is evident from the three major conformations that the guest cannot enter into the host cavity due to its big size. Similarly, for the guest **82**, two major conformations were obtained from the cluster analysis (figure 4.7.1.2).

Figure 4.7.1.1: Most abundant conformations of the host (**116**) - guest (**81**) complex obtained from cluster analysis, a > b > c

a) 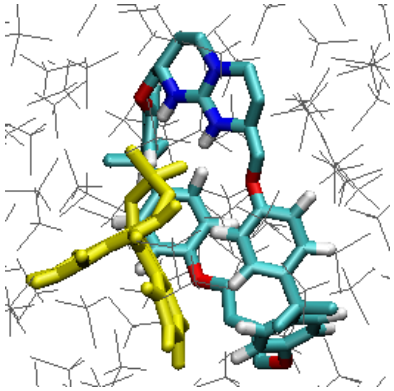

b) 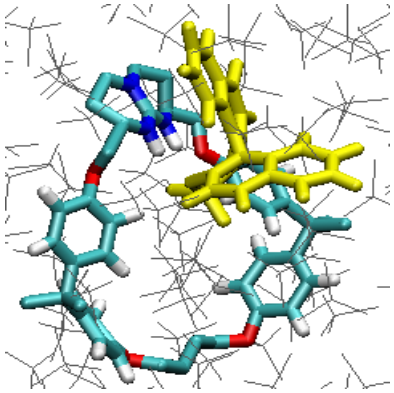

c) 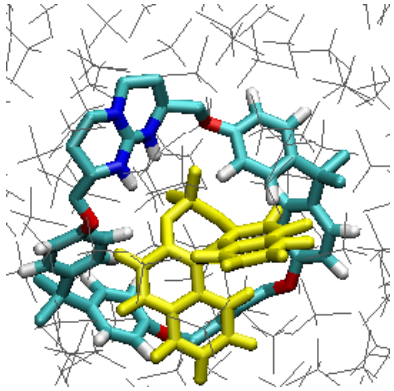

The hydrogen bond analysis of the two complexes is shown in figure 4.7.1.3. The graph shows occurrence of different hydrogen bonds in the structures obtained during the molecular dynamics run. The hydrogen bonds were defined by specifying the maximum cut off distance between the hydrogen and the acceptor and the minimum cut off angle between the donor, the hydrogen and the acceptor. These parameters were set as 0.35 for the maximum distance and 135 for the minimum angle for all the H-bond time series. The acceptor and donor atoms and the hydrogen itself were identified by their masses in a separate input file (massfile).

Figure 4.7.1.2: Most abundant conformations of the host (**116**) - guest (**82**) complex obtained from cluster analysis, a > b

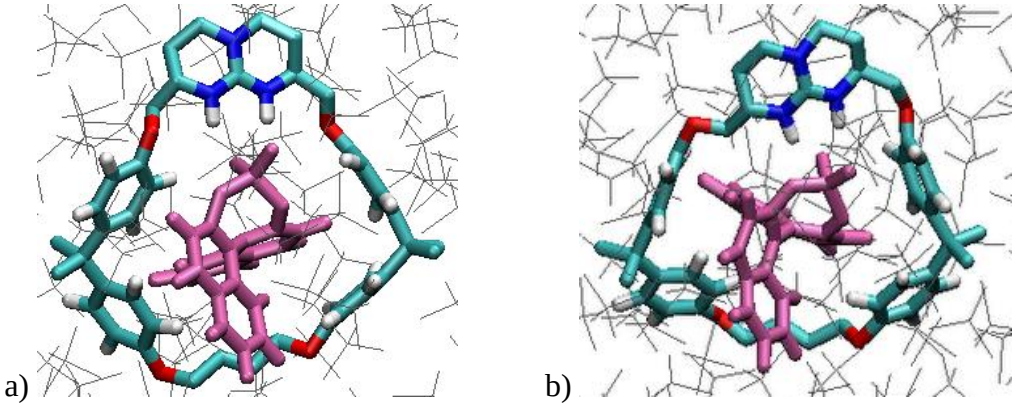

Two groups (A and B) can be defined between which the H–bonds need to be calculated. In all the MD calculations, the host molecule was defined as the donor and the guest molecule was defined as the acceptor as we were concerned with only intermolecular hydrogen bonding. Evidently, there is no chemical basis to the time series obtained for hydrogen bonds, but it gives a fair idea about the H-interactions between the host and the guest molecules. In spite of this, these results can be effectively incorporated in designing a host-guest system by applying the knowledge of chemical properties of the host and the guest.

Figure 4.7.1.3: Possible hydrogen bond interactions depicted in the figure 4.7.1.4

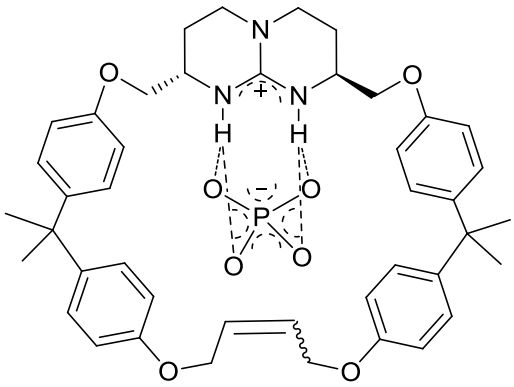

The hydrogen bonds 1-8 correspond to the interaction between guanidinium NH's and electronegative phosphate oxygen atoms (figure 4.7.1.3) in the figure 4.7.1.4. It is evident from the graphs shown in the figure that the non-bonding interaction is dominated by the hydrogen bonds formed between phosphate oxygen atoms and guanidinium NH's. The hydrogen bonds between two units occur exclusively in more than 60% of the possible conformations in the

course of molecular dynamics run during a period of 10 nano seconds. There is some interaction between aromatic CH's and the negatively charged phosphate oxygen as well (H-bond no. 9 and 10 in figure 4.7.2.3), but it accounts only for less than 10% possible conformers.

Figure 4.7.1.3: Time series of hydrogen bond occurrence between; a) **116** and **81**; b) **116** and **82** over a period of 10 ns at 300 K in chloroform.

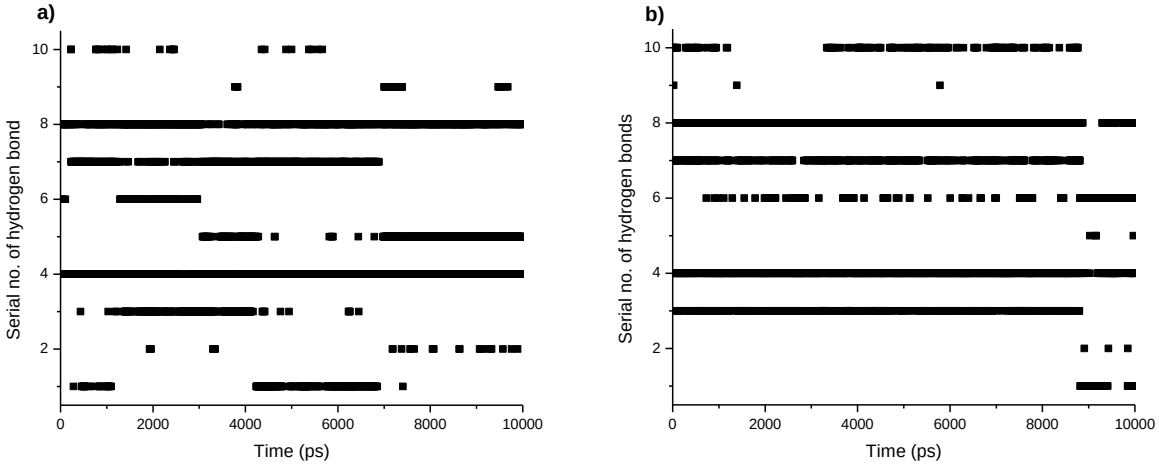

4.7.2 MD simulations of host 116 with phosphinate guests (85 and 86)

Molecular dynamic simulations were performed on host **116** with diastereomeric phosphinate guests **85** and **86** in explicit chloroform solvent at 300 K. The MD calculations of host **116** with **85** and **86** were inconclusive in terms of enantiomeric differentiation of the two guests by the host **116**, but it showed that both the enantiomers could enter into the cavity of the molecule over a trajectory of 10 nano seconds which means that there must be some specific geometric interaction between the host and the guest. Looking at the most abundant cluster structures of the host-guest complexes (figure 4.7.2.1 and 4.7.2.2), it was clear that the phenyl rings of the guests **85** and **86** interacted with the side arms of the host **116**. The electrostatic interaction between the host **116** and the guests **85** and **86** dominated other non-bonding interactions which was evident from the fact that guanidinium carbon and phosphiinate functions were in close vicinity to each other in all the conformations. The conformational structures also suggested that there might be possible CH-π or π-π interaction between the aromatic rings of the host and the guests.

Figure 4.7.2.1: Most abundant conformations of the host (**116**) - guest (**85**) complex obtained from cluster analysis, a > b > c > d.

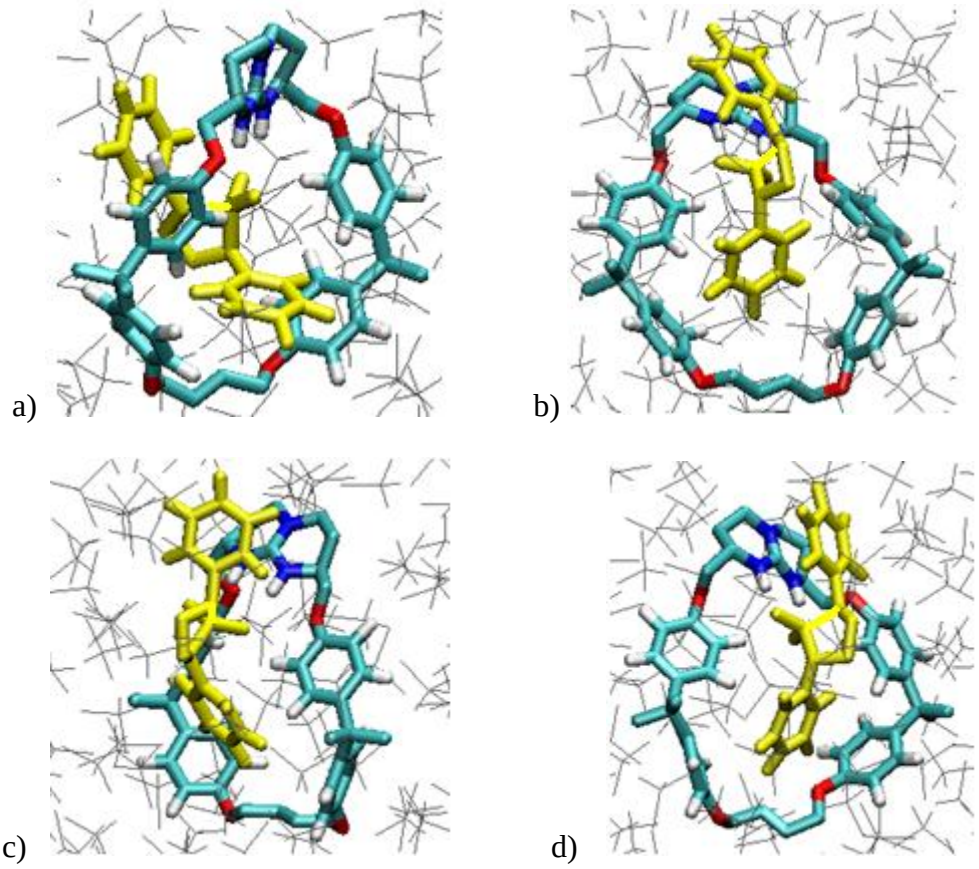

Figure 4.7.2.2: Most abundant conformations of the host (**116**) - guest (**86**) complex obtained from cluster analysis a> b > c > d.

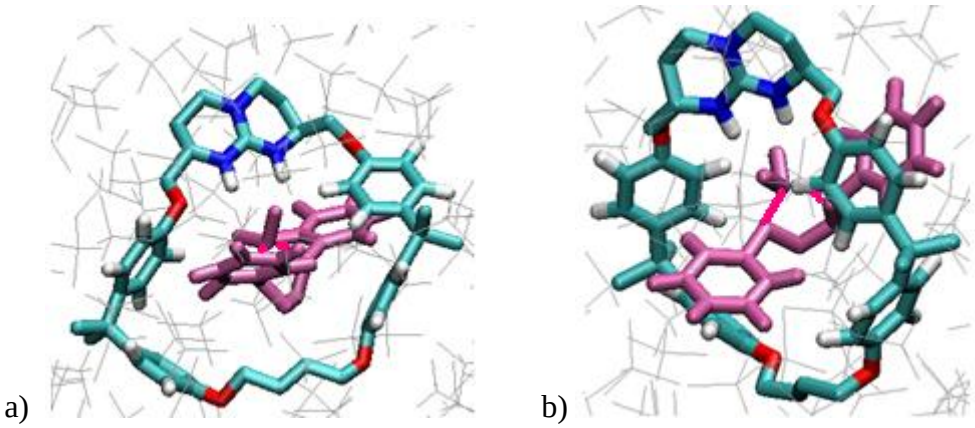

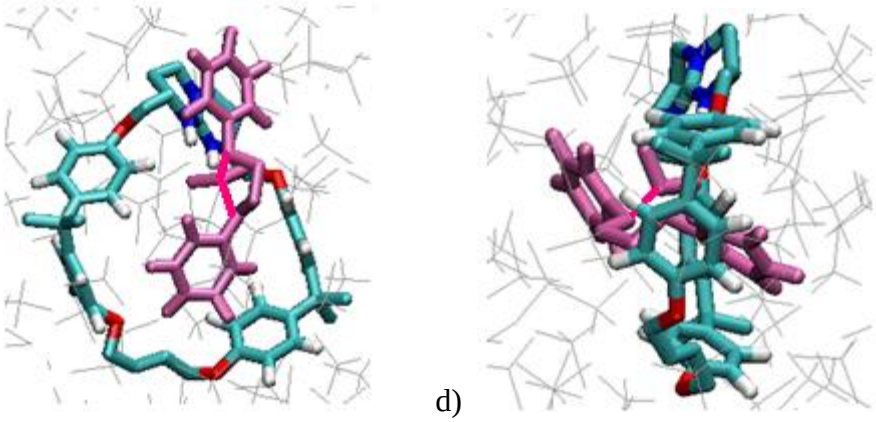

c) d)

Hydrogen bond analysis of the same simulation runs showed that the major contribution came from the hydrogen bonding between the guanidinium NH protons and the phosphinate oxygen atoms (figure 4.7.2.3). The guanidinium NH's are very good hydrogen bond donors because of the high electronegativity of nitrogen and phosphinate oxygen atoms act as excellent hydrogen bond acceptor. But interestingly, other significant hydrogen bonding interactions could also be observed from the time series shown in the figure 4.7.1.3.

Figure 4.7.2.3: Possible hydrogen bond interactions depicted in the figure 4.7.2.4

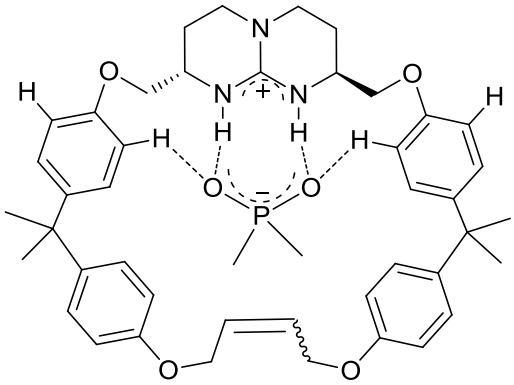

In the graphs shown in the figure, the hydrogen bonds 1-4 belong to the interactions between the phosphinate oxygens and the guanidinium NH's and the hydrogen bonds 5-10 indicate the interaction between aromatic CH's of the host (near to the guanidinium unit) and phosphinate oxygens. This indicated further the possibility of geometric interaction between the host **116** and the guests **85** and **86**.

Figure 4.7.2.4: Time series of hydrogen bond occurrence between; a) **116** and **85**; b) **116** and **86** over a period of 10 ns at 300 K in chloroform.

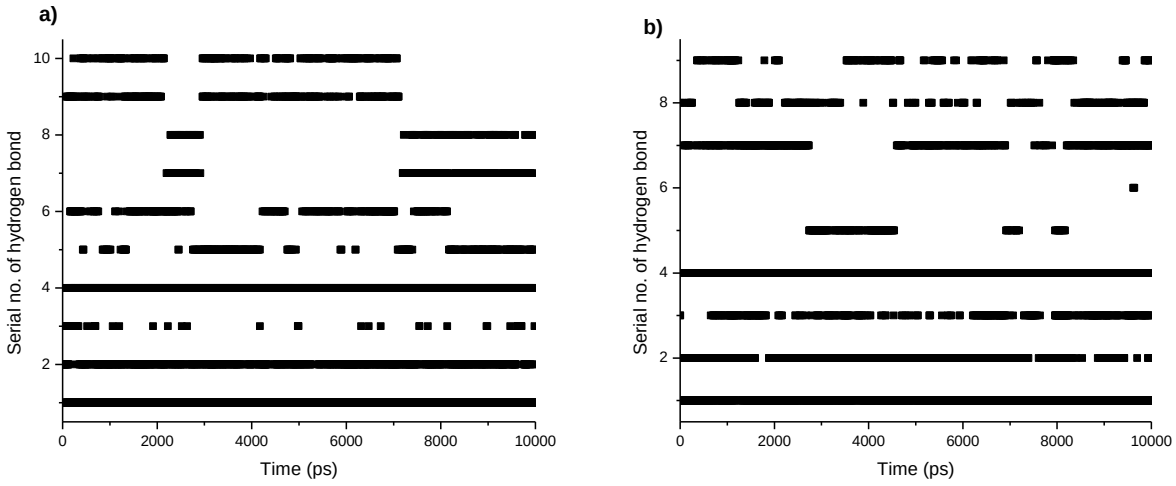

4.7.3 MD simulations of host 116 with mandelate guests (87 and 88)

The molecular dynamics simulations on the host **116** with the guests **87** and **88** were performed at 300 K in explicit chloroform solvent. The cluster analysis of the MD simulations of **116** with **87** and **88** gave three most abundant conformations of the complex formed between the host and the guests (figure 4.7.3.1 and 4.7.3.2). It is clear from the figures that the mandelate anion is too small in comparison to the cavity of the host **116**. And hence, there is very small possibility of any non-bonding interaction between the mandale guests and the hydrophobic side arms of the host **116**. The electrostatic interaction between carboxylate and the guanidinium unit was the driving force between the host and the guest enantiomers in the complexation process.

Figure 4.7.3.1: Most abundant conformations of the host (**116**) - guest (**87**) complex obtained from cluster analysis, a > b > c

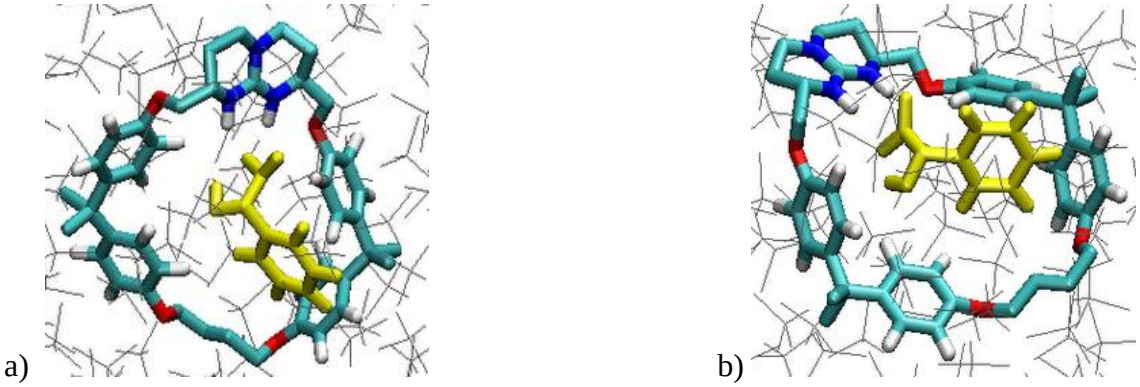

c) 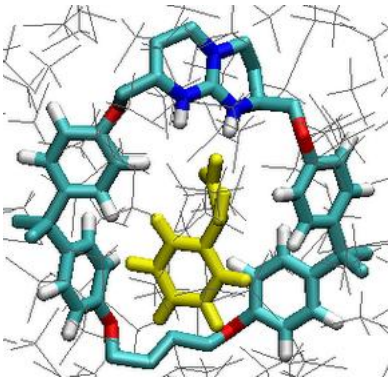

Figure 4.7.3.2: Most abundant conformations of the host (**116**) - guest (**88**) complex obtained from cluster analysis, a > b > c

a) 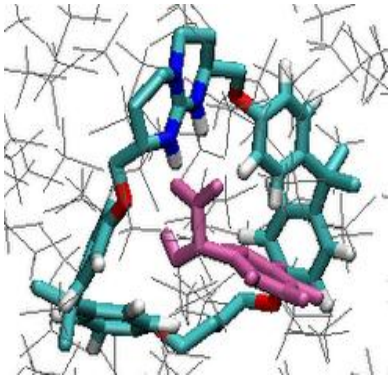

b) 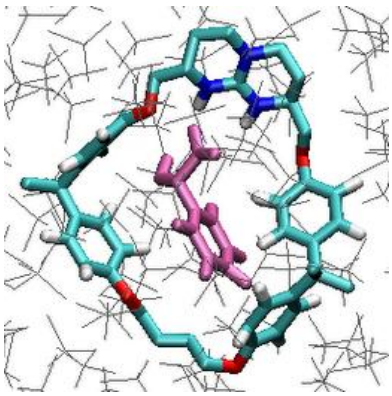

c) 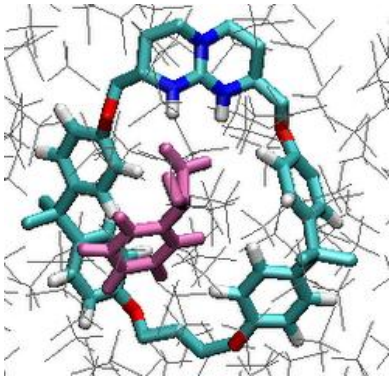

The hydrogen bond analysis between the host and the guest again confirmed that there was no contacts of H-bonding distance between the host side arms and the mandelate anion. The NH···O hydrogen bonding between the guandinium unit and the carboxylate function (hydrogen bond no. 1-4) dominates the possible non-bonding interactions (figure 4.7.3.4).

Figure 4.7.3.3: Possible hydrogen bond interactions depicted in the figure 4.7.3.4

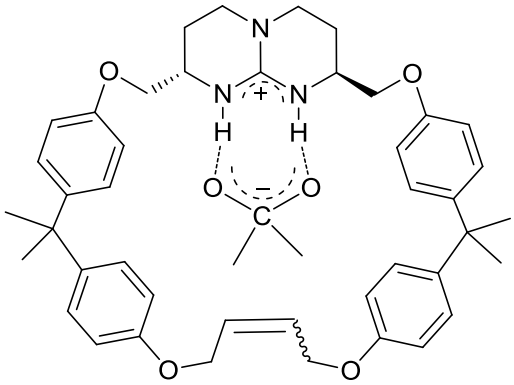

Figure 4.7.3.4: Time series of hydrogen bond occurrence between; a) **116** and **85**; b) **116** and **86** over a period of 10 ns at 300 K in chloroform.

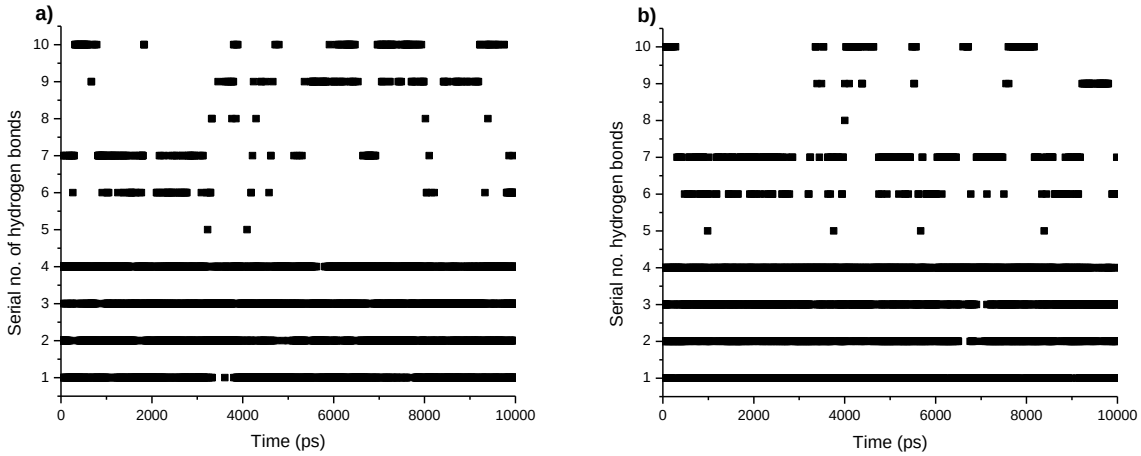

4.7.4 MD simulations of host 115 with mandelate guest 87

The molecular dynamic calculations of interaction between mandelate enantiomer **87** and host **115** showed that the major hydrogen bonding contribution comes from the interaction between guanidinium NH protons and charged oxygen atoms of guest molecules. There are some indications about the preferred geometrical configurations as well. The change in dihedral angle (CH-O-CH_2-CH) of host **115** within the trajectory of 10 nano seconds in the molecular dynamic simulations with mandelate anion clearly indicated that the two arms tend to point in the same direction (figure 4.7.4.1). This might be due to the non-bonding interactions between mandelate anion and guanidinium side chains. The host molecule has very flexible side arms which can move freely in space. This was reflected in the cluster analysis of the MD simulation of the

interaction between host and guest in chloroform at 300 K. There was no preferred conformation in the course of the molecular dynamics simulation as indicated by the cluster analysis.

Figure 4.7.4.1: Initial and final configuration (after molecular dynamics simulation) of the host **115** with the guest **87** in chloroform at 300 K.

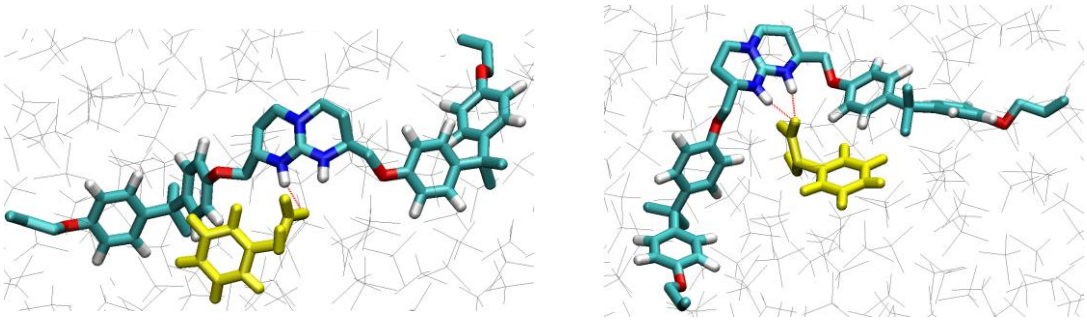

4.7.5 MD simulations of estradiol host 120 with phosphate guests (81 and 82)

The molecular dynamic simulations between host **120** and the binaphthyl guests **81** and **82** were performed at 300 K in chloroform over a period of 10 nano seconds. Like in the case of the host **115**, the host **120** also has a very flexible structure. The number of degree of the freedom of the host molecule is quite high because the steroid side arms are free to move in the space. The cluster analysis (figure 4.7.5.1 and 4.7.5.2) supported this expectation as it did not give any preferred conformation of the complex formed between the host **120** and the guests **81** and **82**.

Figure 4.7.5.1: Initial and final configuration (after molecular dynamics simulation) of the host **120** with the guest **81** in chloroform at 300 K.

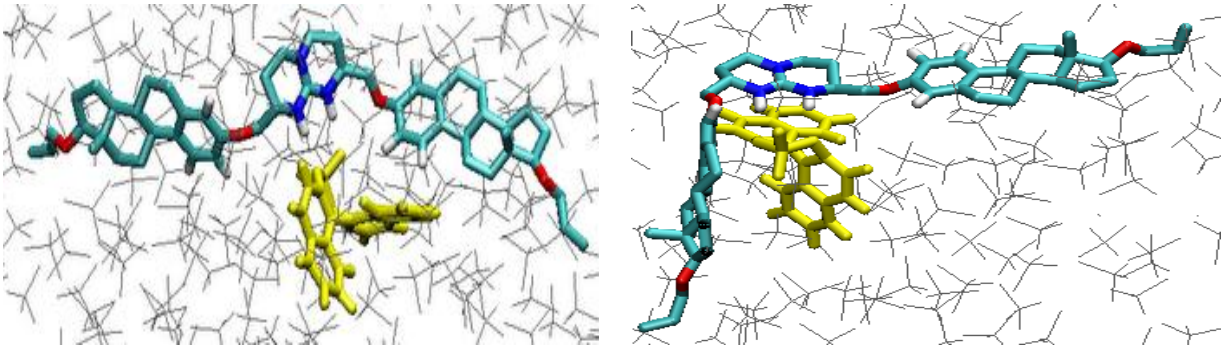

Figure 4.7.5.1: Initial and final configuration (after molecular dynamics simulation) of the host **120** with the guest **81** in chloroform at 300 K.

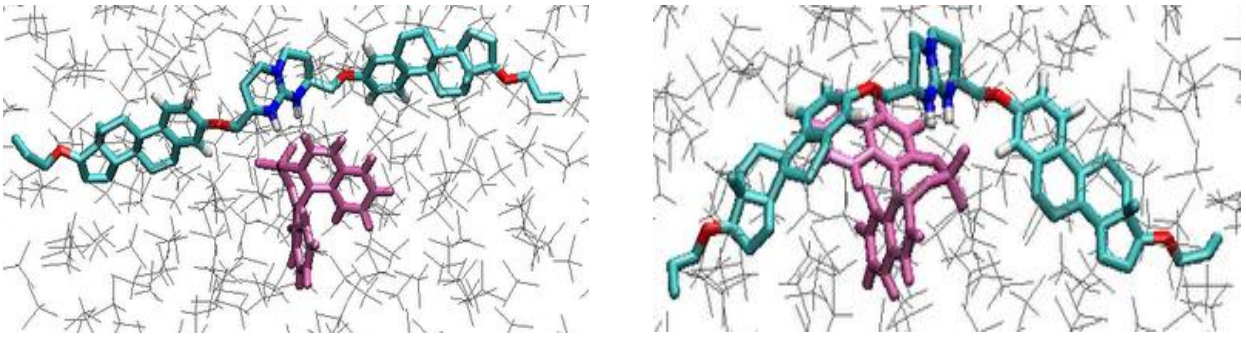

5. Experimental Procedures

5.1 Reagents, Methods and Materials

All reactions were carried out in oven-dried glassware under an inert nitrogen / argon atmosphere. All chemicals were purchased from Sigma-Aldrich, Fluka, ABCR, Strem Chemicals or Fluorochem and used as received for the synthesis. Dry solvents like dichloromethane, acetonitrile and dimethylformamide were purchased from Sigma-Aldrich on molecular sieves and used without further purification. Tetrahydrofuran, toluene and ethanol were dried & purified as described below.

Tetrahydrofuran (THF), Toluene and 1, 4-dioxane

Technical grade solvents from the in-house store were first distilled under nitrogen atmosphere. Sodium wire was pressed into the freshly distilled solvents, benzophenone (about 15 grams/litre as an indicator) was added and the flask was stoppered and was kept in dark overnight. Light blue-green to deep purple colour change during reflux indicated the absence of water in the solvent. Before use, the solvent was refluxed under inert nitrogen for an hour and required quantity of solvent was withdrawn every time.

Absolute ethanol

6 g of sodium metal per litre of freshly distilled ethanol was dissolved and 20 g diethyl phthalate was added and refluxed for 1 h under inert nitrogen atmosphere. Then, the solvent was distilled over a vigreux column and stored on $4A^{o}$ molecular sieves.

All other solvents were distilled before use (first 10-15% fractions were discarded). Triethyl amine and EDIPA were stored on potassium hydroxide before distillation from calcium hydride.

Almost all reactions were monitored by RP-HPLC. HPLC instrumentation includes Merck-Hitachi L-6200A Intelligent Pump, Knauer UV-VIS Filter-Photometer and Sedex 55 LSD detector. The chromatograms were recorded by Kipp & Zonen BD112 two channel recorder. Following are the reverse phase HPLC columns used-

- Macherey-Nagel EC 250/4.6 Nucleodur C18 Pyramid, 3µ
- Macherey-Nagel EC 250/4 Nucleodur 100-5 C18 EC
- Macherey-Nagel EC 250/4 Nucleodur 100-5 CN
- Phenomenex Aqua 125/4 C18, 5µ
- Nucleodur 125/4 100-3 C8 EC

HPLC grade methanol and acetonitrile were purchased from VWR International, Germany. All eluents were prepared by mixing methanol / acetonitrile and water with 0.1 % trifluoroacetic acid as buffer and degassed by ultra-sonification.

Silica gel TLC and Aluminium oxide TLC-PET foils from Fluka were also used occasionally for reaction progress monitoring; visualization was effected with UV and/or by developing in iodine. Uniplate Silica gel GF Prep-TLC's from Analtech Inc., USA and commercially available solid phase extraction (SPE) cartridges from Alltech (High Capacity C18) were used for small scale purifications. Silica gel 100 (0.063-0.200 mm) from Merck was used for medium to large scale purifications.

Moreover, medium pressure reverse phase Flash-Chromatography was performed using C8 or CN-modified silica gel in Michael-Miller columns connected to HPLC Pump 64, UV detector and a recorder (all from Knauer).

Microwave reaction was carried out in a house hold microwave oven, Model MW 20 Digital W / MW 20 Digital S from TechnoStar.

Kugelrohr distillation was performed in a Büchi Glass oven B-585 apparatus connected to a high vacuum pump.

NMR spectra were recorded on a Brucker AV-250 / 360 / 500 MHz spectrometer at 250 / 360 / 500 (^{1}H), 63 / 91 (^{13}C) MHz and 121 MHz (^{31}P) at 298 K. Chemical shifts are reported in δ (ppm) relative to the solvent residual peak [92] $CDCl_3$ / DMSO-d_6 / MeOD / CD_3CN as internal standards (^{1}H and ^{13}C) and H_3PO_4 as external standard for ^{31}P. Data for ^{1}H are reported as follows: chemical shift, multiplicity (s = singlet, d = doublet, t = triplet, bs = broad signal, m = multiplet), coupling constants (*J*) in Hz and integration.

Mass spectra were recorded on LCQ Classic Electrospray-Ionisation (ESI, HPLC-MS). High-resolution mass spectra were recorded under ESI^+ / HRMS using a MicroTOF-Q 77.

IR-Spectra were recorded on JASCO IR-4100 spectrometer (as direct substance or CCl_4 solution). Melting points were measured in open capillary tubes using Fisher-Jones apparatus.

Calorimetric titrations were performed on the Isothermal Titration Calorimeter MCS-ITC from Microcal Inc., USA.

MD simulations were done by using GROMOS'96 software and desktop PC's.

5.2 Synthetic Procedures

4-(2-(4-(allyloxy)phenyl)propan-2-yl)phenol 105.

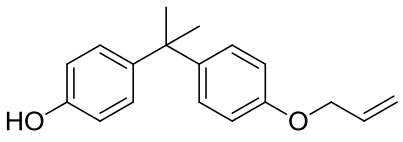

105

Bisphenol A (**104**) (4 g, 17.5 mmol) and potassium carbonate (4.85 g, 35 mmol) were taken in 200 ml of distilled acetone and refluxed at 60°C for 30 minutes. Then allyl bromide (2.1g, 17.5 mmol) was added to this mixture which was refluxed for another 6 hours after which complete conversion of starting material into mono-allylated and bis-allylated product was observed by HPLC analysis. The reaction mixture was filtered to remove insoluble potassium carbonate followed by evaporation of the solvent. The obtained crude residue was dissolved in dichloromethane and quenched with water and brine solution. The DCM fraction was dried over $MgSO_4$ and filtered. Subsequent evaporation of the solvent gave gummy liquid. The mixture of mono- and bis- allylated products was purified by flash silica chromatography using petroleum ether and ethyl acetate (9:1 by volume) for elution. 2.8 g (60% yields) of the mono-allylated product was obtained after purification.

105: $C_{18}H_{20}O_2$ (MW 268.4)

HPLC analysis: R_v= 10ml, 125/4 Nucleodur 100-3 C8 ec, UV_{254}, flow= 1ml/min, gradient from 50% CH_3OH to 90% CH_3OH in 10 min and then 90% CH_3OH for next 5 min, 0.1% TFA as buffer.

^{1}H-NMR (360 MHz; $CDCl_3$): δ= 7.2 (d, 4H, -CC**H**-); 6.85 (d, 4H, -OCC**H**-); 6.4 (s, 1H, -O**H**); 6.1 (m, 1H, CH_2=C**H**-); 5.5 (m, 2H, -CH=C**H**$_2$); 4.58 (d, 2H, -OC**H**$_2$-); 1.7(s, 6H, -CC**H**$_3$-).

^{13}C-NMR (90.56 MHz; $CDCl_3$): δ= 156.2 (-**C**OH); 153.4 (-**C**OCH_2-); 143.4, 142.8 (-C(CH_3)$_2$**C**-); 133.3 (-**C**H=CH_2); 127.8, 127.6 (-C**C**HCH-); 117.5 (-CH=**C**H_2); 114.7, 114.0 (-OC**C**H-); 68.8 (-O**C**H2-); 41.5 (-**C**(CH_3)$_2$); 30.9 (-C(**C**H_3)$_2$).

^{13}C NMR-DEPT (90.56 MHz; $CDCl_3$): δ= 133.3 (-**C**H=CH_2); 127.8, 127.6 (-C**C**HCH-); 117.5 (-CH=**C**H_2); 114.7, 114.0 (-OC**C**H-); 68.8 (-O**C**H2-); 30.9 (-C(**C**H_3)$_2$).

(2*S*,8*S*)-2,8-bis(chloromethyl)-2,3,4,6,7,8-hexahydro-1H-pyrimido[1,2-a]pyrimidin-9-ium chloride 114.

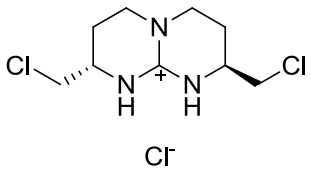

114

118 mg (0.5 mmol) of guanidinium bis-hydroxy compound (**113**) was taken up in 2 ml thionyl chloride and refluxed at 80 °C for 2.5 hours. Then thionyl chloride was removed under reduced pressure condition. The product was recrystallised from acetone/hexane.

114: $C_9H_{15}Cl_3N_3$. HCl (MW 272.6)

MS-ESI: m/z = 236.2 (M^+, 100%)

HPLC analysis: R_v= 12 ml, 125/4 Nucleodur 100-3 C18 ec, UV_{254}, flow= 1ml/min, gradient from 10% CH_3OH to 50% CH_3OH in 10 min and then 50 % CH_3OH to 90% CH_3OH in next 10 min, 0.1% TFA as buffer.

^{1}H-NMR (360 MHz; $CDCl_3$): δ= 9.2 (bs, 2H, -N**H**-); 3.72 (m, 2H, -NHC**H**-); 3.5-3.6 (m, 4H, -C**H**$_2$Cl); 3.36-3.41 (m, 4H, -NC**H**$_2$-); 1.97-2.04 (m, 2H, -CHC**H**$_2$-); 1.8-1.9 (m, 2H, -CHC**H**$_2$-).

^{13}C-NMR (90.56 MHz; $CDCl_3$): δ= 151.01 (guanidinium carbon); 63.5 (-**C**H_2Cl); 50.21 (-**C**HCH_2-); 45.4 (-N**C**H_2-); 22.6 (-CH**C**H_2-).

(2*S*,8*S*)-2,8-bis((4-(2-(4-(allyloxy)phenyl)propan-2-yl)phenoxy)methyl)-2,3,4,6,7,8-hexahydro-1H-pyrimido[1,2-a]pyrimidin-9-ium chloride 115.

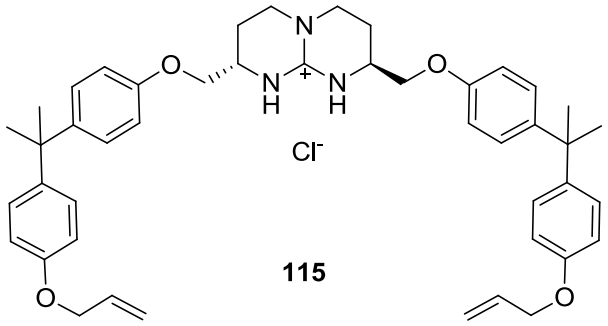

115

Mono allylated compound **105** (531mg, 1.98 mmol) and cesium carbonate (3.2 g, 9.89 mmol) were taken in 10 ml dry acetonitrile under nitrogen atmosphere and stirred at 65 °C for 30 min. Guanidinylating compound **114** (180 mg, 0.66 mmol) was added to this solution and the mixture was continuously stirred at 65 °C. The reaction was monitored by HPLC. The mass analysis of the new peak in HPLC showed the formation of desired bis-substituted compound **115**. After 5 hours, complete conversion of starting compound **114** was observed. The reaction mixture was filtered to remove cesium carbonate and the residue obtained was dissolved in dichloromethane. The DCM solution was quenched with water and brine solution and subsequently dried over magnesium sulphate. Solvent was evaporated and the crude residue was dissolved again in methanol. On addition of sodium tetraphenyl borate (230 mg, 0.67 mmol) solution (in water) to the methanol solution, the substituted product was precipitated as tetraphenylborate salt. The precipitate was washed with methanol and used as it is for the further reactions.

115: $C_{45}H_{53}N_3O_4$.HCl (MW 736.4)

MS-ESI: m/z = 700.5 (M^+, 100%)

HPLC analysis: R_v= 12ml, 125/4 Nucleodur 100-3 C8 ec, UV_{220}, flow= 1ml/min, gradient from 50% CH_3OH to 90% CH_3OH in 10 min and then 90% CH_3OH for next 5 min, 0.1% TFA as buffer.

^{1}H-NMR (360 MHz; $CDCl_3$): δ= 8.9 (bs, 2H, -guanidinium-**H**); 7.15 (d, 8H, aromatic-**H**-); 6.8 (d, 8H, aromatic-**H**); 6.05 (m, 2H, CH_2=C**H**-); 5.4 (m, 4H, -CH=C**H**$_2$); 4.53 (d, 2H, -OC**H**$_2$-); 4.05 (m, 4H, -NC**H**$_2$-); 3.86 (2H, -OCH$_2$C**H**-); 3.4 (m, 4H, -OC**H**$_2$-); 2.15 (m, 4H, -NCH$_2$C**H**$_2$-);1.65(s, 12H, -C(C**H**$_3$)$_2$).

^{13}C-NMR (90.56 MHz; $CDCl_3$): δ= 156.6, 155.9, 144.2, 143.3 (quaternary aromatic); 151.6 (C^+), 133.6 (-**C**H=CH$_2$); 127.8, 114.2 (aromatic **C**H); 117.6 (-CH=**C**H$_2$); 68.8 (-O**C**H2-); 47.7 (-CH$_2$**C**HNH-); 45.3 (-NCH$_2$-); 41.8 (-**C**(CH$_3$)$_2$); 31.1 (-C(**C**H$_3$)$_2$); 23.3 (-NCH$_2$**C**H$_2$-).

^{13}C NMR-DEPT (90.56 MHz; $CDCl_3$): δ= 133.6 (-**C**H=CH$_2$); 127.8, 114.2 (aromatic **C**H); 117.6 (-CH=**C**H$_2$); 68.8 (-O**C**H2-); 47.7 (-CH$_2$**C**HNH-); 45.3 (-NCH$_2$-); 31.1 (-C(**C**H$_3$)$_2$); 23.3 (-NCH$_2$**C**H$_2$-).

Compound 116.

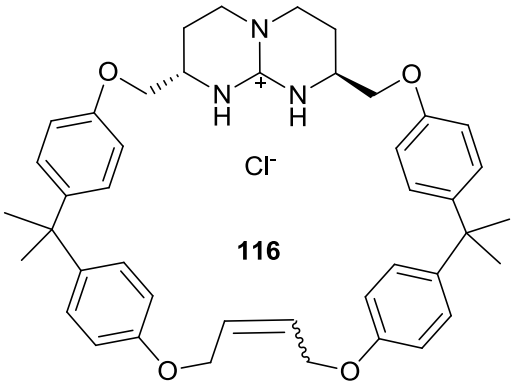

Grubb's (II) catalyst (6 mg, 0.007 mmol) was taken in an oven dried round bottom flask with rubber septum and dissolved in dry dichloroethane (50 ml). Bis-substituted guanidinium compound **115** (65mg, 0.064 mmol) solution (in 10 ml DCE) was added to this solution by plastic syringe and the flask was charged with nitrogen. The reaction mixture was heated under microwave irradiation at 240 watt power. The reaction was monitored by HPLC after every 1 minute heating. HPLC analysis showed an equilibrium mix of cyclised product and starting compound after 4 minutes. Reaction was quenched with water and brine solution and dried over $MgSO_4$. The solvent was evaporated and the crude residue was dissolved in acetonitrile to remove any polymeric substances. The solution obtained after centrifugation was subjected to

perchlorate ion exchange resin. Finally, the pure compound was obtained by MPLC (MeOH:water = 65:35).

116: $C_{43}H_{49}N_3O_4$.HCl (MW 708.3)

MS-ESI: m/z = 672.4 (M^+, 100%)

HPLC analysis: R_v= 17ml, 125/4 Nucleodur 100-3 C8 ec, UV_{220}, flow= 1ml/min, gradient from 50% CH_3OH to 70% CH_3OH in 10 min, then 70% MeOH to 90% MeOH in next 5 min and then 90% CH_3OH for next 5 min, 0.1% TFA as buffer.

^{1}H-NMR (360 MHz; $CDCl_3$): δ= 8.12 (bs, 2H, -guanidinium-**H**); 7.07 (d, 8H, aromatic-**H**-); 6.77 (d, 8H, aromatic-**H**); 5.97 (m, 2H, C**H**=C**H**-); 4.56 (d, 4H, -OC**H**$_2$CH=); 4.06, 3.96 (m, 4H, -OC**H**$_2$-); 3.68 (2H, -OCH$_2$C**H**-); 3.35, 3.28 (m, 4H, -NC**H**$_2$-); 2.08, 1.91 (m, 4H, -NCH$_2$C**H**$_2$-);1.62 (s, 12H, -C(C**H**$_3$)$_2$).

^{13}C-NMR (90.56 MHz; $CDCl_3$): δ= 156.6, 155.9, 144.2, 143.3 (quaternary aromatic); 151.6 (C^+), 128.45 (-**C**H=**C**H-); 127.8, 114.5 (aromatic **C**H); 69.86 (-O**C**H$_2$CH-); 67.7 (-O**C**H$_2$CH=); 47.3 (-CH$_2$**C**HNH-); 45.6 (-NCH$_2$-); 41.6 (-**C**(CH$_3$)$_2$); 30.8 (-C(**C**H$_3$)$_2$); 23.3 (-NCH$_2$**C**H$_2$-).

^{13}C NMR-DEPT (90.56 MHz; $CDCl_3$): δ= 128.45 (-**C**H=**C**H-); 127.8, 114.5 (aromatic **C**H); 69.84 (-O**C**H$_2$CH-); 67.8 (-O**C**H$_2$CH=); 47.3 (-CH$_2$**C**HNH-); 45.6 (-NCH$_2$-); 30.8 (-C(**C**H$_3$)$_2$); 23.3 (-NCH$_2$**C**H$_2$-).

Compound 117.

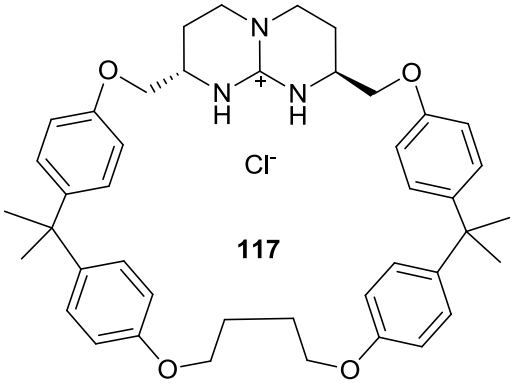

The cyclised product **116** (30 mg, .04 mmol) obtained after ring closing metathesis was dissolved in dry tetrahydrofuran (5 ml) and palladium catalyst on activated charcoal (10 %) was added to

this solution at room temperature. The mixture was stirred and hydrogen was bubbled through the solution. After 2 hours of stirring under hydrogen, complete conversion of starting compound **116** was observed. The mixture was filtered and purified by solvent phase extraction C-18 column.

117: $C_{43}H_{51}N_3O_4$.HCl (MW 710.3)

MS-ESI: m/z = 674.5 (M^+, 100%)

HPLC analysis: R_v= 11ml, 125/4 Nucleodur 100-3 C8 ec, UV_{220}, flow= 1ml/min, gradient from 50% CH_3OH to 90% CH_3OH in 10 min, then 90% MeOH to 90% MeOH in next 5 min, 0.1% TFA as buffer.

^{1}H-NMR (360 MHz; $CDCl_3$): δ= 8.6 (bs, 2H, -guanidinium-**H**); 7.07 (d, 8H, aromatic-**H**-); 6.77 (d, 8H, aromatic-**H**); 4.0-3.7 (m, 8H, -OC**H**$_2$CH-, -OC**H**$_2$-); 3.68 (2H, -CH_2C**H**NH-); 3.30 (m, 4H, -NC**H**$_2$-); 1.95-2.14 (m, 8H, -NCH_2C**H**$_2$-, -OCH_2C**H**$_2$-); 1.61 (s, 12H, -C(C**H**$_3$)$_2$).

^{13}C-NMR (90.56 MHz; $CDCl_3$): δ= 156.6, 155.9, 144.2, 143.3 (quaternary aromatic); 151.6 (C^+); 127.95, 127.8, 114.5, 114.0 (aromatic **C**H); 69.81 (-O**C**H$_2$CH-); 67.1 (-O**C**H_2CH_2-); 47.7 (-CH_2**C**HNH-); 45.8 (-NCH_2-); 41.7 (-**C**$(CH_3)_2$); 30.8 (-C(**C**$H_3)_2$); 25.7 (-NCH_2**C**H_2-); 23.1 (-OCH_2**C**H_2).

^{13}C NMR-DEPT (90.56 MHz; $CDCl_3$): 127.95, 127.8, 114.5, 114.0 (aromatic **C**H); 69.81 (-O**C**H$_2$CH-); 67.1 (-O**C**H_2CH_2-); 47.7 (-CH_2**C**HNH-); 45.8 (-NCH_2-); 30.8 (-C(**C**$H_3)_2$); 25.7 (-NCH_2**C**H_2-); 23.1 (-OCH_2**C**H_2-).

HMQC ($CDCl_3$): δ= [(7.07, 128.13), (7.05, 128.18), (6.81, 115.28), (6.74, 114.32); aromatic –**CH**-]; ((4.12, 3.96), 70.43; -O**C**H$_2$CH-); (3.99, 67.39; -O**C**H_2CH_2-); (3.73, 47.28; -CH_2**C**HNH-); ((3.42, 3.29), 45.7; -NC**H**$_2$); (1.61, 30.99; -C(**C**$H_3)_2$); ((1.95, 1.90), 25.97; -NCH_2**C**H_2-); (2.12, 23.56; -OCH_2**C**H_2-).

(13*R*,17*R*)-17-(allyloxy)-13-methyl-7,8,9,11,12,13,14,15,16,17-decahydro-6H-cyclopenta[a]phenanthren-3-ol 119.

Preparation of the catalytic stock solution

Chinolin-2-carboxylic acid (17.3 mg, 100 µmol) and Cp*Ru$(CH_3CN)_3PF_6$ (43.5 mg, 100 µmol) were weighed into a 10 ml measuring flask and filled to the mark with dry dichloromethane.

ß-estradiol -3-benzoate **118** (68 mg, 0.18 mmol) was added with allylalcohol (21 mg, 0.36 mmol) to 2 ml of dry dichloromethane. 190 µl of the catalyst solution, prepared as given above, was added and the solution was refluxed at 48 °C under nitrogen atmosphere. Almost complete conversion of the starting compound was observed by HPLC after 24 hours. The solvent was removed and the crude residue was dissolved in MeOH/1 N NaOH (aq.) (3:2) solvent. The mixture was refluxed at 80 °C under nitrogen. Complete conversion into the deprotected product was observed after 3 hours. The solution was extracted with heptane to remove traces of starting compound. MeOH/H_2O solution was neutralized with 4N HCl and was then extracted with heptane/ether (1:1) to isolate the final product. The solvent was evaporated and the residue was dissolved in dichloromethane and extracted with water and brine solution, then dried over $MgSO_4$ and filtered. The compound was recrystallised from DCM/hexane.

119: $C_{21}H_{28}O_2$.HCl (MW 312.4)

HPLC analysis: R_v= 13ml, 125/4 Nucleodur 100-3 C8 ec, UV_{254}, flow= 1ml/min, gradient from 50% CH_3OH to 90% CH_3OH in 10 min and then 90% CH_3OH for next 10 min, 0.1% TFA as buffer.

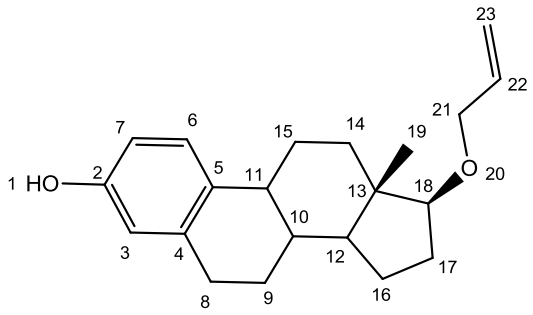

119

^{1}H-NMR (360 MHz; $CDCl_3$): δ= 7.17 (d, 1H, aromatic-**H**-); 6.61(d, 1H, aromatic-**H**); 6.56 (s, 1H, aromatic-**H**); 5.9 (m, 1H, CH_2=C**H**-); 5.2 (dd, 2H, -CH=C**H**$_2$); 4.04 (d, 2H, -OC**H**$_2$-); 3.47 (t, 1H, -CC**H**$_2$-); 2.8 (m, 2H, -CC**H**-, -CC**H**$_2$-); 1.2-2.25 (m, 13H, aliphatic-**H**)

^{13}C-NMR (90.56 MHz; $CDCl_3$): δ= 153.4 (-**C**OH); 138.4 (aromatic quaternary-C); 133.9 (CH2=**C**H-); 132.9 (aromatic quaternary-**C**); 126.7, 115.4, 112.8 (aromatic **C**H); 116.36 (**C**H_2=CH-); 88.6 (-CH_2O**C**H-); 71.05 (-O**C**H_2); 50.37 (**C12**); 44.07 (**C11**); 43.45 (**C13**); 38.74 (**C10**); 38.10 (**C14**); 29.77 (**C8**); 28.2 (**C17**); 27.3 (**C9**); 26.6 (**C15**); 23.2 (**C16**); 11.87 (**C**H_3).

^{13}C NMR-DEPT (90.56 MHz; $CDCl_3$): δ= 133.9 (CH2=**C**H-); 126.7, 115.4, 112.8 (aromatic **C**H); 116.36 (**C**H_2=CH-); 88.6 (-CH_2O**C**H-); 71.0 (-O**C**H_2); 50.33 (**C12**); 44.03 (**C11**); 38.69 (**C10**); 38.05 (**C14**); 29.73 (**C8**); 28.2 (**C17**); 27.26 (**C9**); 26.54 (**C15**); 23.2 (C16); 11.83 (**C**H_3).

HMQC ($CDCl_3$): δ= (7.20, 126.84; aromatic **C**); (6.71, 112.56; aromatic **C**); (6.65, 115.21; aromatic **C**); (5.93, 136.71; **C22**); ((5.30, 5.16), 116.6; **C23**); (3.46, 88.62; **C18**); (4.04, 71.05; **C21**); (1.19, 50.37; **C12**); (2.19, 44.07; **C11**); (1.44, 38.73; **C14**); (1.38, 38.09; **C10**); ((2.80, 2.88), 29.77; **C8**); (1.52, 27.30; **C9**); (1.86, 27.30; **C17**); (0.8, 11.87; **C19**); (1.69, 23.23; **C16**); (1.62, 26.58; **C15**)

(2*S*,8*S*)-2,8-bis((((13*R*,17*R*)-17-(allyloxy)-13-methyl-7,8,9,11,12,13,14,15,16,17-decahydro-6H-cyclopenta[a]phenanthren-3-yl)oxy)methyl)-2,3,4,6,7,8-hexahydro-1H-pyrimido[1,2-a]pyrimidin-9-ium chloride 120.

Mono allylated estradiol compound **119** (50 mg, 0.16 mmol) was dissolved in dry acetonitrile, cesium carbonate (261mg, 0.8 mmol) was added under nitrogen atmosphere, and the misture was heated at 70 °C for 30 min. 2,8-bischloro-methyl-guanidin compound **114** (17.5 mg, 0.06 mmol) was added to this solution and heating was continued. The reaction was monitored by HPLC. Mass analysis of the newly formed peak in HPLC showed the formation of the desired bis-substituted product. After 6 hours, complete conversion of starting compound **114** was observed. The reaction mixture was filtered to remove cesium carbonate and the crude residue obtained was dissolved in dichloromethane. The solution was extracted with water and brine solution and dried over magnesium sulphate. Subsequently, the solvent was evaporated and the crude remainder was taken up again in methanol. The methanol solution was made basic upto a pH of ~12 by addition of sodium hydroxide solution which led to the precipitation of the substituted product. The suspension was centrifuged and the precipitate was washed with methanol again two times and was used as is in the further reactions.

120: $C_{21}H_{28}O_2$.HCl (MW 824.6)

MS-ESI: m/z = 788.5 (M^+, 100%)

HPLC analysis: R_v= 15ml, 125/4 Nucleodur 100-3 C8 ec, UV_{254}, flow= 1ml/min, gradient from 50% CH_3OH to 90% CH_3OH in 10 min and then 90% CH_3OH for next 5 min, 0.1% TFA as buffer.

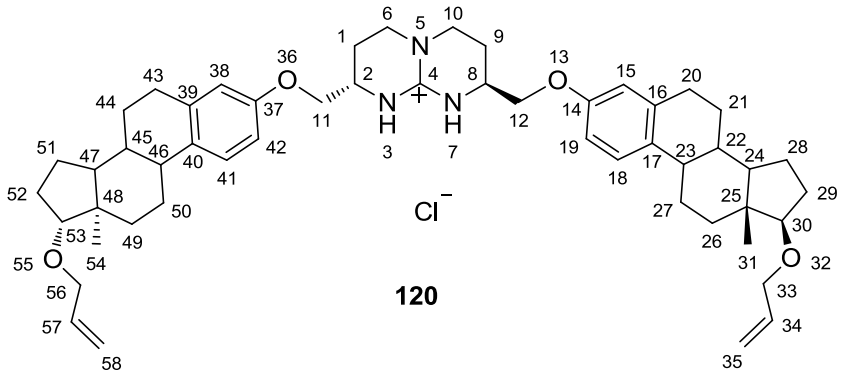

120

^{1}H-NMR (500 MHz; $CDCl_3$): δ= 7.17 (d, 2H, aromatic-**H**-); 6.68-6.61 (s, 4H, aromatic-**H**); 5.93 (m, 2H, CH_2=C**H**-); 5.26 (m, 4H, -CH=C**H**$_2$); 4.03, 3.82 (dd, 4H, -C**H**$_2$OAr-); 4.05 (d, 4H, H_2**C33**); 3.68 (m, 2H, -NHC**H**-); 3.47 (m, 2H, -C**H**CH_2-); 3.17 (m, 4H, -NCH_2CH_2-); 1.2-2.85 (m, 34H, aliphatic-**H**)

^{13}C-NMR (90.56 MHz; $CDCl_3$): δ= 153.4 (-**C**OCH_2-); 151.32 (quaternary C^+); 138.32 (-CH=**C-, ** aromatic); 135.77 (**C34**); 133.71 (-CH=**C**-, aromatic); 126.7, 115.4, 112.8 (aromatic **C**); 116.36 (**C35**); 88.57 (**C30**); 71.01 (**C33**); 69.06 (**C12**); 50.36 (**C24**); 47.57 (**C8**); 45.30 (**C10**); 44.08 (**C23**); 43.45 (**C25**); 38.74 (**C22**); 38.10 (**C26**); 29.90 (**C20**); 28.22 (**C29**); 27.3 (**C27**); 26.58 (**C21**); 23.59 (**C9**); 23.2 (**C28**); 11.87 (**C31**).

^{13}C NMR-DEPT (90.56 MHz; $CDCl_3$): δ= 135.77 (**C34**); 126.7, 115.4, 112.8 (aromatic **C**); 116.36 (**C35**); 88.57 (**C30**); 71.01 (**C33**); 69.06 (**C12**); 50.36 (**C24**); 47.57 (**C8**); 45.30 (**C10**); 44.08 (**C23**); 38.74 (**C22**); 38.10 (**C26**); 29.90 (**C20**); 28.22 (**C29**); 27.3 (**C27**); 26.58 (**C21**); 23.59 (**C9**); 23.2 (**C28**); 11.87 (**C31**).

HMQC ($CDCl_3$): (7.20, 126.88; aromatic **C**); (6.72, 112.70; aromatic **C**); (6.66, 114.85; aromatic **C**); (5.93, 136.09; **C34**); ((5.30, 5.16), 116.35; **C35**); (3.45, 88.77; **C30**); (4.02, 71.22; **C33**); ((3.82,4.00), 69.07; **C12**); (3.66, 47.86; **C8**); (1.20, 50.54; **C24**); ((3.24, 3.17), 45.30; **C10**); (2.17, 44.22; **C23**); (1.39, 38.71; **C22**); ((2.07, 1.40), 38.07; **C26**); ((2.82, 2.17), 30.05; **C20**); ((2.05, 1.56), 28.45; **C29**); ((1.86, 1.35); 27.51; **C27**); ((1.45, 2.26), 26.76; **C21**); ((1.71, 2.05), 23.59; **C9**); ((1.69, 1.35), 23.38; **C28**); (0.78, 11.89; **C31**)

(2*S*,8*S*)-2,8-bis((((13*R*,17*R*)-17-hydroxy-13-methyl-7,8,9,11,12,13,14,15,16,17-decahydro-6H-cyclopenta[a]phenanthren-3-yl)oxy)methyl)-2,3,4,6,7,8-hexahydro-1H-pyrimido[1,2-a]pyrimidin-9-ium chloride 122.

Estradiol compound **121** (100 mg, 0.37 mmol) was dissolved in dry acetonitrile, treated with cesium carbonate (598 mg, 1.84 mmol) under nitrogen atmosphere and heated at 70 °C for 30 min. 2,8-bischloro-methyl-guanidine compound **114** (33 mg, 0.12 mmol) was added to this solution and heating was continued. The reaction was monitored by HPLC. Mass analysis of the newly formed peak in HPLC showed the formation of desired bis-substituted product. After 5 hours, complete conversion of starting compound **114** was observed. The reaction mixture was filtered to remove cesium carbonate and the crude residue obtained was redissolved in dichloromethane. The solution was washed with water and brine solution and dried over magnesium sulphate. Subsequently, the solvent was evaporated and the residue was dissolved again in methanol. The methanol solution was made basic up to a pH~12 by addition of sodium hydroxide solution which led to the precipitation of the substituted product. The solution was centrifuged and the precipitate was washed with methanol two times and was used as is in the further reactions.

122: $C_{45}H_{61}N_3O_4$.HCl (MW 744.4)

MS-ESI: m/z = 708.7 (M^+, 100%)

HPLC analysis: R_v= 10ml, 125/4 Nucleodur 100-3 C8 ec, UV_{254}, flow= 1ml/min, gradient from 50% CH_3OH to 90% CH_3OH in 10 min and then 90% CH_3OH for next 5 min, 0.1% TFA as buffer.

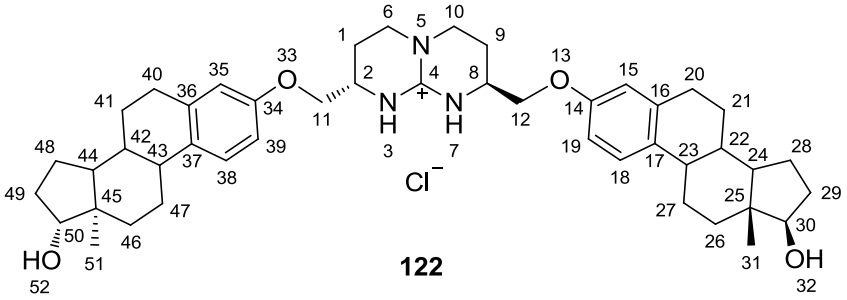

COSY (500 MHz; $CDCl_3$): δ= 7.20 (d, 2H, aromatic-**H**-); 6.72, 6.67 (s, 4H, aromatic-**H**); 5.33 (d, 2H, -O**H**); 4.22, 3.89 (dd, 4H, -C**H**$_2$OAr-); 3.75 (m, 2H, -C**H**OH-); 3.85 (m, 2H, -NHC**H**-) 3.42, 3.33 (m, 4H, -NC**H**$_2$-); 1.2- 2.5 (m, 34H, aliphatic-**H**); 0.79 (s, 6H, -C**H**$_3$).

HSQC ($CDCl_3$): δ= (7.20, 126.88; aromatic **C**); (6.72, 112.70; aromatic **C**); (6.66, 114.85; aromatic **C**); (3.75, 82.28; **C30**); ((3.89,4.22), 69.17; **C12**); (3.85, 47.79; **C8**); (1.21, 50.38; **C24**); ((3.42, 3.33), 45.39; **C10**); (2.19, 44.24; **C23**); (1.44, 39.11; **C22**); ((1.30, 1.97), 37.10; **C26**); ((1.51, 2.14), 30.99; **C29**); ((1.28, 2.85), 30.10; **C20**); ((1.32, 1.89); 27.39; **C27**); ((1.49, 2.31), 26.64; **C21**); ((1.38, 1.72), 23.48; **C28**); ((1.72, 2.04), 23.88; **C9**); (0.79, 11.15**; C31**)

Compound 124.

Open chain guanidinium compound **122** (50 mg, 0.067 mmol) was dissolved in dry 1,2-dichloroethane and $BF_3.Et_2O$ (25 µl) was added to it. The solution was heated to 80 °C under nitrogen atmosphere. Then bis(4-isocyanatophenyl)methane **123** (20 mg, 0.08 mmol) was added to this solution. The reaction was monitored by HPLC and mass analysis. A precipitate was formed during the reaction, but the HPLC analysis showed that it was a salt. Complete conversion of the starting material was observed after 4 hours in HPLC. The product formed was analyzed by ESI-MS and it showed the correct mass of the 1:1 adduct. The reaction mixture was then filtered and the solvent was evaporated. The obtained crude was dissolved in acetonitrile to remove any polymerization product. The pure cyclized compound was obtained by C-18 solvent phase extraction column (65% MeOH in water). Infrared spectroscopy was performed on the product to see if there was any isocyanate peak. No peak was observed in the isocaynate stretching frequency region in IR spectrum which confirms that both isocyanate functions of **123** reacted with the starting compound **122**. The symmetry observed in the NMR spectrum again confirmed the identity of the macrocyclic compound **124**. The integration of the aromatic and methylene unit of isocyanate peaks in the ^1H NMR shows 1:1 ratio of the compound **122** and **123** in the final cyclized product **124**.

MS-ESI: m/z = 958.8 (M^+, 100%)

HPLC analysis: R_v= 11ml, 125/4 Nucleodur 100-3 C8 ec, UV_{254}, flow= 1ml/min, gradient from 50% CH_3OH to 90% CH_3OH in 5 min and then 90% CH_3OH for next 10 min, 0.1% TFA as buffer.

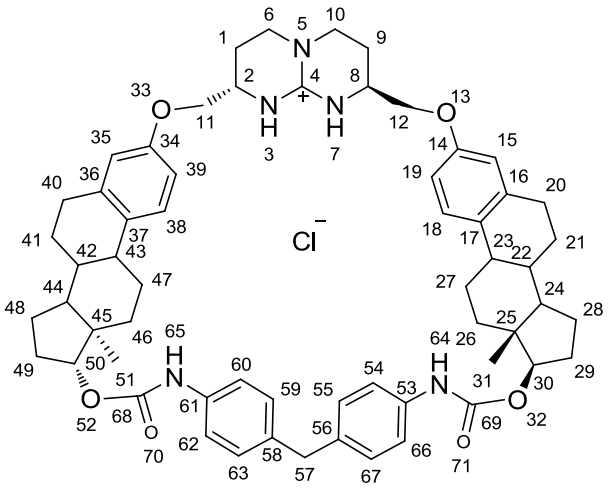

124

^{1}H-NMR (500 MHz; $CDCl_3$): δ= 7.30 (d, 4H, aromatic-**H**); 7.20 (d, 2H, aromatic-**H**-); 7.12 (d, 4H, aromatic **H**); 6.72, 6.67 (s, 4H, aromatic-**H**); 5.26 (bs, 2H, -N**H**-); 4.04, 3.99 (dd, 4H, -C**H**$_2$OAr-); 4.75 (m, 2H, -C**H**OCO-); 3.91 (s, 2H, -ArC**H**$_2$Ar-); 3.87 (m, 2H, -NHC**H**-); 3.46, 3.38 (m, 4H, -NC**H**$_2$-); 1.2- 2.5 (m, 34H, aliphatic-**H**); 0.89 (s, 6H, -C**H**$_3$).

HSQC ($CDCl_3$): δ= (7.30, 119.40; aromatic **C**); (7.20, 126.92; aromatic **C**); (7.12, 129.84; aromatic **C**); (6.70, 112.50; aromatic **C**); (6.65, 114.99; aromatic **C**); (4.75, 84.01; **C30**); ((4.04, 3.99), 69.17; **C12**); (3.87, 47.97; **C8**); (1.32, 50.00; **C24**); ((3.46, 3.38), 45.61; **C10**); (2.22, 44.02; **C23**); (3.91, 40.90; **C57**); (1.46, 38.91; **C22**); ((1.96, 1.46), 37.20; **C26**); ((2.25, 1.65), 27.95; **C29**); ((2.86, 1.29), 29.95; **C20**); ((1.90, 1.37); 27.22; **C27**); ((2.31, 1.49), 26.90; **C21**); ((1.77, 1.43), 23.45; **C28**); ((2.20, 2.09), 23.39; **C9**); (0.89, 12.29**; C31**)

5.3 Experiments in-silico

All the MD simulations were carried out using desktop computers (Pentium PC's) and GROMOS'96 (an acronym of the GROningen MOlecular Simulation) software provided generously by Prof. W.F. van Gunsteren, ETH-Zürich.

All topology files were prepared following the instructions given in GROMOS manual. Co-ordinate files were made by first drawing the molecule structure in ChemSketch (ACD/Labs version 12.0) and saved these *.sk files as *.mol files. Second, with the help of Open Babel program (version 2.2.1) converted the *.mol files into *.gr96 co-ordinate files.

5.3.1 Topology file for guanidinium host 116 (MAC1)

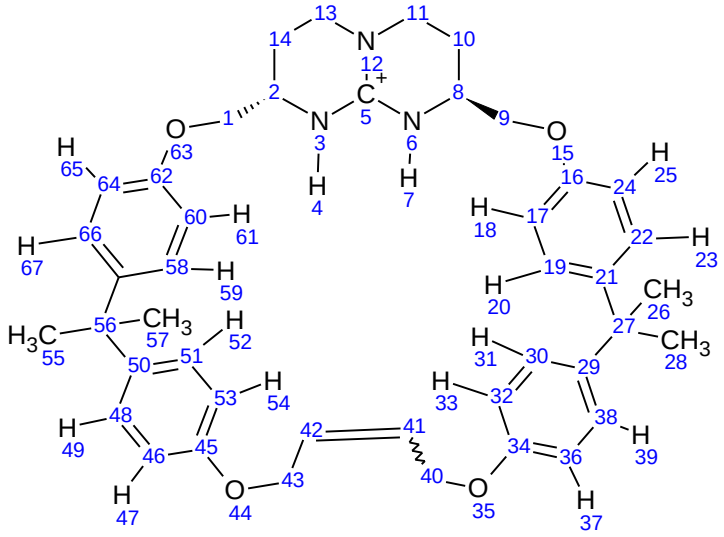

```
MTBUILDBLSOLUTE
# building block
# RNME
MAC1
# number of atoms, number of preceding exclusions
# NMAT, NLIN
    68   0
# ATOM MAE MSAE
# ATOM  ANM  IACM  MASS  CGM  ICGM  MAE  MSAE
     1   C1    13     4   0.00   1    5     2  3 14 63 64
     2   C2    12     3   0.20   0    6     3  4  5 13 14 64
     3   N1    10    14  -0.11   0    5     4  5  6 12 14
     4   HN1   18     1   0.24   0    1     5
     5   C3    11    12   0.34   0    6     6  7  8 11 12 13
     6   N2    10    14  -0.11   0    5     7  8  9 10 12
     7   HN2   18     1   0.24   0    1     8
     8   C4    12     3   0.20   1    4     9  10 11 15
     9   C5    13     4   0.00   1    3    10  15 16
    10   C6    13     4   0.00   1    2    11 12
    11   C7    13     4   0.055  0    2    12 13
    12   N3    10    14  -0.11   0    2    13 14
    13   C8    13     4   0.055  1    1    14
    14   C9    13     4   0.00   1    0
    15   O1     3    16  -0.20   0    7    16 17 18 19 22 24 25
    16   C10   11    12   0.20   1    9    17 18 19 20 21 22 23 24 25
    17   C11   11    12  -0.10   0    8    18 19 20 21 22 24 25 27
    18   HC11  17     1   0.10   1    4    19 20 21 24
    19   C12   11    12  -0.10   0    6    20 21 22 23 24 27
    20   HC12  17     1   0.10   1    3    21 22 27
    21   C13   11    12   0.00   1    8    22 23 24 25 26 27 28 29
    22   C14   11    12  -0.10   0    4    23 24 25 27
    23   HC14  17     1   0.10   1    3    24 25 27
    24   C15   11    12  -0.10   0    2    25 27
    25   HC15  17     1   0.10   1    0
```

```
     26   C16   14      5   0.00   0    3    27 28 29
     27   C17   11     12   0.00   0    8    28 29 30 31 32 36 38 39
     28   C18   14      5   0.00   1    1    29
     29   C19   11     12   0.00   1    9    30 31 32 33 34 36 37 38 39
     30   C20   11     12  -0.10   0    8    31 32 33 34 35 36 38 39
     31   HC20  17      1   0.10   1    4    32 33 34 38
     32   C21   11     12  -0.10   0    7    33 34 35 36 37 38 40
     33   HC21  17      1   0.10   1    3    34 35 36
     34   C22   11     12   0.20   0    7    35 36 37 38 39 40 41
     35   O2     3     16  -0.20   1    6    36 37 38 40 41 42
     36   C23   11     12  -0.10   0    4    37 38 39 40
     37   HC23  17      1   0.10   1    2    38 39
     38   C24   11     12  -0.10   0    1    39
     39   HC24  17      1   0.10   1    0
     40   C25   13     12   0.00   0    2    41 42
     41   C26   16      3   0.00   0    2    42 43
     42   C27   16      3   0.00   0    2    43 44
     43   C28   13     12   0.00   1    2    44 45
     44   O3     3     16  -0.20   0    7    45 46 47 48 51 53 54
     45   C29   11     12   0.20   1    9    46 47 48 49 50 51 52 53 54
     46   C30   11     12  -0.10   0    8    47 48 49 50 51 53 54 56
     47   HC30  17      1   0.10   1    4    48 49 50 53
     48   C31   11     12  -0.10   0    6    49 50 51 52 53 56
     49   HC31  17      1   0.10   1    3    50 51 56
     50   C32   11     12   0.00   1    8    51 52 53 54 55 56 57 58
     51   C33   11     12  -0.10   0    4    52 53 54 56
     52   HC33  17      1   0.10   1    3    53 54 56
     53   C34   11     12  -0.10   0    2    54 56
     54   HC34  17      1   0.10   1    0
     55   C35   14      5   0.00   0    3    56 57 58
     56   C36   11     12   0.00   0    8    57 58 59 60 61 65 67 68
     57   C37   14      5   0.00   1    1    58
     58   C38   11     12   0.00   1    9    59 60 61 62 63 65 66 67 68
     59   C39   11     12  -0.10   0    8    60 61 62 63 64 65 67 68
     60   HC39  17      1   0.10   1    4    61 62 63 67
     61   C40   11     12  -0.10   0    6    62 63 64 65 66 67
     62   HC40  17      1   0.10   1    3    63 64 65
     63   C41   11     12   0.20   0    5    64 65 66 67 68
     64   O4     3     16  -0.20   1    3    65 66 67
     65   C42   11     12  -0.10   0    3    66 67 68
     66   HC42  17      1   0.10   1    2    67 68
     67   C43   11     12  -0.10   0    1    68
     68   HC43  17      1   0.10   1    0
# NB
  74
# IB   JB   MCB              6    7     2             15   16    12
   1    2    26              6    8    20             16   17    15
   1   64    17              8    9    26             16   24    15
   2    3    20              8   10    26             17   18     3
   2   14    26              9   15    17             17   19    15
   3    4     2             10   11    26             19   20     3
   3    5    10             11   12    20             19   21    15
   5    6    10             12   13    20             21   22    15
   5   12    10             13   14    26             21   27    26
```

```
  22   23    3            36   38   15            51   53   15
  22   24   15            38   39    3            53   54    3
  24   25    3            40   41   26            55   56   26
  26   27   26            41   42   12            56   57   26
  27   28   26            42   43   26            56   58   26
  27   29   26            43   44   17            58   59   15
  29   30   15            44   45   12            58   67   15
  29   38   15            45   46   15            59   60    3
  30   31    3            45   53   15            59   61   15
  30   32   15            46   47    3            61   62    3
  32   33    3            46   48   15            61   63   15
  32   34   15            48   49    3            63   64   12
  34   35   12            48   50   15            63   65   15
  34   36   15            50   51   15            65   66    3
  35   40   17            50   56   26            65   67   15
  36   37    3            51   52    3            67   68    3
# NBA
  116
# IB   JB   KB   MCB                19   21   27   24
   2    1   64   12                 22   21   27   24
   1    2    3   12                 21   22   23   24
   1    2   14   12                 21   22   24   26
   3    2   14   12                 23   22   24   24
   2    3    4   17                 22   24   25   24
   2    3    5   26                 22   24   16   26
   4    3    5   17                 16   24   25   24
   3    5    6   27                 21   27   29   12
   3    5   12   27                 29   27   28   12
   6    5   12   27                 26   27   28   12
   5    6    7   17                 21   27   26   12
   5    6    8   26                 21   27   28   12
   7    6    8   17                 26   27   29   12
   6    8    9   12                 27   29   30   24
   6    8   10   12                 27   29   38   24
   9    8   10   12                 30   29   38   26
   8    9   15   12                 29   30   31   24
   8   10   11   12                 29   30   32   26
  10   11   12   12                 31   30   32   24
  11   12   13   26                 30   32   33   24
   5   12   11   26                 30   32   34   26
   5   12   13   26                 33   32   34   24
  12   13   14   12                 32   34   35   24
  13   14    2   12                 32   34   36   26
   9   15   16   11                 35   34   36   24
  15   16   17   26                 34   35   40   11
  15   16   24   26                 34   36   37   24
  17   16   24   26                 34   36   38   26
  16   17   18   24                 37   36   38   24
  16   17   19   26                 36   38   39   24
  18   17   19   24                 36   38   29   26
  17   19   20   24                 29   38   39   24
  17   19   21   26                 35   40   41   12
  20   19   21   24                 40   41   42   26
  19   21   22   26                 41   42   43   26
```

```
  42   43   44    12
  43   44   45    11
  44   45   46    24
  44   45   53    24
  46   45   53    26
  45   46   47    24
  45   46   48    26
  47   46   48    24
  46   48   49    24
  46   48   50    26
  49   48   50    24
  48   50   51    26
  48   50   56    24
  51   50   56    24
  50   51   52    24
  50   51   53    26
  52   51   53    24
  51   53   54    24
  51   53   45    26
  45   53   54    24
  55   56   57    12
  57   56   58    12
  50   56   58    12
  50   56   55    12
  50   56   57    12
  55   56   58    12
  56   58   59    24
  56   58   67    24
  59   58   67    26
  58   59   60    24
  58   59   61    26
  60   59   61    24
  59   61   62    24
  59   61   63    26
  62   61   63    24
  61   63   64    24
  61   63   65    26
  63   64    1    11
  64   63   65    24
  63   65   66    24
  63   65   67    26
  66   65   67    24
  58   67   65    26
  58   67   68    24
  65   67   68    24

# NIDA
  54
# IB   JB   KB   LB   MCB
   2    3    1   14     2
   8    6    9   10     2
   3    2    4    5     1
   5    3    6   12     1
   6    5    7    8     1
  12    5   11   13     1
  16   15   17   24     1
  17   16   18   19     1
  19   17   20   21     1
  21   19   22   27     1
  22   21   23   24     1
  24   16   22   25     1
  16   17   19   21     1
  17   19   21   22     1
  19   21   22   24     1
  21   22   24   16     1
  22   24   16   17     1
  24   16   17   19     1
  29   27   30   38     1
  30   29   31   32     1
  32   30   33   34     1
  34   32   35   36     1
  36   34   37   38     1
  38   36   39   29     1
  29   30   32   34     1
  30   32   34   36     1
  32   34   36   38     1
  34   36   38   29     1
  36   38   29   30     1
  38   29   30   32     1
  45   44   46   53     1
  46   45   47   48     1
  48   46   49   50     1
  50   48   51   56     1
  51   50   52   53     1
  53   45   51   54     1
  45   46   48   50     1
  46   48   50   51     1
  48   50   51   53     1
  50   51   53   45     1
  51   53   45   46     1
  53   45   46   48     1
  58   56   59   67     1
  59   58   60   61     1
  61   59   62   63     1
  63   61   64   65     1
  65   63   66   67     1
  67   65   68   58     1
  58   59   61   63     1
  59   61   63   65     1
  61   63   65   67     1
  63   65   67   58     1
  65   67   58   59     1
  67   58   59   61     1
```

```
# NDA
  28
# IB    JB    KB    LB    MCB                    8     9    15    16     12
  64     1     2    14     17                    9    15    16    17      2
  10     8     9    15     17                   61    63    64     1      2
   1     2     3     4     19                   19    21    27    29     20
   7     6     8     9     19                   21    27    29    30     20
   4     3     5    12      4                   48    50    56    58     20
   7     6     5    12      4                   50    56    58    59     20
   3     2    14    13     17                   32    34    35    40      2
   6     8    10    11     17                   43    44    45    46      2
   8    10    11    12     17                   34    35    40    41     12
   2    14    13    12     17                   35    40    41    42     20
  10    11    12    13     19                   40    41    42    43      4
  11    12    13    14     19                   41    42    43    44     20
   3     5    12    13      5                   42    43    44    45     12
  63    64     1     2     12
END
```

5.3.2 Topology file for guanidinium host 120 (ESTO)

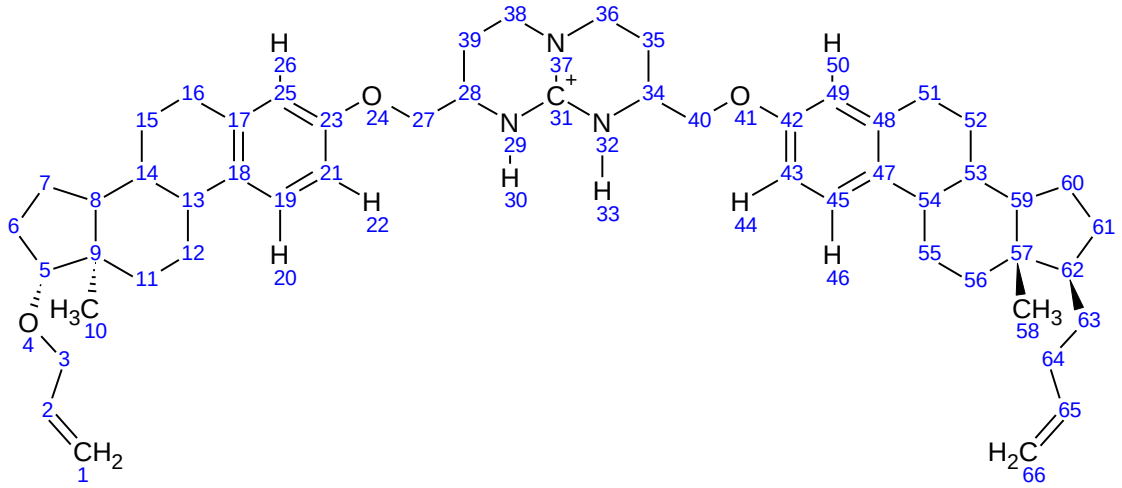


```
MTBUILDBLSOLUTE
# building block
# RNME
ESTO
# number of atoms, number of preceding exclusions
# NMAT, NLIN
    66   0
# ATOM MAE MSAE
# ATOM   ANM   IACM   MASS   CGM   ICGM   MAE   MSAE
     1    C1     13      4   0.00    0     2     2 3
     2    C2     12      3   0.00    0     2     3 4
     3    C3     13      4   0.00    1     2     4 5
     4    O1      3     16  -0.20    0     3     5 6 9
     5    C4     12      3   0.20    1     6     6 7 8 9 10 11
     6    C5     44      4   0.00    0     3     7 8 9
     7    C6     44      4   0.00    1     3     8 9 14
```

```
 8   C7    12     3   0.00   1    6    9 10 11 13 14 15
 9   C8    11    12   0.00   0    4    10 11 12 14
10   C9    14     5   0.00   1    1    11
11   C10   44     4   0.00   0    2    12 13
12   C11   44     4   0.00   1    3    13 14 18
13   C12   12     3   0.00   0    5    14 15 17 18 19
14   C13   12     3   0.00   1    3    15 16 18
15   C14   44     4   0.00   0    2    16 17
16   C15   44     4   0.00   1    3    17 18 25
17   C16   11    12   0.00   1    8    18 19 20 21 23 24 25 26
18   C17   11    12   0.00   1    7    19 20 21 22 23 25 26
19   C18   11    12  -0.10   0    6    20 21 22 23 24 25
20   HC18  17     1   0.10   1    3    21 22 23
21   C19   11    12  -0.10   0    5    22 23 24 25 26
22   HC19  17     1   0.10   1    2    23 25
23   C20   11    12   0.20   0    4    24 25 26 27
24   O2     3    16  -0.20   1    3    25 27 28
25   C21   11    12  -0.10   0    1    26
26   HC21  17     1   0.10   1    0
27   C22   13     4   0.00   1    3    28 29 39
28   C23   12     3   0.20   0    5    29 30 31 38 39
29   N1    10    14  -0.11   0    5    30 31 32 37 39
30   HN1   18     1   0.24   0    1    31
31   C24   11    12   0.34   0    6    32 33 34 36 37 38
32   N2    10    14  -0.11   0    5    33 34 35 37 40
33   HN2   18     1   0.24   0    1    34
34   C25   12     3   0.20   1    4    35 36 40 41
35   C26   13     4   0.00   1    3    36 37 40
36   C27   13     4   0.055  0    2    37 38
37   N3    10    14  -0.11   0    2    38 39
38   C28   13     4   0.055  1    1    39
39   C29   13     4   0.00   1    0
40   C30   13     4   0.00   1    2    41 42
41   O3     3    16  -0.20   0    3    42 43 49
42   C31   11    12   0.20   1    8    43 44 45 46 47 48 49 50
43   C32   11    12  -0.10   0    7    44 45 46 47 48 49 50
44   HC32  17     1   0.10   1    4    45 46 47 49
45   C33   11    12  -0.10   0    5    46 47 48 49 54
46   HC33  17     1   0.10   1    2    47 48
47   C34   11    12   0.00   1    7    48 49 50 51 53 54 55
48   C35   11    12   0.00   1    5    49 50 51 52 54
49   C36   11    12  -0.10   0    2    50 51
50   HC36  17     1   0.10   1    0
51   C37   44     4   0.00   0    2    52 53
52   C38   44     4   0.00   1    3    53 54 59
53   C39   12     3   0.00   0    5    54 55 57 59 60
54   C40   12     3   0.00   1    3    55 56 59
55   C41   44     4   0.00   0    2    56 57
56   C42   44     4   0.00   1    4    57 58 59 62
57   C43   11    12   0.00   0    6    58 59 60 61 62 63
58   C44   14     5   0.00   1    2    59 62
59   C45   12     3   0.00   1    3    60 61 62
60   C46   44     4   0.00   0    2    61 62
61   C47   44     4   0.00   1    2    62 63
```

```
    62   C48   12     3   0.20   0    2    63 64
    63   O4     3    16  -0.20   1    2    64 65
    64   C49   13     4   0.00   0    2    65 66
    65   C50   12     3   0.00   0    1    66
    66   C51   13     4   0.00   1    0
# NB
  75
# IB   JB   MCB              21   23    15              45   46     3
   1    2    12              23   24    12              45   47    15
   2    3    26              23   25    15              47   48    15
   3    4    17              25   26     3              47   54    26
   4    5    17              24   27    17              48   49    15
   5    6    26              27   28    26              48   51    26
   5    9    26              28   29    20              49   50     3
   6    7    26              28   39    26              51   52    26
   7    8    26              29   30     2              52   53    26
   8    9    26              29   31    10              53   54    26
   8   14    26              31   32    10              53   59    26
   9   10    26              31   37    10              54   55    26
   9   11    26              32   33     2              55   56    26
  11   12    26              32   34    20              56   57    26
  12   13    26              34   35    26              57   58    26
  13   14    26              34   40    26              57   59    26
  13   18    26              35   36    26              57   62    26
  14   15    26              36   37    20              59   60    26
  15   16    26              37   38    20              60   61    26
  16   17    26              38   39    26              61   62    26
  17   18    15              40   41    17              62   63    17
  17   25    15              41   42    12              63   64    17
  18   19    15              42   43    15              64   65    26
  19   20     3              42   49    15              65   66    12
  19   21    15              43   44     3
  21   22     3              43   45    15
# NBA
  116
# IB   JB   KB   MCB                  11   12   13    12
   1    2    3    26                  12   13   14    12
   2    3    4    12                  12   13   18    12
   3    4    5    11                  14   13   18    12
   4    5    6    12                  13   14   15    12
   4    5    9    12                   8   14   13    12
   6    5    9    12                   8   14   15    12
   5    6    7    12                  14   15   16    12
   6    7    8    12                  15   16   17    12
   7    8    9    12                  16   17   18    26
   7    8   14    12                  16   17   25    26
   9    8   14    12                  18   17   25    26
   8    9   10    12                  17   18   13    26
   8    9   11    12                  17   18   19    26
   8    9    5    12                  13   18   19    26
   5    9   11    12                  18   19   20    24
   5    9   10    12                  18   19   21    26
  10    9   11    12                  20   19   21    24
   9   11   12    12                  19   21   22    24
```

```
  19   21   23    26
  22   21   23    24
  21   23   24    24
  21   23   25    26
  24   23   25    24
  23   24   27    11
  23   25   26    24
  23   25   17    26
  26   25   17    24
  24   27   28    12
  27   28   29    12
  27   28   39    12
  29   28   39    12
  28   29   30    17
  28   29   31    26
  30   29   31    17
  29   31   32    27
  29   31   37    27
  32   31   37    27
  31   32   33    17
  31   32   34    26
  33   32   34    17
  32   34   40    12
  32   34   35    12
  35   34   40    12
  34   35   36    12
  35   36   37    12
  36   37   38    26
  36   37   31    26
  38   37   31    26
  37   38   39    12
  38   39   28    12
  34   40   41    12
  40   41   42    11
  41   42   43    24
  41   42   49    24
  43   42   49    26
  42   43   44    24
  42   43   45    26
  44   43   45    24
# NIDA
  40
# IB   JB   KB   LB   MCB
   5    4    9    6     2
   8    9   14    7     2
  13   18   14   12     2
  14    8   15   13     2
  59   57   60   53     2
  54   47   55   53     2
  53   59   54   52     2
   9    5    8   11     2
  28   29   27   39     2
  34   32   40   35     2
  57   62   56   59     2
  43   45   46    24
  43   45   47    26
  46   45   47    24
  45   47   48    26
  45   47   54    26
  48   47   54    26
  47   48   49    26
  47   48   51    26
  49   48   51    26
  48   49   50    24
  48   49   42    26
  50   49   42    24
  48   51   52    12
  51   52   53    12
  52   53   54    12
  52   53   59    12
  54   53   59    12
  53   54   55    12
  53   54   47    12
  47   54   55    12
  54   55   56    12
  55   56   57    12
  56   57   58    12
  56   57   59    12
  56   57   62    12
  58   57   59    12
  58   57   62    12
  59   57   62    12
  57   59   60    12
  57   59   53    12
  53   59   60    12
  59   60   61    12
  60   61   62    12
  61   62   63    12
  61   62   57    12
  57   62   63    12
  62   63   64    11
  63   64   65    12
  64   65   66    26
  62   63   61   57     2
  18   13   17   19     1
  17   16   18   25     1
  19   18   20   21     1
  21   19   22   23     1
  23   21   25   24     1
  25   17   26   23     1
  17   18   19   21     1
  18   19   21   23     1
  19   21   23   25     1
  21   23   25   17     1
  25   17   18   19     1
```

```
  23   25   17   18    1                48   47   49   51    1
  29   28   30   31    1                49   48   50   42    1
  31   29   32   37    1                42   43   45   47    1
  32   31   33   34    1                43   45   47   48    1
  37   31   36   38    1                45   47   48   49    1
  42   41   43   49    1                47   48   49   42    1
  43   42   44   45    1                48   49   42   43    1
  45   43   46   47    1                49   42   43   45    1
  47   45   48   54    1
# NDA
  59
# IB   JB   KB   LB   MCB               56   55   54   53   17
   1    2    3    4   20                12   13   14   15   17
  66   65   64   63   20                55   54   53   52   17
   2    3    4    5   12                 7    8   14   15   17
  65   64   63   62   12                60   59   53   52   17
   3    4    5    6   12                13   14   15   16   17
  64   63   62   61   12                54   53   52   51   17
   3    4    5    9   12                14   15   16   17   17
  64   63   62   57   12                53   52   51   48   17
   4    5    6    7   17                15   16   17   18   20
   4    5    6    7    7                52   51   48   49   20
  63   62   61   60   17                12   13   18   19   20
  63   62   61   60    7                53   54   47   48   20
   5    6    7    8   17                21   23   24   27    2
  62   61   60   59   17                43   42   41   40    2
   6    7    8    9   17                23   24   27   28   12
  61   60   59   57   17                42   41   40   34   12
   7    8    9   10   20                24   27   28   39   17
   4    5    9   10    7                41   40   34   35   17
   6    5    9   10   20                27   28   29   30   19
   4    5    9   10   17                40   34   32   33   19
  60   59   57   56   20                30   29   31   37    4
  63   62   57   56   17                33   32   31   37    4
  63   62   57   56    7                29   28   39   38   17
  61   62   57   56   20                32   34   35   36   17
   8    9   11   12   20                34   35   36   37   17
  59   57   56   55   20                37   38   39   28   17
   9   11   12   13   17                35   36   37   38   19
  57   56   55   54   17                36   37   38   39   19
  11   12   13   14   17                29   31   37   38    5
END
```

5.3.3 Topology file for binaphthyl phosphate guests 81 and 82 (RBNP and SBNP)

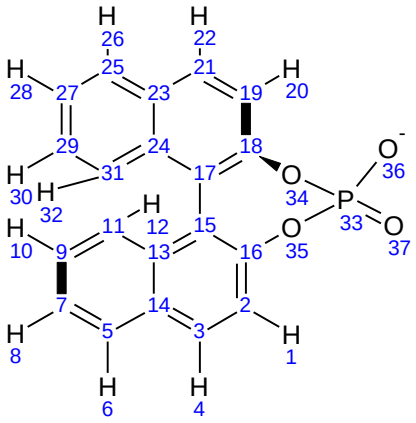


```
MTBUILDBLSOLUTE
# building block
# RNME
RBNP
# number of atoms, number of preceding exclusions
# NMAT, NLIN
    37         0
# ATOM MAE MSAE
# ATOM   ANM   IACM   MASS   CGM   ICGM   MAE   MSAE
     1   HCA     17      1   0.10     0     7      2   3   4 14 15 16 35
     2    CA     11     12 -0.10     1    10      3   4   5 13 14 15 16 17 33 35
     3    CB     11     12 -0.10     0     9      4   5   6  7 11 13 14 15 16
     4   HCB     17      1   0.10     1     4      5 13 14 16
     5    CC     11     12 -0.10     0     9      6   7   8  9 10 11 13 14 15
     6   HCC     17      1   0.10     1     5      7   8   9 13 14
     7    CD     11     12 -0.10     0     7      8   9 10 11 12 13 14
     8   HCD     17      1   0.10     1     4      9 10 11 14
     9    CE     11     12 -0.10     0     6     10 11 12 13 14 15
    10   HCE     17      1   0.10     1     3     11 12 13
    11    CF     11     12 -0.10     0     6     12 13 14 15 16 17
    12   HCF     17      1   0.10     1     3     13 14 15
    13    CG     11     12   0.00     0     7     14 15 16 17 18 24 35
    14    CH     11     12   0.00     1     3     15 16 17
    15    CI     11     12   0.00     0    10     16 17 18 19 23 24 31 33 34 35
    16    CJ     11     12   0.00     1     8     17 18 24 33 34 35 36 37
    17    CK     11     12   0.00     0    13     18 19 20 21 23 24 25 29 31 32
33 34 35
    18    CL     11     12   0.00     1    12     19 20 21 22 23 24 31 33 34 35
36 37
    19    CM     11     12 -0.10     0     8     20 21 22 23 24 25 33 34
    20   HCM     17      1   0.10     1     4     21 22 23 34
    21    CN     11     12 -0.10     0     7     22 23 24 25 26 27 34
    22   HCN     17      1   0.10     1     3     23 24 25
    23    CO     11     12   0.00     0     8     24 25 26 27 28 29 31 32
    24    CP     11     12   0.00     1     7     25 26 27 29 30 31 32
    25    CQ     11     12 -0.10     0     6     26 27 28 29 30 31
    26   HCQ     17      1   0.10     1     3     27 28 29
```

```
    27   CR    11    12 -0.10    0    5    28 29 30 31 32
    28  HCR    17     1  0.10    1    3    29 30 31
    29   CS    11    12 -0.10    0    3    30 31 32
    30  HCS    17     1  0.10    1    2    31 32
    31   CT    11    12 -0.10    0    1    32
    32  HCT    17     1  0.10    1    0
    33   P1    27    31  0.99    0    4    34 35 36 37
    34   O1     3    16 -0.36    0    3    35 36 37
    35   O2     3    16 -0.36    0    2    36 37
    36   O3     2    16 -0.635   0    1    37
    37   O4     2    16 -0.635   1    0
# NB
  41
# IB   JB   MCB              11   13    15              23   24    15
   1    2     3              13   14    15              23   25    15
   2    3    15              13   15    15              24   31    15
   2   16    15              15   16    15              25   26     3
   3    4     3              15   17    15              25   27    15
   3   14    15              16   35    12              27   28     3
   5    6     3              17   18    15              27   29    15
   5    7    15              17   24    15              29   30     3
   5   14    15              18   19    15              29   31    15
   7    8     3              18   34    12              31   32     3
   7    9    15              19   20     3              33   34    27
   9   10     3              19   21    15              33   35    27
   9   11    15              21   22     3              33   36    23
  11   12     3              21   23    15              33   37    23
# NBA
  68
#
IB   JB   KB   MCB                        5   14   13    26
   1    2    3    24                     13   15   16    26
   1    2   16    24                     13   15   17    26
   3    2   16    26                     16   15   17    26
   2    3    4    24                      2   16   15    26
   2    3   14    26                      2   16   35    18
   4    3   14    24                     15   16   35    18
   6    5    7    24                     15   17   18    26
   6    5   14    24                     15   17   24    26
   7    5   14    26                     18   17   24    26
   5    7    8    24                     17   18   34    18
   5    7    9    26                     17   18   19    26
   8    7    9    24                     19   18   34    18
   7    9   10    24                     18   19   20    24
   7    9   11    26                     18   19   21    26
  10    9   11    24                     20   19   21    24
   9   11   12    24                     19   21   22    24
   9   11   13    26                     19   21   23    26
  12   11   13    24                     22   21   23    24
  11   13   14    26                     21   23   24    26
  11   13   15    26                     21   23   25    26
  14   13   15    26                     24   23   25    26
   3   14   13    26                     17   24   23    26
   3   14    5    26                     17   24   31    26
```

```
  23   24   31    26                    29   31   24    26
  23   25   26    24                    24   31   32    24
  23   25   27    26                    34   33   35     4
  26   25   27    24                    35   33   36    13
  25   27   28    24                    36   33   37    28
  25   27   29    26                    37   33   34    13
  28   27   29    24                    34   33   36    13
  27   29   30    24                    35   33   37    13
  27   29   31    26                    18   34   33    25
  30   29   31    24                    16   35   33    25
  29   31   32    24
# NIDA
  49
# IB   JB   KB   LB   MCB               15   16    2    3     1
   2    1    3   16     1               16    2    3   14     1
   3    2    4   14     1                5    7    9   11     1
  14    3    5   13     1                7    9   11   13     1
   5    6    7   14     1                9   11   13   14     1
   7    5    8    9     1               11   13   14    5     1
   9    7   10   11     1               13   14    5    7     1
  11    9   12   13     1               14    5    7    9     1
  13   11   14   15     1               17   18   19   21     1
  15   13   16   17     1               18   19   21   23     1
  16    2   15   35     1               19   21   23   24     1
  17   15   18   24     1               21   23   24   17     1
  18   17   19   34     1               23   24   17   18     1
  19   18   20   21     1               24   17   18   19     1
  21   19   22   23     1               24   23   25   27     1
  23   21   24   25     1               23   25   27   29     1
  25   23   26   27     1               25   27   29   31     1
  27   25   28   29     1               27   29   31   24     1
  29   27   30   31     1               29   31   24   23     1
  31   24   29   32     1               31   24   23   25     1
  24   17   23   31     1               16   15   17   18     1
   2    3   14   13     1               13   15   17   24     1
   3   14   13   15     1               16   15   17   24     1
  14   13   15   16     1               13   15   17   18     1
  13   15   16    2     1               17   18   24   15     2
# NDA
   6
#
IB   JB   KB   LB   MCB                16   35   33   37    11
  15   16   35   33     2               18   34   33   36     9
  17   18   34   33     2               18   34   33   36    11
  16   35   33   37     9
END
```

The topology file of guest **82** was created similarly by reversing the atom priorities while defining the improper dihedral angle around the chiral center.

5.3.4 Topology file for diphenyl phosphinate guests 85 and 86 (RDPP and SDPP)

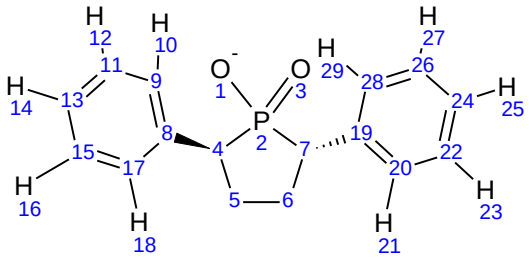


```
MTBUILDBLSOLUTE
# building block
# RNME
SDPP
# number of atoms, number of preceding exclusions
# NMAT, NLIN
    29         0
# ATOM MAE MSAE
# ATOM  ANM  IACM  MASS  CGM  ICGM  MAE  MSAE
     1   O1     2    16 -0.635   0    4   2 3 4 7
     2    P    27    31  0.27    0    7   3 4 5 6 7 8 19
     3   O2     2    16 -0.635   1    2   4 7
     4   C1    12     3  0.00    0    6   5 6 7 8 9 17
     5   C2    13     4  0.00    0    3   6 7 8
     6   C3    13     4  0.00    0    2   7 19
     7   C4    12     3  0.00    1    3   19 20 28
     8   C5    11    12  0.00    1    9   9 10 11 12 13 15 16 17 18
     9   C6    11    12 -0.10    0    8   10 11 12 13 14 15 17 18
    10  HC6    17     1  0.10    1    4   11 12 13 17
    11   C7    11    12 -0.10    0    6   12 13 14 15 16 17
    12  HC7    17     1  0.10    1    3   13 14 15
    13   C8    11    12 -0.10    0    5   14 15 16 17 18
    14  HC8    17     1  0.10    1    3   15 16 17
    15   C9    11    12 -0.10    0    3   16 17 18
    16  HC9    17     1  0.10    1    2   17 18
    17  C10    11    12 -0.10    0    1   18
    18  HC10   17     1  0.10    1    0
    19  C11    11    12  0.00    1    9   20 21 22 23 24 26 27 28 29
    20  C12    11    12 -0.10    0    8   21 22 23 24 25 26 28 29
    21  HC12   17     1  0.10    1    4   22 23 24 28
    22  C13    11    12 -0.10    0    6   23 24 25 26 27 28
    23  HC13   17     1  0.10    1    3   24 25 26
    24  C14    11    12 -0.10    0    5   25 26 27 28 29
    25  HC14   17     1  0.10    1    3   26 27 28
    26  C15    11    12 -0.10    0    3   27 28 29
    27  HC15   17     1  0.10    1    2   28 29
    28  C16    11    12 -0.10    0    1   29
    29  HC16   17     1  0.10    1    0
# NB
  31
# IB   JB   MCB              2    3    23              2    7    51
   1    2    23              2    4    51              4    5    25
```

```
   4    8    26              11   13    15              20   22    15
   5    6    25              13   14     3              22   23     3
   6    7    25              13   15    15              22   24    15
   7   19    26              15   16     3              24   25     3
   8    9    15              15   17    15              24   26    15
   8   17    15              17   18     3              26   27     3
   9   10     3              19   20    15              26   28    15
   9   11    15              19   28    15              28   29     3
  11   12     3              20   21     3
# NBA
  50
# IB   JB   KB   MCB                      14   13   15    24
   1    2    3    51                      13   15   16    24
   1    2    4    50                      13   15   17    26
   1    2    7    50                      16   15   17    24
   3    2    4    50                      15   17   18    24
   3    2    7    50                      15   17    8    26
   4    2    7    49                       8   17   18    24
   2    4    8    52                       7   19   20    26
   2    4    5    52                       7   19   28    26
   5    4    8     7                      20   19   28    26
   4    5    6     7                      19   20   21    24
   5    6    7     7                      19   20   22    26
   6    7   19     7                      21   20   22    24
   6    7    2    52                      20   22   23    24
   2    7   19    52                      20   22   24    26
   4    8    9    26                      23   22   24    24
   4    8   17    26                      22   24   25    24
   9    8   17    26                      22   24   26    26
   8    9   10    24                      25   24   26    24
  10    9   11    24                      24   26   27    24
   8    9   11    26                      24   26   28    26
   9   11   12    24                      27   26   28    24
   9   11   13    26                      26   28   29    24
  12   11   13    24                      26   28   19    26
  11   13   14    24                      19   28   29    24
  11   13   15    26
# NIDA
  26
# IB   JB   KB   LB   MCB                   9   11   13   15     1
   8    4    9   17     1                  11   13   15   17     1
   9    8   10   11     1                  13   15   17    8     1
  11    9   12   13     1                  15   17    8    9     1
  13   11   14   15     1                  17    8    9   11     1
  15   13   16   17     1                  19   20   22   24     1
  17   15   18    8     1                  20   22   24   26     1
  19    7   20   28     1                  22   24   26   28     1
  20   19   21   22     1                  24   26   28   19     1
  22   20   23   24     1                  26   28   19   20     1
  24   22   25   26     1                  28   19   20   22     1
  26   24   27   28     1                   4    2    8    5     2
  28   26   29   19     1                   7    2   19    6     2
   8    9   11   13     1
# NDA
```

```
   13
# IB   JB   KB   LB   MCB                    5    4    8    9     6
   1    2    4    5    42                    2    7    6    5     7
   1    2    7    6    42                    2    7   19   20     6
   1    2    4    8    41                    6    7   19   20     6
   1    2    7   19    41                    4    5    6    7    17
   2    4    5    6     7                    6    7    2    4    14
   2    4    8    9     6                    7    2    4    5    14
END
```

The topology file of guest **85** was created similarly by reversing the atom priorities while defining the improper dihedral angle around the chiral center.

5.3.5 Topology file for mandelate guests 87 and 88 (MANR and MANS)

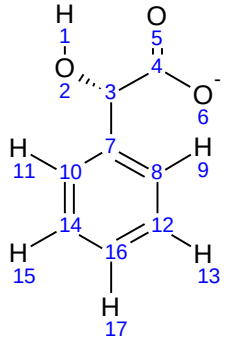


```
MTBUILDBLSOLUTE
# building block (residue, nucleotide, etc.)
# RNME
MANS
# number of atoms, number of preceding exclusions
# NMAT, NLIN
    17     0
#ATOM ANM  IACM MASS     CGMI CGM MAE MSAE
    1  HM    18    1   0.398    0   2    2    3
    2  OM1    3   16  -0.548    0   3    3    4    7
    3  CM1   12    3   0.150    1  10    4    5    6    7    8    9   10
11   12   14
    4  CM2   11   12   0.270    0   3    5    6    7
    5  OM2    2   16  -0.635    0   1    6
    6  OM3    2   16  -0.635    1   0
    7  CM3   11   12   0.000    0   9   8  9 10  11  12  13  14  15   16
    8  CM4   11   12  -0.100    0   8   9  10  11   12   13   14   16   17
    9  HM4   17    1   0.100    0   4   10   12   13   16
   10  CM5   11   12  -0.100    0   6   11   12   14   15   16   17
   11  HM5   17    1   0.100    0   3   14   15   16
   12  CM6   11   12  -0.100    0   5   13   14   15   16   17
   13  HM6   17    1   0.100    0   3   14   16   17
   14  CM7   11   12  -0.100    0   3   15   16   17
   15  HM7   17    1   0.100    0   2   16   17
   16  CM8   11   12  -0.100    0   1   17
```

```
   17  HM8   17    1   0.100    1   0
#  NB
   17
#  IB   JB  MCB                4    6    5               10   14   15
    1    2    1                7    8   15               12   13    3
    2    3   12                7   10   15               12   16   15
    3    4   26                8    9    3               14   15    3
    3    7   26                8   12   15               14   16   15
    4    5    5               10   11    3               16   17    3
# NBA
   25
#  IB   JB   KB  MCB                        7   10   14   26
    1    2    3   11                        8    7   10   26
    2    3    4   14                        8   12   13   24
    2    3    7   14                        8   12   16   26
    3    4    5   21                        9    8   12   24
    3    4    6   21                       10   14   15   24
    3    7    8   26                       10   14   16   26
    3    7   10   26                       11   10   14   24
    4    3    7   14                       12   16   14   26
    5    4    6   37                       12   16   17   24
    7    8    9   24                       13   12   16   24
    7    8   12   26                       14   16   17   24
    7   10   11   24                       15   14   16   24
# NIDA
   15
#  IB   JB   KB   LB  MCB                  14   16   15   10    1
    4    3    6    5    1                  10    7   14   11    1
    3    2    4    7    2                   8    7   10   14    1
    3    7    8    9    1                   7   10   14   16    1
    7    3    8   10    1                  10   14   16   12    1
    8    7    9   12    1                  14   16   12    8    1
   12    8   13   16    1                  16   12    8    7    1
   16   12   17   14    1                  12    8    7   10    1
#  NDA
   3
#  IB   JB   KB   LB  MCB                   2    3    4    5   20
    1    2    3    7   12                   2    3    7   10   20
END
```

The topology file of guest **87** was created similarly by reversing the atom priorities while defining the improper dihedral angle around the chiral center.

6. Summary

The work presented here describes the design, synthesis and binding studies of open-chain and macrocyclic chiral bicyclic guanidinium receptors specially designed for enantiorecognition of oxoanions. The receptor **115** was designed such that it would have a bicyclic guanidinium group as the main binding motif flanked by mono-allylated bisphenol A substituents on both sides. Ring closing metathesis was performed on **115** to obtain the macrocyclic host **116** possessing a rigid conformational structure. Host **117** was derived from **116** by reduction of the double bond. Hosts **115**, **117** and **116** are in the decreasing order of the number of degrees of freedom and the effect of structural confinement of the hosts could be observed in their enantio-recognition ability of the chiral oxoanions in the ITC titrations.

Host **116** showed the best enantiodifferentiation between guests **85** and **86**, binding **85** preferentially by a factor of ~360. On the other hand, host **115** did not show any significant preference for any of the enantiomers of the chiral guest pairs tested. Host **117**, which possesses intermediate structural rigidity, bound **85** preferentially over **86** by a factor of ~26. Analysis of the energetic signatures of the ITC titrations of the host **116** and guests **85** and **86** gave an insight into the driving factors behind the enantiorecognition shown. The one-site-binding model gave association constants as K_{ass}= 3.97x10^5 M^{-1} ($\Delta H°$= -5.94 kcal mol^{-1}, $\Delta S°$= +6.0 e.u.) for **85** and K_{ass}= 1,095 M^{-1} ($\Delta H°$= -7.07 kcal mol^{-1}, $\Delta S°$= -9.4 e.u.) for **86**. It was clear from the data obtained than the higher binding constant of **85** over **86** derived from the huge difference in the entropy released during the two complexation processes.

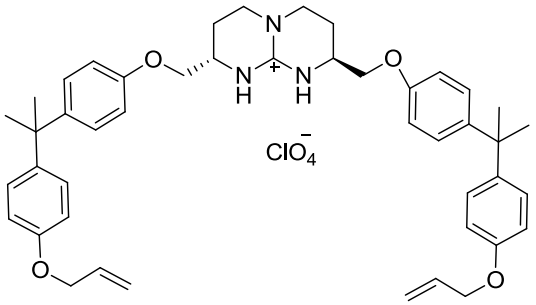

115

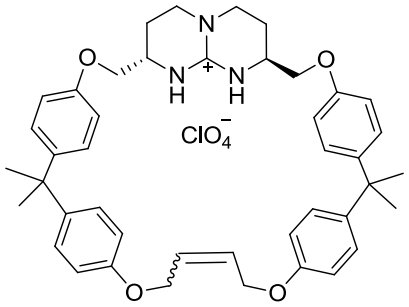

116

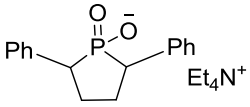

85 and **86**

Another series of chiral bicyclic guanidinium hosts was also designed exploiting estradiol side chains. Host **120** was obtained by substitution of mono-allylated estradiol to the guanidinium unit, but efforts to synthesize the cyclic host by ring closing metathesis on terminal alkenes were

not successful in this case. So, the open-chain host **122** was synthesized as an alternative approach. Then the macrocyclic host **124** was prepared by using bis-(4-isocyanatophenyl) methane as the linker group. Host **124** was not completely satisfactory in terms of the desired structural rigidity, because of the flexible spacer group. Expectedly, hosts **120** and **122** did not show any significant enantiorecognition for any of the chiral guest pairs according to ITC titrations. Host **124** showed moderate enantiodifferentiation for binaphthyl phosphate guests **81** and **82** in 1,2-dichloroethane.

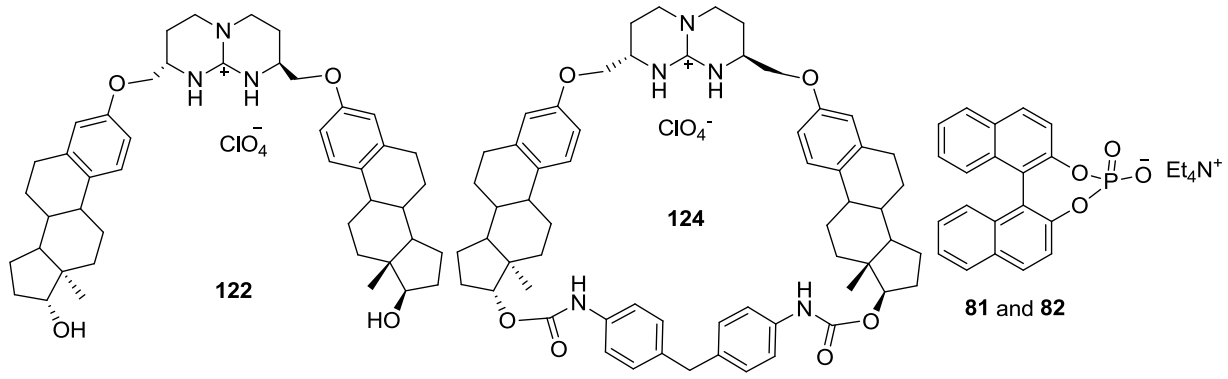

Molecular dynamics simulation studies on host **116** and various oxoanion guests were performed in chloroform at 300 K using the GROMOS'96 software. MD studies gave a preliminary idea of the size compatibility between host **116** and oxoanion guests. The cluster analysis and H-bond analysis suggested that the diphenyl phosphinate guests **85** and **86** were the most compatible with respect to the size of the cavity of host **116** while binaphthyl phosphate guests **81** and **82** were too big to enter the host cavity.

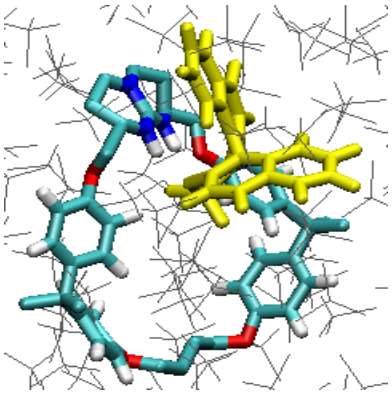

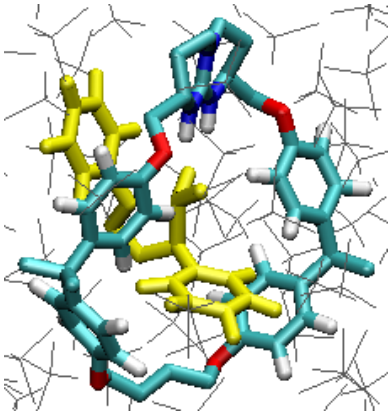

7. References

1. (a) Schmidtchen, F. P., Reflections on the construction of anion receptors: Is there a sign to resign from design? *Coord. Chem. Rev.* **2006,** *250* (23-24), 2918; (b) Schmidtchen, F. P., Artificial host molecules for the sensing of anions. In *Anion Sensing*, **2005**; p 1; (c) Schmidtchen, F. P.; Berger, M., Artificial organic host molecules for anions. *Chemical Reviews* **1997,** *97* (5), 1609.

2. (a) Gale, P. A., Anion coordination and anion-directed assembly: highlights from 1997 and 1998. *Coord. Chem. Rev.* **2000,** *199* (1), 181; (b) Gale, P. A., Anion and ion-pair receptor chemistry: highlights from 2000 and 2001. *Coord. Chem. Rev.* **2003,** *240* (1-2), 191; (c) Gale, P. A.; Anzenbacher Jr, P.; Sessler, J. L., Calixpyrroles II. *Coord. Chem. Rev.* **2001,** *222* (1), 57; (d) Beer, P. D.; Gale, P. A., Anion recognition and sensing: The state of the art and future perspectives. *Angew. Chem., Int. Ed.* **2001,** *40* (3), 486; (e) Fitzmaurice, R. J.; Kyne, G. M.; Douheret, D.; Kilburn, J. D., Synthetic receptors for carboxylic acids and carboxylates. *J. Chem. Soc., Perkin Trans. 1* **2002,** (7), 841; (f) Choi, K.; Hamilton, A. D., Macrocyclic anion receptors based on directed hydrogen bonding interactions. *Coord. Chem. Rev.* **2003,** *240* (1-2), 101.

3. Martínez-Máñez, R.; Sancenón, F., Fluorogenic and chromogenic chemosensors and reagents for anions. *Chem. Rev.* **2003,** *103* (11), 4419.

4. Bondy, C. R.; Loeb, S. J., Amide based receptors for anions. *Coord. Chem. Rev.* **2003,** *240* (1-2), 77.

5. Best, M. D.; Tobey, S. L.; Anslyn, E. V., Abiotic guanidinium containing receptors for anionic species. *Coord. Chem. Rev.* **2003,** *240* (1-2), 3.

6. Hiroshi, T., Armed crown ether complexes in supramolecular assembly. *Coord. Chem. Rev.* **1996,** *148* (0), 1.

7. Tsukube, H.; Shinoda, S., Lanthanide complexes in molecular recognition and chirality sensing of biological substrates. *Chem. Rev.* **2002,** *102* (6), 2389.

8. (a) Ward, T. J.; Hamburg, D.-M., Chiral separations. *Anal. Chem.* **2004,** *76* (16), 4635; (b) Pirkle, W. H.; Pochapsky, T. C., Considerations of chiral recognition relevant to the liquid chromatography separation of enantiomers. *Chem. Rev.* **1989,** *89* (2), 347.

9. Schmidtchen, F. P., Hosting anions. The energetic perspective. *Chem. Soc. Rev.* **2010,** *39* (10), 3916.

10. Stibor, I.; Zlatušková, P., Chiral recognition of anions. In *Anion Sensing*, 2005; p 31.

11. Schug, K. A.; Lindner, W., Noncovalent binding between guanidinium and anionic groups: focus on biological- and synthetic-based Arginine/Guanidinium interactions with phosph[on]ate and sulf[on]ate residues. *Chem. Rev.* **2004,** *105* (1), 67.

12. Kim, D. H.; Park, J.-I., The nature of interaction between the carboxylate of substrates and the guanidinium moiety of Arg-145 in carboxypeptidase A probed by inhibitors of the enzyme. *Bioorg. & Med. Chem. Lett.* **1996,** *6* (24), 2967.

13. Wang, P.-F.; McLeish, M. J.; Kneen, M. M.; Lee, G.; Kenyon, G. L., An Unusually low pKa for Cys282 in the active site of human muscle creatine kinase *Biochemistry* **2001,** *40* (39), 11698.

14. Mowat, C. G.; Moysey, R.; Miles, C. S.; Leys, D.; Doherty, M. K.; Taylor, P.; Walkinshaw, M. D.; Reid, G. A.; Chapman, S. K., Kinetic and crystallographic analysis of the key active site acid/base arginine in a soluble fumarate reductase *Biochemistry* **2001,** *40* (41), 12292.

15. Bell, J. K.; Yennavar, H. P.; Right, S. K.; Thompson, J. R.; Viola, R. E.; Banaszak, L. J., structural analyses of a malate dehydrogenase with a variable active site *J. Biol. Chem.* **2001,** *276*, 31156.

16. Kubik, S.; Reyheller, C.; Stüwe, S., Recognition of anions by synthetic receptors in aqueous solution. *J. Incl. Phenom. and Macrocyclic Chem.* **2005,** *52* (3), 137.

17. Echavarren, A.; Galan, A.; Lehn, J. M.; de Mendoza, J., Chiral recognition of aromatic carboxylate anions by an optically active abiotic receptor containing a rigid guanidinium binding subunit. *J. Am. Chem. Soc.* **1989,** *111* (13), 4994.

18. Metzger, A.; Gloe, K.; Stephan, H.; Schmidtchen, F. P., Molecular recognition and phase transfer of underivatized amino acids by a foldable artificial host. *J. Org. Chem.* **1996,** *61* (6), 2051.

19. Lawless, L. J.; Blackburn, A. G.; Ayling, A. J.; Perez-Payan, M. N.; Davis, A. P., Steroidal guanidines as enantioselective receptors for N-acyl [small alpha]-amino acids. Part 1. 3[small alpha]-Guanylated carbamates derived from cholic acid. *J. Chem. Soc., Perkin Trans. 1* **2001,** (11), 1329.

20. Schmuck, Carsten, carboxylate binding by 2-(guanidiniocarbonyl)pyrrole receptors in aqueous solvents: improving the binding properties of guanidinium cations through additional hydrogen bonds. *Chem. - Eur. J.* **2000,** *6* (4), 709.

21. Dietrich, B.; M., F. T.; Lehn, J. M.; Pease, L. G.; Fyles, D. M., *J. Chem. Soc., Chem. Commun.* **1978**, 934.

22. Galan, A.; Andreu, D.; Echavarren, A. M.; Prados, P.; de Mendoza, J., A receptor for the enantioselective recognition of phenylalanine and tryptophan under neutral conditions. *J. Am. Chem. Soc.* **1992,** *114* (4), 1511.

23. Fang, L.; Guo-Yuan, L.; Wei-Jiang, H.; Ming-Hua, L.; Long-Gen, Z.; Hou-Ming, W., Molecular recognition of nucleotides by a calix[4]arene derivative with two alkyl guanidinium groups at the air-water interface. *New J. Chem.* **2002,** *26* (5), 601.

24. Alcázar, V.; Segura, M.; Prados, P.; de Mendoza, J., A preorganized macrocycle based on a bicyclic guanidinium subunit with six convergent hydrogen bonds for anion recognition. *Tetrahedron Lett.* **1998,** *39* (9), 1033.

25. Jadhav, V. D.; Schmidtchen, F. P., A novel synthesis of chiral guanidinium receptors and their use in unfolding the energetics of enantiorecognition of chiral carboxylates. *J. Org. Chem.* **2007,** *73* (3), 1077.

26. Doyle, M. P.; Morgan, J. P.; Fettinger, J. C.; Zavalij, P. Y.; Colyer, J. T.; Timmons, D. J.; Carducci, M. D., "Matched/mismatched" diastereomeric dirhodium(II) carboxamidate catalyst pairs. structure-selectivity correlations in diazo decomposition and hetero-Diels-Alder reactions. *J. Org. Chem.* **2005,** *70* (13), 5291.

27. Exner, O., Entropy-enthalpy compensation and anticompensation: solvation and ligand binding. *Chem. Commun.* **2000,** (17), 1655.

28. Williams, D. H.; Bardsley, B., The vancomycin group of antibiotics and the fight against resistant bacteria. *Angew. Chem. Int. Ed.* **1999,** *38* (9), 1172.

29. Antonisse, M. G. M.; Reinhoudt, N. D., Neutral anion receptors: design and application. *Chem. Commun.* **1998,** (4), 443.

30. Prohens, R.; Tomàs, S.; Morey, J.; Deyà, P. M.; Ballester, P.; Costa, A., Squaramido-based receptors: Molecular recognition of carboxylate anions in highly competitive media. *Tetrahedron Lett.* **1998,** *39* (9), 1063.

31. Pelizzi, N.; Casnati, A.; Ungaro, R., Calix[4]arenes with perfluorinated alcoholic functions at the upper rim: a new class of neutral anion receptors. *Chem. Commun.* **1998,** (23), 2607.

32. (a) Pu, L., 1,1‘-Binaphthyl dimers, oligomers, and polymers: molecular recognition, asymmetric catalysis, and new materials. *Chem. Rev.* **1998,** *98* (7), 2405; (b) Chen, Y.; Yekta, S.; Yudin, A. K., Modified BINOL ligands in asymmetric catalysis. *Chem. Rev.* **2003,** *103* (8), 3155; (c) Kočovský, P.; Vyskočil, Š.; Smrčina, M., Non-symmetrically substituted 1,1‘-binaphthyls in enantioselective catalysis. *Chem. Rev.* **2003,** *103* (8), 3213; (d) Brunel, J. M., BINOL: A versatile chiral reagent. *Chem. Rev.* **2005,** *105* (3), 857.

33. Yoon, J.; Cram, D. J., Chiral recognition properties in complexation of two asymmetric hemicarcerands1. *J. Am. Chem. Soc.* **1997,** *119* (49), 11796.

34. Lin, J.; Zhang, H.-C.; Pu, L., Bisbinaphthyl macrocycle-based highly enantioselective fluorescent sensors for α-hydroxycarboxylic acids. *Org. Lett.* **2002,** *4* (19), 3297.

35. Li, Z.-B.; Lin, J.; Zhang, H.-C.; Sabat, M.; Hyacinth, M.; Pu, L., Macrocyclic bisbinaphthyl fluorophores and their acyclic analogues: signal amplification and chiral recognition. *J. Org. Chem.* **2004,** *69* (19), 6284.

36. Li, Z.-B.; Lin, J.; Pu, L., A cyclohexyl-1,2-diamine-derived bis(binaphthyl) macrocycle: enhanced sensitivity and enantioselectivity in the fluorescent recognition of mandelic acid. *Angew. Chem. Int. Ed.* **2005,** *44* (11), 1690.

37. Liu, H.-L.; Hou, X.-L.; Pu, L., enantioselective precipitation and solid-state fluorescence enhancement in the recognition of α-hydroxycarboxylic acids. *Angew. Chem. Int. Ed.* **2009,** *48* (2), 382.

38. Lu, Q.-S.; Dong, L.; Zhang, J.; Li, J.; Jiang, L.; Huang, Y.; Qin, S.; Hu, C.-W.; Yu, X.-Q., Imidazolium-functionalized BINOL as a multifunctional receptor for chromogenic and chiral anion recognition. *Org. Lett.* **2009,** *11* (3), 669.

39. Sambasivan, S.; Kim, D.-s.; Ahn, K. H., Chiral discrimination of [small alpha]-amino acids with a C2-symmetric homoditopic receptor. *Chem. Commun. 46* (4), 541.

40. Xu, K.-X.; Yang, L.-R.; Wang, Y.-X.; Zhao, J.; Wang, C.-J., Synthesis and enantioselective fluorescent sensors for amino acid derivatives based on BINOL. *Supramol. Chem.* **2010,** *22* (10), 563.

41. Xu, K.-X.; Cheng, P.-F.; Zhao, J.; Wang, C.-J., Enantioselective fluorescent sensors for amino acid derivatives based on BINOL bearing S-tryptophan unit: synthesis and chiral recognition. *J. Fluorescence* **2011,** *21* (3), 991.

42. Swamy, K.; Singh, J. N.; Yoo, J.; Kwon, S.; Chung, S.-Y.; Lee, C.-H.; Yoon, J., Chiral binaphthyl receptors bearing imidazolium or urea groups for the recognition of anions. *J. Incl. Phenom. and Macrocyclic Chem.* **2010,** *66* (1), 107.

43. Zhao, J.; Davidson, M. G.; Mahon, M. F.; Kociok-Köhn, G.; James, T. D., An enantioselective fluorescent sensor for sugar acids. *J. Am. Chem. Soc.* **2004,** *126* (49), 16179.

44. Ragusa, A.; Rossi, S.; Hayes, J. M.; Stein, M.; Kilburn, J. D., Novel enantioselective receptors for N-protected glutamate and aspartate. *Chem –Eur. J.* **2005,** *11* (19), 5674.

45. Ragusa, A.; Hayes, J. M.; Light, M. E.; Kilburn, J. D., A combined computational and experimental approach for the analysis of the enantioselective potential of a new macrocyclic receptor for N-protected α-amino acids. *Chem. – Eur. J.* **2007,** *13* (9), 2717.

46. Gonzalez, S.; Pelaez, R.; Sanz, F.; Jimenez, M. B. N.; Moran, J. N. R.; Caballero, M. C., Macrocyclic chiral receptors toward enantioselective recognition of naproxen. *Org. Lett.* **2006,** *8* (21), 4679.

47. Kim, Y. K.; Lee, H. N.; Singh, N. J.; Choi, H. J.; Xue, J. Y.; Kim, K. S.; Yoon, J.; Hyun, M. H., Anthracene derivatives bearing thiourea and glucopyranosyl groups for the highly selective chiral recognition of amino acids: opposite chiral selectivities from similar binding units. *J. Org. Chem.* **2007,** *73* (1), 301.

48. Chen, Z.-H.; He, Y.-B.; Hu, C.-G.; Huang, X.-H., Preparation of a metal–ligand fluorescent chemosensor and enantioselective recognition of carboxylate anions in aqueous solution. *Tetrahedron: Asymmetry* **2008,** *19* (17), 2051.

49. Miyaji, H.; Hong, S.-J.; Jeong, S.-D.; Yoon, D.-W.; Na, H.-K.; Hong, J.; Ham, S.; Sessler, J. L.; Lee, C.-H., A Binol-Strapped Calix[4]pyrrole as a Model Chirogenic Receptor for the Enantioselective Recognition of Carboxylate Anions. *Angew. Chem. Int. Ed.* **2007,** *46* (14), 2508.

50. Fan, A.; Kah Hong, H.; Valiyaveettil, S.; Vittal, J. J., A urea-incorporated receptor for aromatic carboxylate anion recognition. *J. Supramol. Chem. 2* (1-3), 247.

51. Barnard, A.; Dickson, S. J.; Paterson, M. J.; Todd, A. M.; Steed, J. W., Enantioselective lactate binding by chiral tripodal anion hosts derived from amino acids. *Org. & Biomol. Chem.* **2009,** *7* (8), 1554.

52. Lin, P.-H.; Tong, S.-J.; Louis, S. R.; Chang, Y.; Chen, W.-Y., Thermodynamic basis of chiral recognition in a DNA aptamer. *Phys. Chem. Chem. Phys.* **2009,** *11* (42), 9744.

53. Su, X.; Luo, K.; Xiang, Q.; Lan, J.; Xie, R., Enantioselective recognitions of chiral molecular tweezers containing imidazoliums for amino acids. *Chirality* **2009,** *21* (5), 539.

54. Kim, S.-M.; Choi, K., A practical solvating agent for the chiral NMR discrimination of carboxylic acids. *Eur. J. Org. Chem.* **2011,** *2011* (25), 4747.

55. Griesbeck, A. G.; Hanft, S.; Diaz Miara, Y., Colorimetric detection of achiral anions and chiral carboxylates by a chiral thiourea-phthalimide dyad. *Photochemical & Photobiological Sci.* **2010,** *9* (10), 1385.

56. (a) Villemin, D., Synthese de macrolides par methathese. *Tetrahedron Lett.* **1980,** *21* (18), 1715; (b) Tsuji, J.; Hashiguchi, S., Application of olefin metathesis to organic synthesis. Syntheses of civetone and macrolides. *Tetrahedron Lett.* **1980,** *21* (31), 2955.

57. (a) Schrock, R. R., Multiple metal–carbon bonds for catalytic metathesis reactions (nobel lecture). *Angew. Chem. Int. Ed.* **2006,** *45* (23), 3748; (b) Grubbs, R. H., Olefin-metathesis catalysts for the preparation of molecules and materials (nobel lecture). *Angew. Chem. Int. Ed.* **2006,** *45* (23), 3760.

58. (a) The application of olefin metathesis to the synthesis of biologically active macrocyclic agents. *Current Topics in Medicinal Chemistry* **2005,** *5*, 1495; (b) Kaliappan, K. P.; Kumar, N., Efficient metathesis route to the B-ring of eleutherobin and other medium-sized cyclic ethers. *Tetrahedron* **2005,** *61* (31), 7461.

59. (a) Kiyota, H.; Nishida, A.; Nagata, T.; Nakagawa, M., Strategies for the synthesis of manzamine alkaloids. In *Marine Natural Products*, Springer Berlin / Heidelberg: 2006; Vol. 5, p 255; (b) Gradillas, A.; Pérez-Castells, J., Macrocyclization by ring-closing metathesis in the total synthesis of natural products: reaction conditions and limitations. *Angew. Chem. Int. Ed.* **2006,** *45* (37), 6086.

60. (a) Ivin, K. J.; Mol, J. C., Introduction. in o*lefin metathesis and metathesis polymerization (2)*, Academic Press: London, 1997; p 1; (b) Jean-Louis Hérisson, P.; Chauvin, Y., Catalyse de transformation des oléfines par les complexes du tungstène. II. Télomérisation

des oléfines cycliques en présence d'oléfines acycliques. *Die Makromolekulare Chemie* **1971,** *141* (1), 161.

61. Conrad, J. C.; Eelman, M. D.; Silva, J. o. A. D.; Monfette, S.; Parnas, H. H.; Snelgrove, J. L.; Fogg, D. E., Oligomers as intermediates in ring-closing metathesis. *J. Am. Chem. Soc.* **2007,** *129* (5), 1024.

62. Yamamoto, K.; Biswas, K.; Gaul, C.; Danishefsky, S. J., Effects of temperature and concentration in some ring closing metathesis reactions. *Tetrahedron Lett.* **2003,** *44* (16), 3297.

63. Lee, C. W.; Grubbs, R. H., Stereoselectivity of macrocyclic ring-closing olefin metathesis. *Org. Lett.* **2000,** *2* (14), 2145.

64. Constable, D. J. C.; Jimenez-Gonzalez, C.; Henderson, R. K., Perspective on solvent use in the pharmaceutical industry. *Org. Process R&D* **2006,** *11* (1), 133.

65. Kidd, T. J.; Leigh, D. A.; Wilson, A. J., Organic "magic rings": The hydrogen bond-directed assembly of catenanes under thermodynamic control. *J. Am. Chem. Soc.* **1999,** *121* (7), 1599.

66. Kirkland, T. A.; Grubbs, R. H., Effects of olefin substitution on the ring-closing metathesis of dienes. *J. Org. Chem.* **1997,** *62* (21), 7310.

67. (a) Sieck, S. R.; McReynolds, M. D.; Schroeder, C. E.; Hanson, P. R., Metathesis studies to cyclic enol phosphonamidates. *J. Org. Chem.* **2006,** *691* (24-25), 5307; (b) Xu, Z.; Johannes, C. W.; Houri, A. F.; La, D. S.; Cogan, D. A.; Hofilena, G. E.; Hoveyda, A. H., Applications of Zr-catalyzed carbomagnesation and Mo-catalyzed macrocyclic ring closing metathesis in asymmetric synthesis. enantioselective total synthesis of Sch 38516 (Fluvirucin B1). *J. Am. Chem. Soc.* **1997,** *119* (43), 10302; (c) El-azizi, Y.; Schmitzer, A.; Collins, S. K., Exploitation of perfluorophenyl–phenyl interactions for achieving difficult macrocyclizations by using ring-closing metathesis. *Angew. Chem. Int. Ed.* **2006,** *45* (6), 968.

68. (a) Marsella, M. J.; Maynard, H. D.; Grubbs, R. H., Template-directed ring-closing metathesis: synthesis and polymerization of unsaturated crown ether analogs. *Angew. Chem., Int. Ed.* **1997,** *36* (10), 1101; (b) Akine, S.; Kagiyama, S.; Nabeshima, T., Oligometallic template strategy for ring-closing olefin metathesis: A highly cis- and trans-selective synthesis of a 32-membered macrocyclic tetraoxime. *Inorg. Chem.* **2007,** *46* (23), 9525.

69. Kilbinger, A. F. M.; Cantrill, S. J.; Waltman, A. W.; Day, M. W.; Grubbs, R. H., Magic ring rotaxanes by olefin metathesis. *Angew. Chem., Int. Ed.* **2003,** *42* (28), 3281.

70. Hamilton, G. D.; Feeder, N.; Teat, J. S.; Sanders, K. M. J., Reversible synthesis of [small pi]-associated [2]catenanes by ring-closing metathesis: towards dynamic combinatorial libraries of catenanes. *New J. Chem.* **1998,** *22* (10), 1019.

71. Fürstner, A.; Langemann, K., Total syntheses of (+)-ricinelaidic acid lactone and of (-)-gloeosporone Based on transition-metal-catalyzed C-C bond formations. *J. Am. Chem. Soc.* **1997,** *119* (39), 9130.

72. Mitchell, L.; Parkinson, J. A.; Percy, J. M.; Singh, K., Selected substituent effects on the rate and efficiency of formation of an eight-membered ring by RCM. *J. Org. Chem.* **2008,** *73* (6), 2389.

73. Pentzer, E. B.; Gadzikwa, T.; Nguyen, S. T., Substrate encapsulation: An efficient strategy for the RCM synthesis of unsaturated Ïμ-Lactones. *Org. Lett.* **2008,** *10* (24), 5613.

74. Varray, S.; Gauzy, C.; Lamaty, F.; Lazaro, R.; Martinez, J., Synthesis of cyclic amino acid derivatives via ring closing metathesis on a poly(ethylene glycol) supported substrate. *J. Org. Chem.* **2000,** *65* (20), 6787.

75. Mayo, K. G.; Nearhoof, E. H.; Kiddle, J. J., Microwave-accelerated ruthenium-catalyzed olefin metathesis. *Org. Lett.* **2002,** *4* (9), 1567.

76. Efskind, J.; Undheim, K., High temperature microwave-accelerated ruthenium-catalysed domino RCM reactions. *Tetrahedron Lett.* **2003,** *44* (14), 2837.

77. Schmidtchen, F.P, A novel synthesis of chiral guanidinium molecular hosts. *Tetrahedron Lett.* **1990,** *31* (16), 2269.

78. Kurzmeier, H.; Schmidtchen, F. P., Abiotic anion receptor functions. A facile and dependable access to chiral guanidinium anchor groups. *J. Org. Chem.* **1990,** *55* (12), 3749.

79. (a) Coquerel, Y.; Rodriguez, J., Microwave-assisted olefin metathesis. *Eur. J. Org. Chem.* **2008,** *2008* (7), 1125; (b) Yang, Q.; Li, X.-Y.; Wu, H.; Xiao, W.-J., Microwave-assisted ring-closing metathesis of diallylamines: a rapid synthesis of pyrrole and pyrroline derivatives. *Tetrahedron Lett.* **2006,** *47* (23), 3893.

80. (a) Griesbaum, K., Problems and possibilities of the free-radical addition of thiols to unsaturated compounds. *Angew. Chem., Int. Ed.* **1970,** *9* (4), 273; (b) Mayo, F. R.; Walling, C., The peroxide effect in the addition of reagents to unsaturated compounds and in rearrangement reactions. *Chem. Rev.* **1940,** *27* (2), 351.

81. (a) Morgan, C. R.; Magnotta, F.; Ketley, A. D., Thiol/ene photocurable polymers. *J. Polymer Sci.: Polymer Chem. Ed.* **1977,** *15* (3), 627; (b) Hoyle, C. E.; Lee, T. Y.; Roper, T., Thiol–enes: Chemistry of the past with promise for the future. *J. Polymer Sci. Part A: Polymer Chem.* **2004,** *42* (21), 5301.

82. Grunwald, E.; Steel, C., Solvent reorganization and thermodynamic enthalpy-entropy compensation. *J. Am. Chem. Soc.* **1995,** *117* (21), 5687.

83. (a) van Gunsteren, W. F.; Bakowies, D.; Baron, R.; Chandrasekhar, I.; Christen, M.; Daura, X.; Gee, P.; Geerke, D. P.; Glättli, A.; Hünenberger, P. H.; Kastenholz, M. A.; Oostenbrink, C.; Schenk, M.; Trzesniak, D.; van der Vegt, N. F. A.; Yu, H. B., Biomolecular Modeling: Goals, Problems, Perspectives. *Angew. Chem., Int. Ed.* **2006,** *45* (25), 4064; (b) van Gunsteren, W. F.; Mark, A. E., On the interpretation of biochemical data by molecular dynamics computer simulation. *Eur. J. Biochem.* **1992,** *204* (3), 947; (c) Huber, T.; van Gunsteren, W. F., SWARM-MD: Searching conformational space by cooperative molecular dynamics. *J. Phys. Chem. A* **1998,** *102* (29), 5937; (d) Scott, W. R. P.; Hünenberger, P. H.; Tironi, I. G.; Mark, A. E.; Billeter, S. R.; Fennen, J.; Torda, A. E.; Huber, T.; Krüger, P.; van Gunsteren, W. F., The GROMOS biomolecular simulation program package. *J. Phys. Chem. A* **1999,** *103* (19), 3596; (e) Phillips, J. C.; Braun, R.; Wang, W.; Gumbart, J.; Tajkhorshid, E.; Villa, E.; Chipot, C.; Skeel, R. D.; Kalé, L.; Schulten, K., Scalable molecular dynamics with NAMD. *J. Comp. Chem.* **2005,** *26* (16), 1781; (f) Case, D. A.; Cheatham, T. E.; Darden, T.; Gohlke, H.; Luo, R.; Merz, K. M.; Onufriev, A.; Simmerling, C.; Wang, B.; Woods, R. J., The Amber biomolecular simulation programs. *J. Comp. Chem.* **2005,** *26* (16), 1668.

84. Cecchini, M.; Krivov, S. V.; Spichty, M.; Karplus, M., Calculation of free-energy differences by confinement simulations. Application to peptide conformers. *J. Phys. Chem. B* **2009,** *113* (29), 9728.

85. Trzesniak, D.; Glättli, A.; Jaun, B.; van Gunsteren, W. F., Interpreting NMR data for β-peptides using Molecular dynamics simulations. *J. Am. Chem. Soc.* **2005,** *127* (41), 14320.

86. van Gunsteren, W. F.; Hünenberger, P. H.; Mark, A. E.; Smith, P. E.; Tironi, I. G., Computer simulation of protein motion. *Comp. Phys. Commun.* **1995,** *91* (1-3), 305.

87. van Gunsteren, W. F.; Berendsen, H. J. C., Computer simulation of molecular dynamics: Methodology, Applications, and Perspectives in Chemistry. *Angew. Chem., Int. Ed.* **1990,** *29* (9), 992.

88. Oostenbrink, C.; Villa, A.; Mark, A. E.; Van Gunsteren, W. F., A biomolecular force field based on the free enthalpy of hydration and solvation: The GROMOS force-field parameter sets 53A5 and 53A6. *J. Comp. Chem.* **2004,** *25* (13), 1656.

89. (a) van der Vegt, N. F. A.; van Gunsteren, W. F., Entropic contributions in cosolvent binding to hydrophobic solutes in water. *J. Phys. Chem. B* **2003,** *108* (3), 1056; (b) van der Vegt, N. F. A.; Trzesniak, D.; Kasumaj, B.; van Gunsteren, W. F., energy–entropy compensation in the transfer of nonpolar solutes from water to cosolvent/water mixtures. *Chem. Phys. Chem.* **2004,** *5* (1), 144.

90. van Gunsteren, W. F.; Billeter, S. R.; Eising, A. A.; Hünenberger, P. H.; Krüger, P.; Mark, A. E.; Acott, W. R. P.; Tironi, I. G., , *Biomolecular Simulation: The Gromos 96 Manual and User Guide*, Hochschulverlag AG: ETH-Zurich. **1996**.

91. de Boer, J. J.; Bright, D., The crystal and molecular structure of 5-hydroxydibenzo-5H-phosphole-5-oxide, $C_{12}H_9O_2P$. *Acta Cryst. Sec. B* **1974,** *30* (3), 797.

92. Gottlieb, H. E.; Kotlyar, V.; Nudelman, A., NMR chemical shifts of common laboratory solvents as trace impurities. *J. Org. Chem.* **1997,** *62* (21), 7512.